9-2009

Tailoring the Surface-Coating of Gold Nanoparticles for Bio-applications

Partha S. Ghosh
University of Massachusetts Amherst, parthabharat@gmail.com

TAILORING THE SURFACE-COATING OF GOLD NANOPARTICLES FOR BIO-APPLICATIONS

A Dissertation Presented

by

PARTHA S. GHOSH

Submitted to the Graduate School of the
University of Massachusetts Amherst in partial fulfillment
of the requirements for the degree of

DOCTOR OF PHILOSOPHY

September 2009

Chemistry

TAILORING THE SURFACE-COATING OF GOLD NANOPARTICLES FOR BIO-APPLICATIONS

A Dissertation Presented

by

PARTHA S. GHOSH

Approved as to style and content by:

_____
Vincent M. Rotello, Chair

_____
Craig T. Martin, Member

_____
Michael J. Knapp, Member

_____
David J. Gross, Member

_____
Edward G. Voigtman, Jr., Associate Head,
Department of Chemistry

DEDICATION

To my grandparents who passed away

ACKNOWLEDGMENTS

I am extremely thankful to my advisor, Prof. Vincent M. Rotello, for his guidance and support over the past five years. His advice and constant encouragement made this thesis work possible. I appreciate the kind of freedom he gave me. It helped me a lot in taking the right path when things were not going well.

I would like to thank my committee members, Prof. Craig T. Martin, Prof. Michael J. Knapp and Prof. David J. Gross, for their constructive comments throughout this research, and academic support.

For their healthy collaboration, I want to thank Prof. Michael J. Knapp, Prof. Neil S. Forbes, Prof. Jean Chmielewski, Prof. Richard W. Vachet and Prof. Kathleen F. Arcaro. I also thank to Halil, Kim, Bhoosan, Dawn and Eva for their help during these collaborations.

I really owe a lot to all the members of the Rotello group, whoever with I came in touch. The friendly and collaborative environment in the lab was a real treat to work. Although every member helped me with more or less, I must mention some names, like Chang-Cheng, Belma, Gang, Oscar and the “delivery gang” (Chae-kyu, Xiaochao, Chiara, Api, Sarit and Rochelle), for their enormous help.

I want to express my heartfelt gratitude to my family, relatives and friends. Without their love and support this work would have been impossible. My special thanks go to Shanti for her endless help in writing my papers/documents, and teaching me English and Biology. My friends (“Bappa”, Sarit, Nitai, Oscar, Debu, Pakkada, Dipankar, Subinoy, Krishnendu, Rishi, Amitda, Abby, Dada, Subhendu, Mal…) were always with me in fun as well as difficult times.

At last but not the least, I am grateful to Department of Chemistry and University of Massachusetts at Amherst for giving me such a nice platform.

ABSTRACT

TAILORING THE SURFACE-COATING OF GOLD NANOPARTICLES FOR BIO-APPLICATIONS

SEPTEMBER 2009

PARTHA S. GHOSH, B.Sc., RAMAKRISHNA MISSION VIDYAMANDIRA

M.Sc., INDIAN INSTITUTE OF TECHNOLOGY KANPUR

Ph.D., UNIVERSITY OF MASSACHUSETTS AMHERST

Directed by: Professor Vincent M. Rotello

Functionalized gold nanoparticles (AuNPs) provide an excellent scaffold for numerous biological applications. In these systems, the gold core imparts stability to the assembly, while the monolayer allows tuning of surface characteristics such as charge and hydrophobicity. The nano-scale size and tunable surface properties have made them an ideal candidate for manipulating protein-protein/protein-nucleic acid interactions, and delivery of therapeutics. In this thesis work, it has been demonstrated how the surface coating plays an important role in achieving a desired goal. Using organic synthesis as a tool, the monolayer was tailored to afford useful particles with biocompatibility and the ability to respond in the cellular environment. The recognition units present on the periphery of particles dictates/controls their interactions with biomolecular or cell surfaces. As described here, these engineered particles exhibited a number of bio-applications, including folding of a peptide into an α-helix, binding with DNA, and cellular delivery of genes and proteins.

TABLE OF CONTENTS

Page

LIST OF TABLES

Table Page

LIST OF FIGURES

Figure Page

CHAPTER 1

INTRODUCTION

1.1 Nanoparticles: An Excellent Scaffold for Biological Applications

Nanobiotechnology has emerged as a new exciting field in recent years with much promise.[1] The use of nanomaterials in biotechnology merges the fields of material science and biology. Nanoparticles offer a useful platform, providing unique properties with potentially wide-ranging therapeutic applications.[2] The field of nanoparticles in biology is certainly a burgeoning one, with the estimated number of papers in the area (based on Web of Science) rising from 11 in 1991 to over 3400 in 2008.

The utility of nanoparticles (NPs) arises from a variety of desirable structural attributes, including the similar size of nanoparticles and biomolecules such as proteins and polynucleic acids (Figure 1.1).[3] Additionally, nanoparticles can be fashioned with a wide range of metal and semiconductor core materials that impart useful properties such as fluorescence and magnetic behavior.[4] The applicable properties of some well known core materials and corresponding possible ligands used for surface functionalization with their possible applications are summarized in Table 1.1.

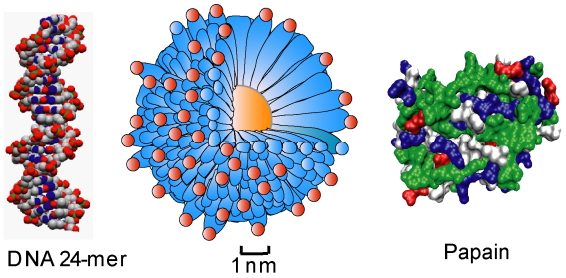

Figure 1.1: Schematic representation of a 2 nm core gold nanoparticle with 11-mercaptoundecanoic acids monolayer and relative sizes of papain and a 24-mer DNA duplex.

Nanoparticles are promising candidates for various biomedical applications, including biosensing, diagnostics, and therapy.[5,6,7,8,9] My research was focused on the use of gold nanoparticles in cellular delivery. As a background to this work, two related areas have been discussed here, namely nanoparticle-biomolecule interactions and nanoparticles as drug delivery systems.

Table 1.1: Characteristics, ligands and representative applications for various metal and semiconductor materials.

Core material	Characteristics	Ligand	Applications
Au	Optical absorption, fluorescence and fluorescence quenching, stability	Thiol, disulfide, phosphine, amine	Biomolecular recognition, delivery, sensing
Ag	Surface-enhanced fluorescence	Thiol	Sensing
Pt	Catalytic property	Thiol, phosphine, amine, isocyanide	Bio-catalyst, sensing
CdSe	Luminescence, photo-stability	Thiol, phosphine, pyridine	Imaging, sensing
Fe_2O_3	Magnetic property	Diol, dopamine derivative, amine	MR imaging and biomolecule purification
SiO_2	Biocompatibility	Alkoxysilane	Biocompatible by surface coating

1.2 Nanoparticle-Biomolecule Interactions

Creation of nanoparticle-based artificial receptors for biomacromolecular surface recognition provides a potential tool for controlling cellular and extracellular processes in numerous biological applications such as transcription regulation, enzymatic inhibition, delivery and sensing.

The conjugation of nanoparticles with biomolecules, such as proteins and DNA, can be done using two different approaches: direct covalent linkage and non-covalent interactions.[10,11,12,13,14] The most direct approach involves covalent attachment.[15] This conjugation can be achieved through either chemisorption of the biomolecule to the particle surface or through the use of heterobifunctional linkers. Chemisorption of proteins onto the surface of nanoparticles (usually containing a core of Au, ZnS, CdS and CdSe/ZnS) can be done through cysteine residues that are present on the protein surface (e.g. oligopeptide, serum albumin),[16] or chemically using 2-iminothiolane (Traut's reagent).[17,18] Bifunctional linkers provide a more versatile means of bioconjugation. Biomolecules are often covalently linked to ligands on the NP surface via traditional coupling strategies such as carbodiimide-mediated amidation and esterfication.[19] For biological applications, OEG or PEG is used in the linker to enhance the stability of the attached biomolecules and minimize non-specific adsorption of other materials.

Non-covalent assembly provides a highly modular approach to the biofunctionalization of nanoparticles. One example is DNA-NP binding, which can be effected through electrostatic interactions, groove binding, intercalation and complementary single strand DNA binding.[20] In this case, nanoparticles provide an attractive receptor for nucleic acids, representing a close analogy to protein-DNA interactions.[21,22] One approach to particle-DNA assembly uses complementary electrostatic interactions to promote high affinity of nanoparticle-DNA binding. The use of cationic ligands on the nanoparticle surface provides a complementary surface for binding the negatively charged backbone of DNA, for example the use of **NP 1** to bind to a 37-mer DNA duplex (Figure 1.2).[23] The binding of DNA inhibited transcription by T7

RNA polymerase, indicating the high affinity of the NP-DNA complex and pointing out a potential use of these systems in gene regulation. Intercalation provides yet another mechanism for DNA binding, as demonstrated by Murray *et al.*[24] A third approach to DNA conjugation exploits the high affinity and specificity of base-paring between DNA strands (Figure 1.2c).[25]

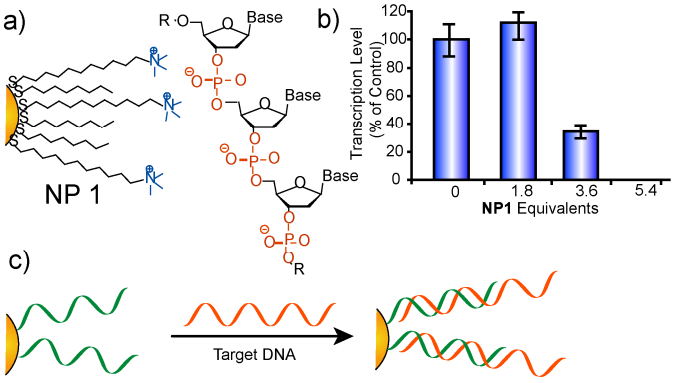

Figure 1.2: The DNA-nanoparticle interactions. (a) Structure of **NP 1** scaffold and the DNA backbone. (b) Transcription level as a function of DNA-**NP 1** stoichiometry. (c) Binding of DNA through complementary oligonucleotide hybridization.

Nanoparticle-protein interactions have also been studied extensively. One system that has been explored in our lab is the binding of chymotrypsin (ChT) - targeting the ring of cationic residues around active site of ChT (Figure 1.3).[26] Time-dependent inhibition of ChT activity was observed upon incubation with negatively charged **NP 2**.[27] A two-step binding process with a fast reversible association followed by a slower irreversible denaturation was observed.[28] This interaction could be reversed using cationic surfactants (Figure 1.3b), which restored ChT activity.[29] Based on the DLS data, two distinct mechanisms for this reversal were postulated: alkyl surfactants **3** and **4** form a bilayer

structures, whereas cationic thiol **5** and alcohol **6** directly modify the monolayer to liberate the bound proteins.

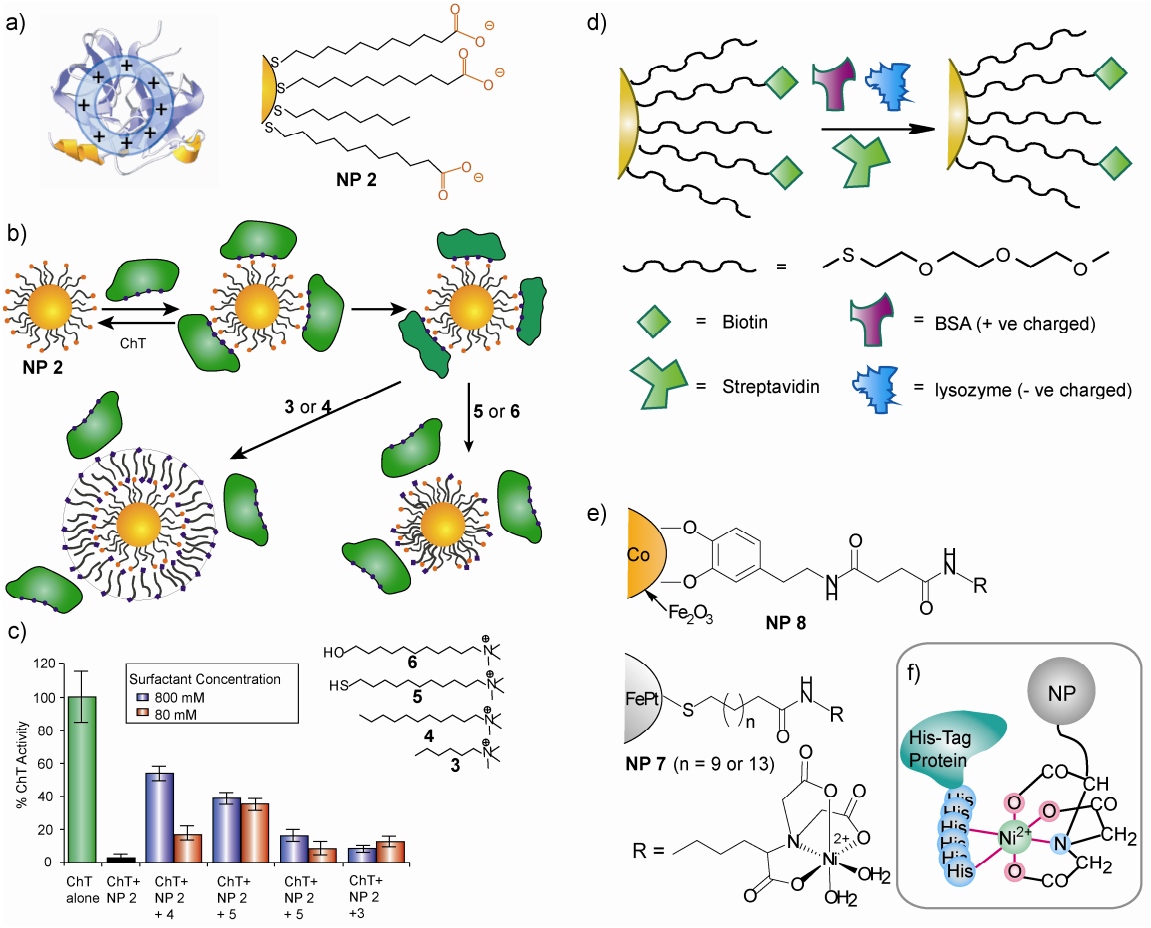

Figure 1.3: Protein-nanoparticle conjugation and the applications. (a) Electrostatic targeting of ChT by anionic **NP 3** b) Complexation of ChT with anionic nanoparticle and its release mechanisms by addition of various surfactants. c) Different degrees of restoration of enzymatic activity of nanoparticle-bound ChT by addition of various positively charged surfactants. (d) Specific interaction of biotin functionalized nanoparticles with streptavidin. (e) Structure of NTA-modified magnetic nanoparticles. (f) The NTA-Ni^{2+} functionalized magnetic nanoparticles selectively bind to histidine-tagged proteins.

The use of simple alkyl-based monolayers resulted in protein denaturation, an unfavorable outcome for a number of applications in delivery and biotechnology. Relying on the resistance of OEG to nonspecific interactions with biomolecules,[30] tetra(ethylene

glycol) spacers were introduced at the nanoparticle-protein interface.[31] Structural data obtained from fluorescence and CD studies revealed that the nanoparticle-bound ChT maintained its native structure. Further studies demonstrated that nanoparticle-protein complexation can considerably stabilize the bound proteins against denaturation at the air-water interface.[32]

Specific biomacromolecular interactions, such as streptavidin/biotin complementarity ($K_a \sim 10^{14}$ M^{-1}),[33] have been used to provide specific protein-NP binding. Zheng and Huang introduced biotin and glutathione-functionalized gold nanoparticles functionalized with tri(ethylene glycol)-terminated thiols.[34] These particles bind specifically to streptavidin and glutathione-*S*-transferase, respectively, to give stable complexes with minimal nonspecific binding with other proteins (Figure 1.3d). Biotin functionalized QDs were also used for specific protein binding in time-resolved fluoroimmunoassay.[35] Another way to specifically bind proteins is through the use of transition metal complexes that bind with surface-exposed histidines of proteins.[36] Xu *et al.* fabricated FePt nanoparticles (magnetic, **NP 7)**, with nickel-terminated nitrilotriacetic acid (NTA).[37] These NPs show high affinity and specificity towards histidine-tagged proteins (proteins with six consecutive histidines residues) (Figure 1.3e). In comparison to commercial magnetic microbeads, these NPs have a large protein binding capacity due to their high surface/volume ratio. This concept can be employed to manipulate the histidine-tagged recombinant proteins and bind other biological substrates at low concentrations.[38,39]

1.3 Nanoparticles as Drug Delivery Systems

Drug delivery systems (DDSs) can improve several crucial properties of 'free' drugs, such as solubility, *in vivo* stability, pharmacokinetics and biodistribution, thus enhancing their efficacy.[40] In a recent example of cellular delivery, mixed monolayer protected gold clusters were exploited for *in vitro* delivery of a hydrophobic fluorophore (BODIPY); an analog of hydrophobic drugs.[41] The cationic surface of the nanoprticles facilitated the penetration of cell membrane, and payload release was triggered by intracellular glutathione (GSH), relying on the ~1000-fold higher intracellular concentration of GSH relative to the extracellular environment (Figure 1.4a). Release of the dye was established by fluorogenesis upon release of the dye from the nanoparticle (Figure 1.4b,c). The controlled release of the fluorophore was observed in mouse embryonic fibroblast (MEF) cells, containing ~ 50% lower GSH levels than Hep G2, through incubation with glutathione monoethyl ester (GSH-OEt), which is processed to GSH by esterases for transiently increasing intracellular GSH concentrations (Figure 1.4d).

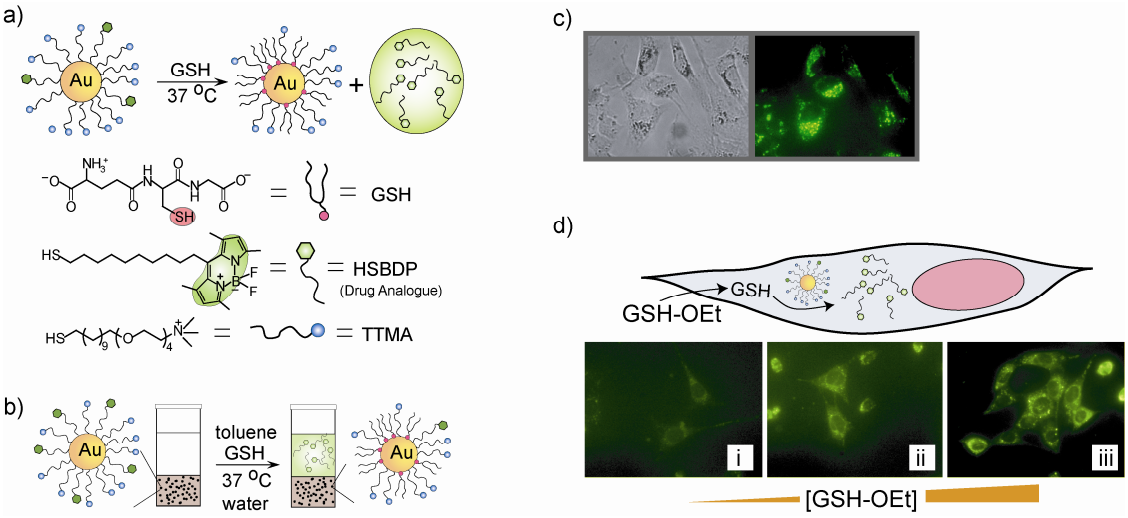

Figure 1.4: a) Schematic illustration of GSH-mediated surface monolayer exchange reaction/payload release. b) *in cuvette* release of BODIPY ligand mediated by GSH. c)

The bright field and fluorescence images of Human Hep G2 cells incubated with AuNP for 96 hours. d) Fluorescence images of MEF cells displaying GSH controlled release of the fluorophore after incubation with of 0, 5, and 20 mM GSH-OEt.

Lin et al. have demonstrated that thiols, such as dihydrolipoic acid (DHLA) and dithiothreitol (DTT), can likewise act as stimuli to remove pore caps in mesoporous silica nanoparticles, releasing trapped molecules inside the pores.[42,43] The pores were capped with removable CdS or Fe_3O_4 nanoparticles through disulphide linkers that are selectively cleaved in a reducing environment. Release of encapsulated-FITC from magnetic nanoparticle-capped MCM-41 was observed in cancer cells due to the presence of a significant amount of intracellular DHLA.

pH-responsive nanomateials provide an alternate mechanism for release, relying on the relatively acidic condition inside tumor and inflamed tissues (pH ~ 6.8), and cellular compartments including endosomes (pH ~ 5.5-6) and lysosomes (pH ~ 4.5-5.0).[44] Toward this end, magnetic nanoparticles (Fe_3O_4) were covalently functionalized with doxorubicin (DOX), an anticancer drug, through an acid labile hydrazone linker.[45] The carrier was then encapsulated with a thermosensitive polymer for temperature controlled release of the drug. The hybrid system released DOX efficiently in mild acidic buffer solution of pH 5.3. Schoenfisch et al. have likewise shown that nitric oxide (NO) can be efficiently released at acidic pH from gold nanoparticles.[46]

Besides the surface chemistry of nanoparticles, the unique physical properties of nanoparticles have been utilized in the design of DDSs. Ford *et al.* have designed a water-soluble nanocontainer for NO storage based on electrostatic assembly of DHLA-coated quantum dots and cationic dinitro complexes that uses energy transfer from the core to release NO.[47] In another approach, doping of Ag/Au nanoparticles serves as an

antenna to absorb the energy from a laser beam of 'biologically friendly' near-infrared (NIR) region causing local heating and disruption of microcapsules. More recently, Bhatia *et al.* designed multifunctional superparamagnetic nanoparticles for remote release of bound drugs (Figure 1.5).[48] The particles transduce external electromagnetic force (EMF) at 350–400 kHz into local heating for melting DNA duplexes.

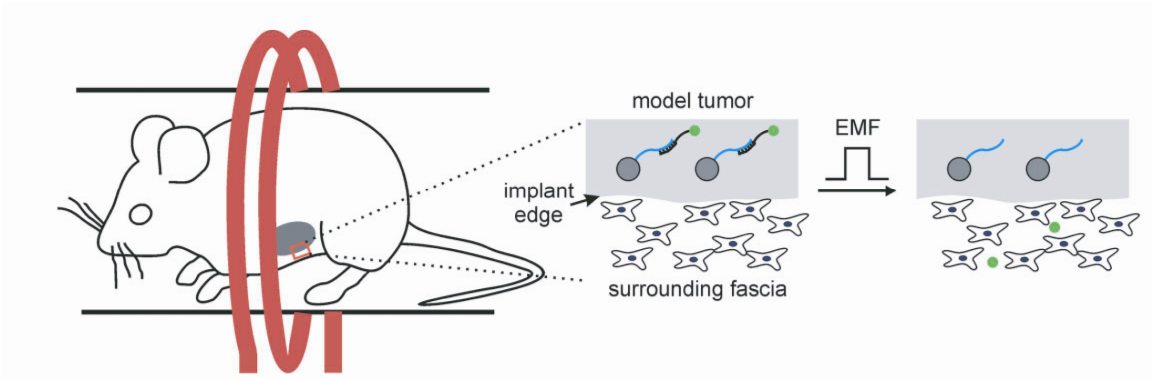

Figure 1.5: Controlled release of payloads using oligonucleotide-modified iron oxide nanoparticles for drug delivery at a remote location (ref. 48).

1.3.1 Nanoparticles as Delivery Vehicles of Biomolecules

Nanoparticles can provide effective carriers for biomolecules such as DNA, RNA, or protein, protecting these materials from degradation and transporting them across the cell-membrane barrier. 'Safe' delivery of these biomolecules provides a means of gene therapy as well as protein-based therapeutic approaches. Gene delivery vectors were designed using a series of cationic nanoparticles with different positive charge coverage and hydrophobicity.[49] In this study, NPs were incubated with a DNA plasmid encoding for β-galactosidase and then used to transfect embryonic kidney cells. Maximizing hydrophobicity without causing precipitation was found to play a key role in enhancing efficiency (Figure 1.6a-c). Building upon these studies, Klibanov *et al.* covalently

attached 2 kDa polyethylenimine (PEI2) onto the surface of gold nanoparticles.[50] The transfection efficiency of these systems varied with the PEI to gold molar ratio in the conjugates, with the best conjugate being 12 times more potent than the unmodified polycation. The efficiency of the delivery could be doubled by the addition of the *N*-dodecyl-PEI2 to the conjugate during complex formation, a further demonstration of the role of hydrophobicity in facilitating transfection. Lin et al. have recently reported mesoporus silica nanoparticles (MSNs)-mediated delivery of DNA into plants.[51]

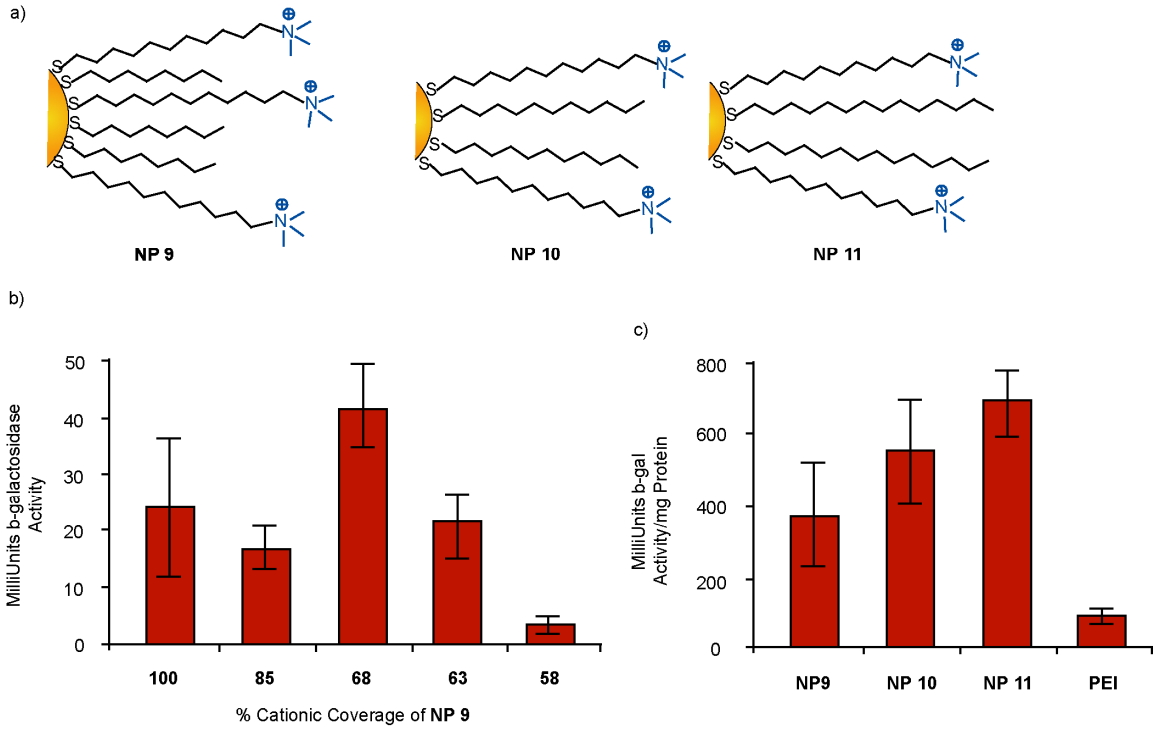

Figure 1.6: a) Structures of nanoparticles used for transfection by Rotello. b) β-Galactosidase transfection using various nanoparticle-DNA complexes at 2200:1. c) Transfection efficiency of nanoparticles **9**, **10**, **11** (2200:1 nanoparticle/DNA ratio) and PEI (60 kDa). All transfections were performed in the presence of 100 μM chloroquine and 10% serum.

In contrast to polycation-mediated transfection, cellular internalization of oligonucleotide functionalized gold nanoparticles carrying high negative surface potential

has emerged as a new approach to gene therapy.[52] Antisense nanoparticles (ASNP) were effective at low concentrations to suppress EGFP translation in C166 cells. Investigation on the mechanism of cellular uptake of ASNP revealed that endocytosis is initiated by adsorption of a large number of serum proteins onto the particle surface.[53]

We have functionalized the monolayer of gold nanoparticles with a photo-cleavable *o*-nitrobenzyl ester moiety that dissociates upon light irradiation to alter the surface potential from positive to negative, thereby releasing adsorbed DNA (Figure 1.7a),[54] as established *in cuvette* by a T7 RNA polymerase assay (Figure 1.7b). FITC-labeled DNA was successfully delivered into mammalian cells with nuclear localization of the released DNA (Figure 1.7c,d), an important requirement for genetic therapy.

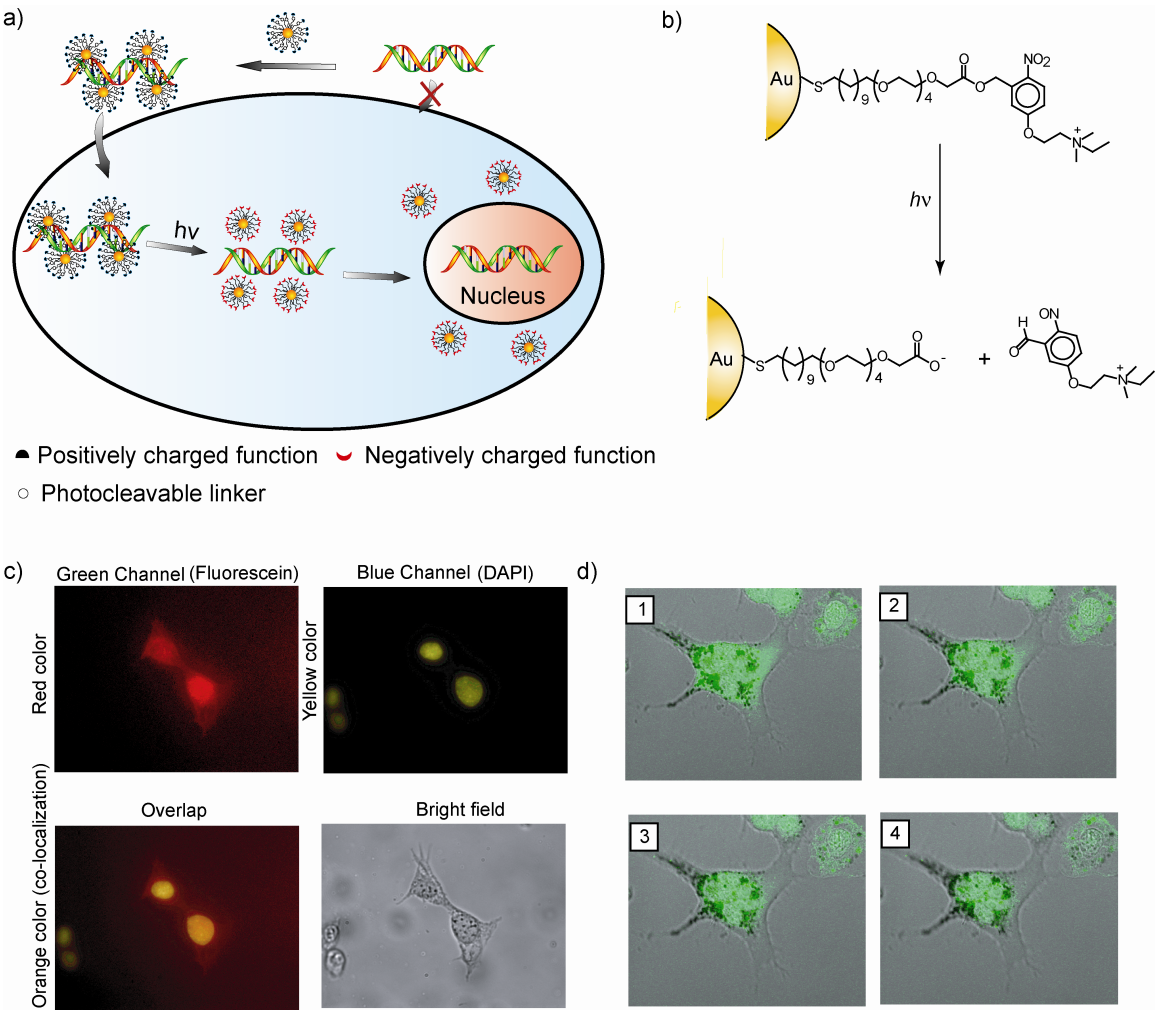

Figure 1.7: a) Depiction of photo-triggered release of DNA inside living cells. b) Illustration of light-induced surface transformation of nanoparticles. c) Fluorescence and bright field micrographs of cells after photo irradiation. To clarify the overlap of F-DNA and nuclei stain DAPI; green (Fluorescein) and blue (DAPI) channel are depicted with red and yellow color, respectively. d) Confocal microscopy images illustrating that the photo-released DNA accumulates inside the nucleus. Panel 1, 2, 3 and 4 show four consecutive slices of middle sections of z-series confocal images (Interval= 1.0 µm).

RNA technology has emerged as a potential tool for curing disease at an early stage. A small interfering RNA (siRNA), generally consisting of 19-21 base pairs, can efficiently silence expression of a gene of interest. For *in vitro* delivery, siRNA has been conjugated to variety of nanoparticles, such as gold,[55] quantum dots,[56] or iron oxide,[57] with a thiol linker. Moore *et al.* has designed a multi-functional superparamagnetic

nanoparticle that can: (1) carry the siRNA, (2) deliver it in a site-specific manner, and (3) probe the delivery by magnetic resonance and optical imaging.[57] The multifunctional nanoparticle was effective for *in vitro* and *in vivo* gene silencing via a specific pathway.

Protein delivery is complementary to nucleic acid therapies in the field of biomedicine. As described in section 1.2, nanoparticles can efficiently bind to proteins, and hence can be used as protein delivery systems. Lin *et al.* have fabricated MCM-41 type mesoporous silica nanoparticles (MSN) as protein carriers (Figure 1.8a).[58] These MSN particles can incorporate cytochrome *c*, a membrane-impermeable protein, into their large pores (diameter = 5.4 nm), and can slowly release the proteins in active form under physiological conditions.

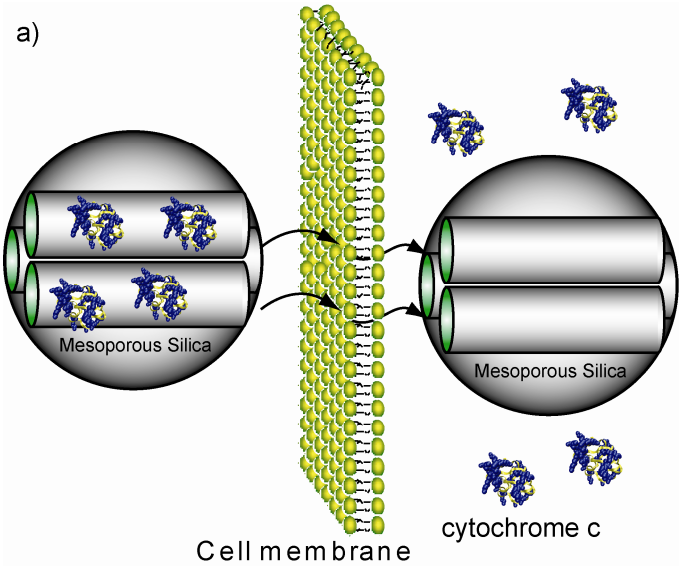

Figure 1.8: Schematic illustration of cellular delivery of cytochrome *c* using mesoporous silica nanoparticles.

1.4 Dissertation Overview

The monolayer structure and peripheral groups of nanoparticles (NPs) play crucial roles for their potential applications in therapy, sensing and imaging. During my PhD

work, I designed and synthesized functional particles and studied their interactions with biomolecules. These studies provided a background for using nanoparticles in delivery applications.

1.4.1 Functionalized Gold Nanoparticles for Surface Recognition

Protein and Peptide Surface. Disruption of protein-protein interactions through surface recognition using synthetic scaffolds provides a powerful tool for biomedical and clinical applications. In a model study, we aimed to interrupt the cytochrome c-cytochrome c peroxidase (Cyt c-CCP) binary adduct, which is formed mainly by ion-pairing at the interface.[59] To this end, cationic, anionic and neutral particles were synthesized. The functionalized nanoparticles interacted with proteins more strongly compared to the protein-protein interaction and bound selectively to either Cyt c or CCP based upon charge complementarity (Figure 1.9a and CHAPTER 2). The ubiquitous nature of protein-protein interactions based on α-helix recognition has contributed to the great interest in designing α-helix mimics as therapeutic modalities. We have demonstrated the nanoparticle-promoted folding of an anionic coiled-peptide into an α-helix in completely aqueous media. The strategy was to allow favorable electrostatic interactions between the nanoparticle and the peptide when the negatively charged residues were positioned in a cofacial manner along the helix. The monolayer was tailored via incorporation of tetraethylene glycol (TEG) unit to prevent non-specific interactions and the surface was decorated with trimethyl ammonium as an electrostatic recognition unit (Figure 1.9b and CHAPTER 2).[60]

DNA surface. DNA binding scaffolds are useful as gene regulators and transfection vectors. A library of nanoparticles functionalized with various amino acids

was fabricated for use in investigating the effects of different non-covalent interactions at the nanoparticle-DNA interface (Figure 1.9c and CHAPTER 3). This study indicated that particles with basic side chains interacted with DNA stronger than hydrophobic ones.[61]

Cell surface. A series of nanoparticles were synthesized and their cellular uptake efficiency was assessed.[62] Furthermore, in this study a method was developed for quick determination of cellular uptake of functionalized particles (Figure 1.9d and CHAPTER 4). The method was based on laser desorption/ionization mass spectrometry (LDI-MS). In this technique, the gold cores facilitated ionization of attached ligands whose mass-to-charge ratios (m/z) acted as "mass barcodes". This barcode technique allowed identification of a specific particle in presence of another. After treating cells with even four different NPs simultaneously, the relative uptake of individual particles was successfully quantified, demonstrating multiplexed screening ability of this method.

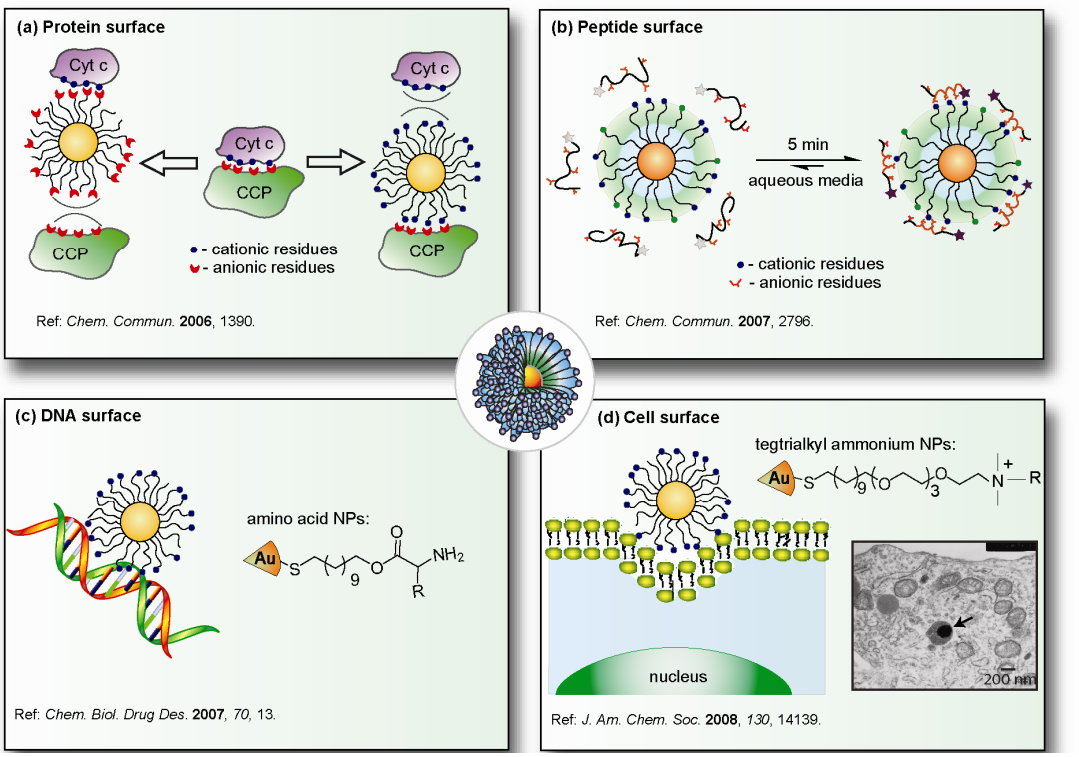

Figure 1.9: Functionalized gold nanoparticles for surface recognition. (a) Functionalized particles for effective recognition of protein surface and disruption of CCP:Cyt c couple.

(b) Nanoparticle-induced folding of a random coil peptide into α-helix in completely aqueous media. (c) Amino acid NPs and ammonium NPs to probe nanoparticle-DNA interactions. (d) Cellular uptake of functionalized nanoparticles. The TEM image showing cellular internalization of NPs.

1.4.2 Nanoparticles-Mediated Delivery of Therapeutics

DNA delivery. Transfection vectors were designed by varying the charge density on particle surfaces (Figure 1.10a and CHAPTER 5).[63] Efficient gene delivery was observed using lysine and lysine dendron functionalized particles without any apparent cytotoxicity. These amino acid-based nanoparticles were responsive to intracellular glutathione levels, providing a tool for controlled release and concomitant expression of DNA.

Protein delivery. In designing a vector for protein delivery, a peptide was tagged on the periphery of particles for protein recognition and subsequent cellular entry (Figure 1.10b and CHAPTER 6). These particles promoted intracellular delivery of β-galactosidase, a membrane-impermeable protein with high molecular weight (465 kDa).[64] Furthermore, these particles were able to transport functional proteins into a diverse array of cell lines and showed no obvious cytotoxicity.

Drug delivery. Zwitterionic gold particles were fabricated as a nanocarrier for small molecule drugs (Figure 1.10c and a brief discussion in CHAPTER 7).[65] We demonstrated that hydrophobic drugs and dyes could be encapsulated into hydrophobic pocket of NPs and stable nanoparticle-drug conjugates formed. The encapsulated drugs were released into cells via cell membrane mediated transportation. The released drug decreased the cell viability as expected, however, the particles were largely excluded from the cell body.

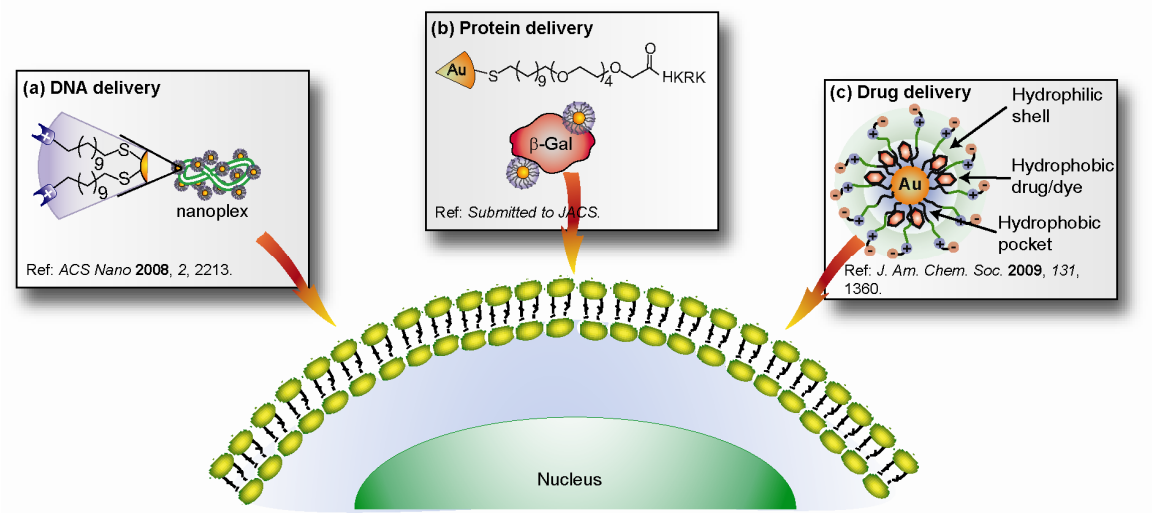

Figure 1.10: Functionalized gold nanoparticles for delivery applications. (a) Cationic nanoparticles condensed a large DNA into nanoplex and the complex efficiently transfected cells. (b) Peptide coated nanoparticles bound with proteins and showed protein transduction into mammalian cells. (c) Zwitterionic particles as a nanocarriers of hydrophobic drugs.

1.5 References

Notes

1. Peer, D.; Karp, J.; Hong, S.; Farokhzad, O.; Margalit, R.; Langer, R. *Nature Nanotech.* **2007**, *2*, 751.

2. Gao, X.; Cui, Y.; Levenson, R. M.; Chung, L. W. K.; Nie, S. *Nat. Biotechnol.* **2004**, *22*, 969.

3. Verma, A.; Rotello, V. M. *Chem. Commun.* **2005**, 303.

4. Ferrari, M. *Nat. Rev. Cancer* **2005**, *5*, 161.

5. Rosi, N. L.; Mirkin, C. A. *Chem. Rev.* **2005**, *105*, 1547.

6. Boisselier, E.; Astruc, D. *Chem. Soc. Rev.* **2009**, *38*, 1759.

7. Daniel, M. C.; Astruc, D. *Chem. Rev.* **2004**, *104*, 293.

8. Murphy, C. J.; Gole, A. M.; Stone, J. W.; Sisco, P. N.; Alkilany, A. M.; Goldsmith, E. C.; Baxter, S. C. *Acc. Chem. Res.* **2008**, *41*, 1721.

9. De, M.; Ghosh P. S.; Rotello, V. M. *Adv. Mater.* **2008**, *20*, 4225.

10. Niemeyer, C. M. *Angew. Chem., Int. Ed.* **2001**, *40*, 4128.

11. Sastry, M.; Rao, M.; Ganesh, K. N. *Acc. Chem. Res.* **2002**, *35*, 847.

12. Katz, E.; Willner, I. *Angew. Chem., Int. Ed.* **2004**, *43*, 6042.

13. Pellegrino, T.; Kudera, S.; Liedl, T.; Javier, A. M.; Manna, L.; Parak, W. J. *Small* **2005**, *1*, 48.

14. You, C. C.; De, M.; Rotello, V. M. *Curr. Opin. Chem. Biol.* **2005**, *9*, 639.

15. Caruso, F. *Adv. Matter.* **2001,** *13*, 11.

16. Naka, K.; Itoh, H.; Tampo, Y.; Chujo, Y. *Langmuir* **2003,** *19*, 5546.

17. Ghosh, S. S.; Kao, P. M.; McCue, A.W.; Chappelle, H. L. *Bioconjugate Chem*. **1990**, *1*, 71.

18. Droz, E.; Taborelli, M.; Descouts, P.; Wells, T. N. C.; Werlen, R. C. *J. Vac. Sci. Technol. B* **1996**, *14*, 1422.

19. Wang, J. *Anal. Chim. Acta* **2003**, *500*, 247.

20. Armitage, B. A. *DNA Binders and Related Subjects*, **2005**, *253*, 55.

21. Mahtab, R.; Harden, H. H.; Murphy, C. J. *J. Am. Chem. Soc.* **2000**, *122*, 14.

22. Lakowicz, J. R.; Gryczynski, I.; Gryczynski, Z.; Nowaczyk, K.; Murphy, C. J. *Anal. Biochem.* **2000**, *280*, 128.

23. McIntosh, C. M.; Esposito, E. A.; Boal, A. K.; Simard, J. M.; Martin, C. T.; Rotello, V. M. *J. Am. Chem. Soc.* **2001**, *123*, 7626.

24. Wang, G. L.; Zhang, J.; Murray, R. W. *Anal. Chem.* **2002**, *74*, 4320.

25. Mirkin, C. A.; Letsinger, R. L.; Mucic, R. C.; Storhoff, J. J. *Nature* **1996**, *382*, 607.

26. Blow, D. M. *Acc. Chem. Res.* **1976**, *9*, 145.

27. Fischer, N. O.; McIntosh, C. M.; Simard, J. M.; Rotello, V. M. *Proc. Natl. Acad. Sci. U. S. A.* **2002**, *99*, 5018.

28. Ramsden, J. J. *Q. Rev. Biophys.* **1993,** *27*, 41.

29. Fischer, N. O.; Verma, A.; Goodman, C. M.; Simard, J. M.; Rotello, V. M. *J. Am. Chem. Soc.* **2003**, *125*, 13387.

30. Love, J. C.; Estroff, L. A.; Kriebel, J. K.; Nuzzo, R. G.; Whitesides, G. M. *Chem. Rev.* **2005**, *105*, 1103.

31. Hong, R.; Fischer, N. O.; Verma, A.; Goodman, C. M.; Emrick, T.; Rotello, V. M. *J. Am. Chem. Soc.* **2004**, *126*, 739.

32. Jordan, B. J.; Hong, R.; Gider, B.; Hill, J.; Emrick, T.; Rotello, V. M. *Soft Matter* **2006**, *2*, 558.

33. Holmberg, A.; Blomstergren, A.; Nord, O.; Lukacs, M.; Lundeberg, J.; Uhlen, M. *Electrophoresis* **2005**, *26*, 501.

34. Zheng, M.; Huang, X. Y. *J. Am. Chem. Soc.* **2004**, *126*, 12047.

35. Hildebrandt, N.; Charbonniere, L. J.; Beck, M.; Ziessel, R. F.; Lohmannsroben, H. G. *Angew. Chem., Int. Ed.* **2005**, *44*, 7612.

36. Fazal, M. A.; Roy, B. C.; Sun, S. G.; Mallik, S.; Rodgers, K. R. *J. Am. Chem. Soc.* **2001**, *123*, 6283.

37. Xu, C. J.; Xu, K. M.; Gu, H. W.; Zhong, X. F.; Guo, Z. H.; Zheng, R. K.; Zhang, X. X.; Xu, B. *J. Am. Chem. Soc.* **2004**, *126*, 3392.

38. Abad, M. ; Mertens, S. F. L. ; Pita, M. ; Fernandez, V. M. ; Schiffrin, D. J. *J. Am. Chem. Soc.* **2005**, *127*, 5689.

39. Gu, H. W. ; Xu, K. M.; Xu, C. J. ; Xu, B. *Chem. Commun.* **2006**, 941.

40. Allen, T. M. ; Cullis, P. R. *Science* **2004**, *303*, 1818.

41. Hong, R.; Han, G.; Fernandez, J. M.; Kim, B. J.; Forbes, N. S.; Rotello, V. M. *J. Am. Chem. Soc*. **2006**, *128*, 1078.

42. Lai, C. Y.; Trewyn, B. G.; Jeftinija, D. M.; Jeftinija, K.; Xu, S.; Jeftinija, S.; Lin, V. S. Y. *J. Am. Chem. Soc.* **2003**, *125*, 4451.

43. Giri, S.; Trewyn, B. G.; Stellmaker, M. P.; Lin, V. S. Y. *Angew. Chem. Int. Ed.* **2005**, *44*, 5038.

44. Yang, Q.; Wang, S. H.; Fan, P. W.; Wang, L. F.; Di, Y.; Lin, K. F.; Xiao, F. S. *Chem. Mater*. **2005**, *17*, 5999.

45. Zhang, J.; Misra, R. D. K. *Acta Biomat.* **2007**, *3*, 838.

46. Polizzi, M. A.; Stasko, N. A.; Schoenfisch, M. H. *Langmuir* **2007**, *23*, 4938.

47. Neuman, D.; Ostrowski, A. D.; Absalonson, R. O.; Strouse, G. F.; Ford, P. C. *J. Am. Chem. Soc.* **2007**, *129*, 4146.

48. Derfus, A. M.; Maltzahn, G.; Harris, T. J.; Duza, T.; Vecchio, K. S.; Ruoslahti, E.; Bhatia, S. N. *Adv. Mater.* **2007**, *19*, 3932.

49. Sandhu, K. K.; McIntosh, C. M.; Simard, J. M.; Smith, S. W.; Rotello, V. M. *Bioconjugate Chem.* **2002**, *13*, 3.

50. Thomas, M.; Klibanov, A. M. *Proc. Natl. Acad. Sci. U. S. A.* **2003**, *100*, 9138.

51. Torney, F.; Trewyn, B. G.; Lin, V. S. Y.; Wang, K. *Nat. Nanotech.* **2007**, *2*, 295.

52. Rosi, N. L.; Giljohann, D. A.; Thaxton, C. S.; Lytton-Jean, A. K. R.; Han, M. S.; Mirkin, C. A. *Science* **2006**, *312*, 1027.

53. Giljohann, D. A.; Seferos, D. S.; Patel, P. C.; Millstone, J. E.; Rosi, N. L.; Mirkin, C. A. *Nano lett.* **2007**, *7*, 3818.

54. Han, G.; You, C. C.; Kim, B. J.; Turingan, R. S.; Forbes, N. S.; Martin, C. T.; Rotello, V. M. *Angew. Chem. Int. Ed.* **2006**, *45*, 3165.

55. Oishi, M.; Nakaogami, J.; Ishii, T.; Nagasaki, Y. *Chem. Lett.***2006**, *35*, 1046.

56. Derfus, A. M.; Chen, A. A.; Min, D. H.; Ruoslahti, E.; Bhatia, S. N. *Bioconjugate Chem.* **2007**, *18*, 1391.

57. Medarova, Z.; Pham, W.; Farrar, C.; Petkova, V.; Moore, A. *Nat. Med.* **2007**, *13*, 372.

58. Slowing, I. I.; Trewyn, B. G.; Lin, V. S. Y. *J. Am. Chem. Soc.* **2007**, *129*, 8845.

59. Bayraktar, H.; Ghosh, P. S.; Rotello, V. M.; Knapp, M. J. *Chem. Commun.* **2006**, 1390.

60. Ghosh, P. S.; Verma, A.; Rotello, V. M. *Chem. Commun.* **2007**, 2796.

61. Ghosh, P. S.; Han, G.; Erdogan, B.; Rosado, O.; Krovi, S. A.; Rotello, V. M. *Chem. Biol. Drug Des.* **2007**, *70*, 13.

62. Zhu, Z. J.; Ghosh, P. S.; Miranda, O. R.; Vachet, R. W.; Rotello, V. M. *J. Am. Chem. Soc.* **2008**, *130*, 14139.
63. Ghosh, P. S.; Kim, C. K.; Han, G.; Forbes, N. S.; Rotello, V. M. *Acs Nano* **2008**, *2*, 2213.

64. Ghosh, P.; Yang, X.; Arvizo, R.; Zhu, Z.-J.; Mo, Z.; Agasti, S. S.; Rotello, V. M. *Submitted to J. Am. Chem. Soc.*

65. Kim, C. K.; Ghosh, P.; Pagliuca, C.; Zhu, Z.-J.; Menichetti, S.; Rotello, V. M. *J. Am. Chem. Soc.* **2009**, *131*, 1360.

CHAPTER 2

NANOPARTICLE-PROMOTED FOLDING OF A RANDOM-COIL PEPTIDE INTO AN α-HELIX

2.1 Introduction

Protein-protein interactions are central to a number of cellular processes, such as signal transduction, cell adhesion, transcription and translation.[1,2,3] Disruption of their interactions by specific recognition using synthetic scaffolds provides a potent tool in biomedical and clinical applications.[4] In collaboration with the Knapp group (UMASS-Amherst), we have shown the ability of nanoparticles to interrupt protein-protein interactions targeting the cytochrome c-cytochrome c peroxidase (Cyt c-CCP) adduct as a model system (Figure 2.1).[5] The formation of this adduct is primarily driven by charge-pairing at the interface between basic Cyt C (pI = 10.3) and acidic CCP (pI = 5.3). The functionalized nanoparticles interacted with proteins more strongly compared to the protein-protein interaction and bound selectively to either Cyt c or CCP based on charge complementarity. We have published this work in *Chemical Communications* (**2006**, 1390-1392).

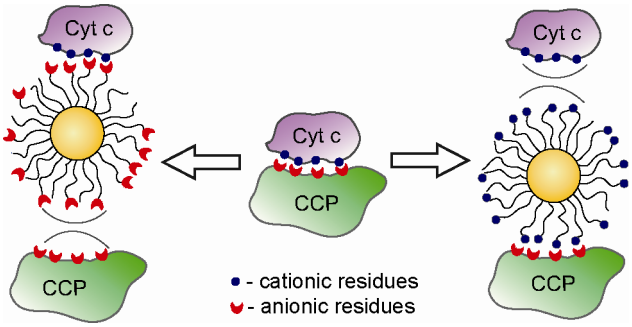

Figure 2.1: A schematic representation of effective recognition of protein surface and disruption of CCP:Cyt c adduct using functionalized particles.

Protein-protein interactions are site-specific and dictated through both non-covalent interactions and shape complementarity.[6] In several cases, the exposed face of a

helical segment interacts with another helical surface or a shallow cleft of the binding partner.[4] For example, hydrophobic residues on the helical surface of p53, a tumour suppressor, bind to a deep hydrophobic cleft of MDM2, an oncoprotein, via steric complementarity.[7] Therefore, the targeting of α-helices provides a promising tool for therapeutics.[8]

A short peptide fragment is very susceptible to proteolytic cleavage and also lacks appreciable secondary structure. The resistance to proteolytic cleavage can be improved by chemical modifications including amidation of the carboxy terminus and acylation of the amino terminus, or by incorporation of non-natural amino acids, such as D-amino acids and β-amino acids.[9,10] In general, the targeted peptide is designed such that the recognition units are positioned at alternating i, i + 3, i + 4 residues of the peptide backbone. Several synthetic strategies have been successfully developed to stabilize short peptides into α-helices. The strategies include the use of metal ion,[11] cyclodextrin dimers[12] and tetraguanidinium-based receptors.[13] However, significant stabilization of peptide α-helices by synthetic scaffolds in completely aqueous media is a challenging task.[14,15,16]

Nanoparticles offer a unique scaffold for biomolecule recognition by proper surface functionalization.[17,18,19] In preliminary studies we used trimethylammonium functionalized gold nanoparticles to stabilize a tetraaspartate peptide (**TAP**) into an α-helix in completely aqueous media.[20] These particles, however, are not biocompatible. Incorporaton of a tetra(ethylene glycol) (TEG) unit renders access to a biocompatible nanoparticle through: (a) increasing the water solubilty,[21] (b) prevention of non specific interactions with biomolecules,[22] and (c) controlled surface recognition.[23] In this chapter,

we have demonstrated stabilization of a peptide into an α-helix by functionalized nanoparticles with a TEG corona (Figure 2.2). Surprisingly, despite the highly flexible structure of the sidechains, these particles display templation to their peptide guests. These results have been reported in *Chemical Communications* (**2007**, 2796-2798).

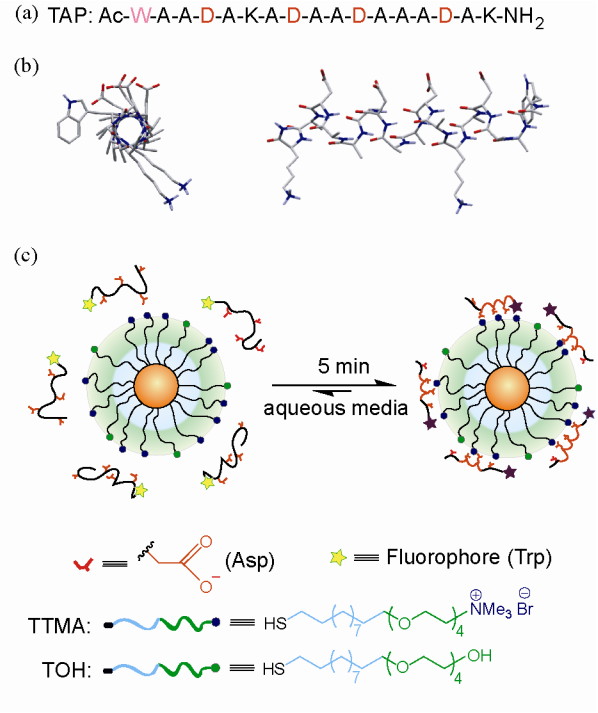

Figure 2.2: (a) Amino acid sequence of the target peptide. (b) End and side view of the tetraaspartate peptide. (c) Schematic depiction of the peptide binding in helical conformation on MMPC surface (shown in relative sizes).

2.2 Results and Discussion

The 17-amino acid peptide **TAP** was engineered such that four aspartate residues were placed at alternating i, i+3, and i+4 positions in order to orient them in one face once the peptide would fold into α-helix (Figure 2.2). The ends of the peptide were capped by acetylation of the amino terminus and amidation of the carboxy terminus to

decrease helix macrodipole effect. Moreover, a tryptophan (trp) residue was integrated at the N-terminal as a fluorescent probe.

Cationic gold mixed monolayer protected clusters (MMPCs) with 2 nm core were used to induce folding of the negatively charged peptide **TAP** into an α-helix. A series of nanoparticles bearing different charge densities on the surface were fabricated (Table 2.1). MMPC **1 – 3** were synthesized via Murray place exchange method[24] by adding different ratios of two ligands, cationic TEG--trimethyl ammonium (TTMA) and neutral TEG-hydroxy (TOH). Water-soluble MMPC **4** was prepared according to the literature procedures.[21]

Table 2.1: The series of nanoparticles used in this study and the percent of their cationic charge density.

Nanoparticles	TTMA : TOH	% of cationic charge
MMPC **1**	1 : 0	~ 100
MMPC **2**	1 : 0.43	~ 70
MMPC **3**	1 : 0.78	~ 55
MMPC **4**	0 : 1	0

The ability of MMPC **1** to induce helicity was monitored in aqueous solution (pH 11) using circular dichroism (CD). Varying concentrations (0 – 10 μM) of nanoparticle were mixed with 15 μM peptide solution, and CD spectra were collected after incubation for 5 min. CD spectra showed significant increase in helicity (maximum at 192 nm, minima at 208 nm and 222 nm) of the peptide in presence of the nanoparticle (Figure 2.3). The percent of helicity induction was calculated by curve fitting using DICHROWEB. The overall helicity was obtained by combining the regular helix and distorted helix. In the absence of nanoparticle, the peptide was in a random coil

conformation showing only ~3% of helicity. Upon addition of cationic MMPC **1** to the peptide solution, there was substantial degree of stabilization in helical conformation with maximum overall helicity up to ~80% (Figure 2.4).

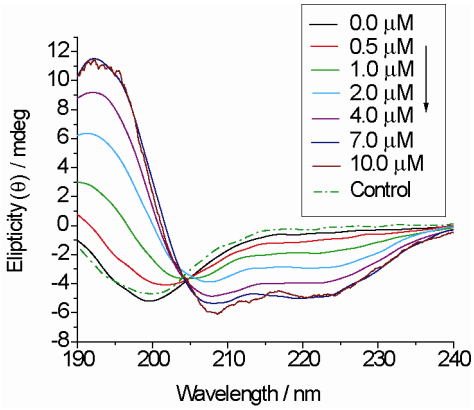

Figure 2.3: CD spectra of the peptide (15 μM) after adding MMPC **1** of various concentrations in water (pH 11).

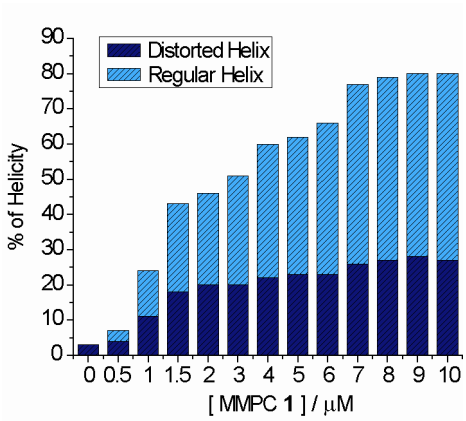

Figure 2.4: DICHROWEB analysis of the CD spectra. 15 μM peptide was titrated against MMPC **1** in pH 11 water: increase in overall helicity (regular and distorted) with increase in nanoparticle concentration.

In contrast, neutral particle (MMPC **4)** was unable to induce helicity in the peptide, which signifies that the recognition of peptide by nanoparticle receptor is due to charge pairing (See control in Figure 2.3). Likewise, addition of salt to the mixture of MMPC **1** and peptide disrupted their interaction resulting in a sharp decrease in helicity

(Figure 2.5), validating electrostatic self-assembly. The electrostatic interaction between particle and peptide was regulated by using MMPCs with different cationic charge density on the surface. CD experiments were performed to observe the effect of charge density on helicity induction. The spectra were obtained after incubation of each of these particles (6 μM) with 15 μM of peptide solution for 5 min and a pronounced change in helicity was observed (Figure 2.5). As expected, helicity decreases with decrease in charge density on the particle surface.

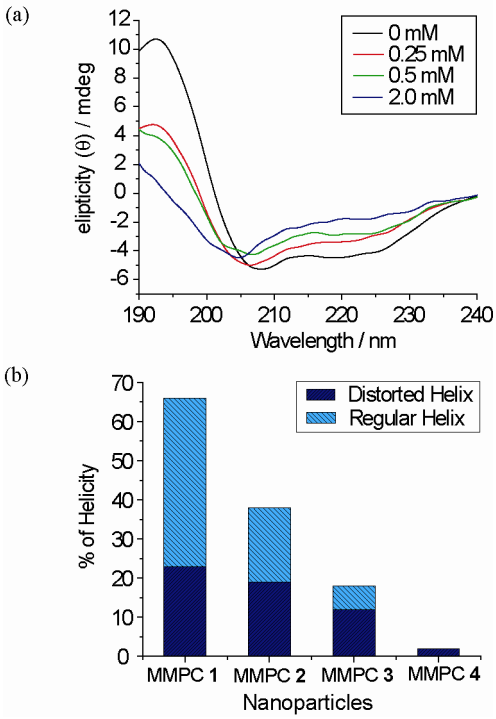

Figure 2.5: (a) CD spectra of a mixture of 15 μM peptide and 6 μM of MMPC **1** at different salt concentration. (b) Calculated overall helicity (regular and distorted) of 15 μM peptide in presence of 6 μM MMPCs in water of pH 11.

The binding affinity of the peptide with MMPCs **1**-**3** was further investigated by fluorescence. Trp-fluorescence was monitored by adding increasing amount of nanoparticle to the 2 μM peptide solution. Upon binding with the peptide, MMPCs quenched the fluorescence due to the gold core. The corrected fluorescence intensities (I /

I_0) were plotted against nanoparticle concentration and fitted with the binding equation (Figure 2.6). The calculated macroscopic binding constant (K_s) were similar for all of the cationic particles (Table 2.2) with ~5-6 peptides binding per particle. The results reflect that the energy required for conformational change is balanced by the favorable enthaply change due to ionic interaction.

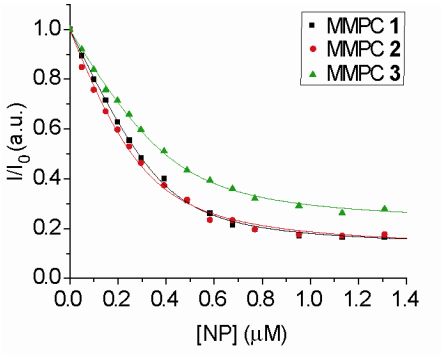

Figure 2.6: Binding curves of 2 μM peptide with different MMPCs from fluorescence titration in pH 11 water. Absorbance of nanoparticles was corrected using neutral MMPC **4**.

Table 2.2: Calculated macroscopic binding constant (K_s), Gibbs free energey change ($-\Delta G$), and binding ratio (n) for the complexation between peptide and cationic nanoparticles in pH 11 water, as determined via fluorescence (The error in binding constants and binding ratios were 25% and 5%, respectively).

Nanoparticles	K_s / 10^6 M^{-1}	$-\Delta G$ / kJ mol^{-1}	n
MMPC **1**	4.1	38.4	5.1
MMPC **2**	2.1	36.7	6.7
MMPC **3**	2.9	37.5	4.7

Gold colloids have the ability to template through maximization of binding enthalpy as the thiols are mobile on the self assembled monolayer (SAM) surface.[20,25] To determine if this was occurring with our particles, the peptide was incubated in the

presence of MMPCs over a period 24 h. As expected, no templation was observed in the case of MMPC **1** due to the complete coverage by the functional group. Significantly, MMPC **2** showed a 16% increase in helicity within a period of 24 h presumably due to the mobility of the ligands on the nanoparticle surface (Figure 2.7). Further decrease in the density of recognition unit for MMPC **3** resulted in no templation. This lack of templation presumably arises from the low concentration of ligands on the surface, increasing the entropic cost of templation.

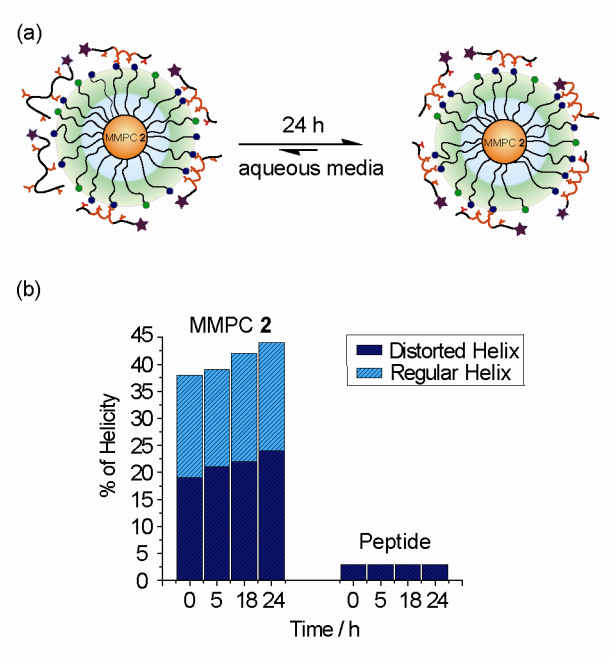

Figure 2.7: Particle-assisted templation of peptide: increase in helicity of TAP with time on incubation with MMPC **2**.

2.3 Conclusion

In summary, we have demonstrated stabilization of α-helices using nanoparticles featuring flexible TEG-terminated sidechains. The electrostatic interaction and hence the extent of helicity induction can be tuned by tailoring the monolayer of MMPCs. Finally, despite the high flexibility of the ligands, MMPC **2** shows templation of the particle

surface to the peptide. In addition to providing enhanced binding and helicity for target peptides, the observed templation highlights the preorganized nature of the nanoparticle monolayer. Clearly, structural information is transmitted via the highly flexible ligands from the particle surface to the terminus, a distance of ~ 3 nm.[26] The nature of this monolayer organization is an open question that a number of groups are exploring,[27,28] providing important insight for both pragmatic and fundamental purposes.

2.4 Experimental Section

General: All the reagents were purchased from Aldrich and used as received. All the recognition experiments were carried out in miliQ water of pH 11. Concentrations of the peptide and particle stock solutions were measured by UV.

Synthesis of ligands: Both the thiol ligands, teghydroxy (TOH) and tegtrimethyl ammonium (TTMA), were synthesized according to the literature procedure.[29,5]

Synthesis of MMPC 1 - 3: 1-pentanethiol-capped gold nanoparticles were dissolved in dichloromethane (DCM) and the ligands were dissolved in DCM alone (for MMPC **1**) or 1:1 DCM-methanol mixture (for MMPC **2** and **3**). Both the solution of particles and ligands were purged with argon separately for 30 min. Then two solutions were admixed and stirred at room temperature for ~ 48 h. MMPC **1** was precipitated out from the solution, while MMPC **2** and **3** remained in solution. In order to remove free ligands, MMPC **1** was washed five times with DCM by centrifugation, and MMPC **2** and **3** were dialyzed in distilled water for a day. The particles were dried and dissolved in D_2O to acquire NMR spectra. The percentage of cationic charge was calculated by NMR end group analysis.

Synthesis of peptide: The tetraaspartate peptide, **TAP**, was synthesized using the Fmoc chemistry-based solid-phase peptide synthesis technique. The crude peptide was purified by reverse-phase HPLC, and subsequently characterized by ESI mass spectrometry (M.W. = 1672.6).

Circular dichroism experiments: 15 μM of peptide with various concentrations of nanoparticles were taken in a quartz cuvette with a 1-mm path length and placed on a Jasco 720 spectrophotometer. After 5 min of equilibration at 23 ºC, CD spectra were acquired by scanning from 250 nm to 190 nm. Average of five scans was recorded at a rate of 20 nm/min with a sample interval of 0.1 nm and 8 sec response. The final spectra were obtained by subtracting the blank one and it was fitted into secondary structure algorithm CDSSTR (protein ref. set 7 comprising of 49 proteins) using DICHROWEB (http://www.cryst.bbk.ac.uk/cdweb/html/home.html). Neutral (TEG-OH) nanoparticle was used for the control experiment.

Fluorescence experiments: Fluorescence spectra were measured in a 1 cm quartz cuvette on a Shimadzu RF-5301 PC spectrofluorophotometer at 30 ºC. Trp fluorescence was monitored at 355 nm wavelength by exciting at 295 nm. 2 μM of peptide solution was titrated with MMPC **1** – **3** in milliQ water of pH 11. The quenching of Trp fluorescence by neutral MMPC **4** was measured to cancel the effect of absorption of nanoparticles. The corrected intensities were plotted against the nanoparticle concentration and fitted into a nonlinear least-squares curve-fitting equation[30] using Origin 7.0 program (Origin Lab Co., Northampton, USA).

2.5 References

Notes

1. Stites, W. E. *Chem. Rev.* **1997,** *97*, 1233.

2. Archakov, A. I.; Govorun, V. M.; Dubanov, A. V.; Ivanov, Y. D.; Veselovsky, A. V.; Lewi, P.; Janssen, P. *Proteomics* **2003,** *3*, 380.

3. Veselovsky, A. V.; Ivanov, Y. D.; Ivanov, A. S.; Archakov, A. I.; Lewi, P.; Janssen, P. *J. Mol. Recog.* **2002,** *15*, 405.

4. Fairlie, D. P.; West, M. L.; Wong, A. K. *Curr. Med. Chem.* **1998**, *5*, 29.

5. Bayraktar, H.; Ghosh, P. S.; Rotello, V. M.; Knapp, M. J. *Chem. Commun.* **2006**, 1390.

6. Jones, S.; Thornton, J. M. *Proc. Natl. Acad. Sci.U. S. A.* **1996**, *93*, 13.

7. Kussie, P. H.; Gorina, S.; Marechal, V.; Elenbaas, B.; Moreau, J.; Levine, A. J.; Pavletich, N. P. *Science* **1996**, *274*, 948.

8. D'Andrea, L. D.; Iaccarino, G.; Fattorusso, R.; Sorriento, D.; Carannante, C.; Capasso, D.; Trimarco, B.; Pedone, C. *Proc. Natl. Acad. Sci. U. S. A.* **2005**, *102*, 14215.

9. Fischer, P. M. *Curr. Protein Pep. Sci.* **2003**, *4*, 339.

10. Cheng, R. P.; Gellman, S. H.; DeGrado, W. F. *Chem. Rev.* **2001**, *101*, 3219.

11. Futaki, S.; Kiwada, T.; Sugiura, Y. *J. Am. Chem. Soc.* **2004**, *126*, 15762.

12. Wilson, D.; Perlson, L.; Breslow, R. *Bioorg. & Med. Chem.* **2003**, *11*, 2649.

13. Haack, T. ; Peczuh, M. W.; Salvatella, X.; Sanchez-Quesada, J. ; de Mendoza, J.; Hamilton, A. D. ; Giralt, E. *J. Am. Chem. Soc.* **1999**, *121*, 11813.

14. Orner, B. P.; Salvatella, X.; Quesada, J. S.; de Mendoza, J.; Giralt, E.; Hamilton, A. D. *Angew. Chem. Int. Ed.* **2002**, *41*, 117.

15. Tsou, L. K.; Tatko, C. D.; Waters, M. L. *J. Am. Chem. Soc.* **2002**, *124*, 14917.

16. Mito-Oka, Y.; Tsukiji, S.; Hiraoka, T.; Kasagi, N.; Shinkai, S.; Hamachi, I. *Tet. Lett.* **2001**, *42*, 7059.

17. Verma, A.; Rotello, V. M. *Chem. Commun.*, **2005**, 303.

18. Hazarika, P.; Kukolka, F.; Niemeyer, C. M. *Angew. Chem. Int. Ed.* **2006**, *45*, 6827.

19. Pasquato, L.; Pengo, P.; Scrimin, P. *J. Mat. Chem.* **2004**, *14*, 3481.

20. Verma, A.; Nakade, H.; Simard, J. M.; Rotello, V. M. *J. Am. Chem. Soc.* **2004**, *126*, 10806.

21. Kanaras, A. G.; Kamounah, F. S.; Schaumburg, K.; Kiely, C. J.; Brust, M. *Chem. Commun.* **2002**, 2294.

22. Zheng, M.; Davidson, F.; Huang, X. Y. *J. Am. Chem. Soc.* **2003**, *125*, 7790.

23. Hong, R.; Fischer, N. O.; Verma, A. ; Goodman, C. M.; Emrick, T.; Rotello, V. M. *J. Am. Chem. Soc.* **2004**, *126*, 739.

24. Templeton, A. C.; Wuelfing, M. P.; Murray, R. W. *Acc. Chem. Res.* **2000**, *33*, 27.

25. Boal, A. K.; Rotello, V. M. *J. Am. Chem. Soc.* **2000**, *122*, 734.

26. The length of TTMA ligand was calculated by using Schrodinger multi processing program in specific Maestro interface. The direct program used was Jaquar v.6.0. Calculations were done at 3.21G* basis set, using DFT, B3LYP. The calculated length was similar to the DLS data (reference 5).

27. Luedtke, W. D.; Landman, U. *J. Phy. Chem. B* **1998**, *102*, 6566.

28. Jackson, A. M.; Myerson, J. W.; Stellacci, F. *Nat. Mat.* **2004**, *3*, 330.

29. Palegrosdemange, C.; Simon, E. S.; Prime, K. L.; Whitesides, G. M. *J. Am. Chem. Soc.* **1991**, *113*, 12.

30. You, C. C.; De, M.; Han, G.; Rotello, V. M. *J. Am. Chem. Soc.* **2005**, *127*, 12873.

CHAPTER 3

AMINO ACID-FUNCTIONALIZED NANOPARTICLES AS DNA RECEPTORS

3.1 Introduction

Synthetic scaffolds that can recognize DNA effectively provide tools for treating various diseases of both genetic and acquired origin.[1] These receptors can recognize DNA via electrostatic interaction, intercalation or major/minor groove binding, thus controlling multiple cellular processes, such as replication and transcription.[2,3,4] Additionally, such materials featuring high affinity towards DNA can also be potential transfection vectors for transporting genetic materials (e.g. plasmid DNA, siRNA or decoy DNA) into living cells *in vitro* and *in vivo*.[5,6,7]

The large protein-DNA interface areas and the diversity of non-covalent interactions at the interface, such as electrostatic, hydrophobic, hydrogen-bonding and π-π interactions must be considered when designing synthetic receptors for DNA recognitions.[8,9] To this end, a variety of synthetic materials has been developed for DNA binding, including polymers,[10,11] dendrimers[12] and functional nanomaterials.[13] These systems have been designed to bind DNA in either non-specific or specific fashion, thus modulating both the structure and function of bound DNA molecules.[14,15]

Gold nanoparticles provide an alternate scaffold for efficient DNA recognition, exploiting both the size and controlled surface functionality of these systems.[16,17] In our earlier studies, we have demonstrated that trimethylammonium functionalized cationic nanoparticles bind with the phosphate backbone of DNA primarily through electrostatic interaction.[18] The binding affinity was high enough to inhibit the transcription by T7

RNA polymerase *in vitro*.[19] Moreover, these cationic nanoparticles facilitate transfection of DNA in mammalian cells.[20]

In addition to the electrostatic interaction between cationic nanoparticles and the phosphate backbone of DNA, other non-covalent interactions should have an important impact on DNA binding.[21] To explore the structural effects of the head groups on DNA binding, a library of cationic nanoparticles was fabricated via functionalization with naturally occurring L-amino acids (Figure 3.1). The structural diversity of amino acid side chains provides an additional handle to probe the effect of different noncovalent interactions in DNA binding. This study has been reported in *Chemical Biology & Drug Design* (**2007**, *70*, 13-18).

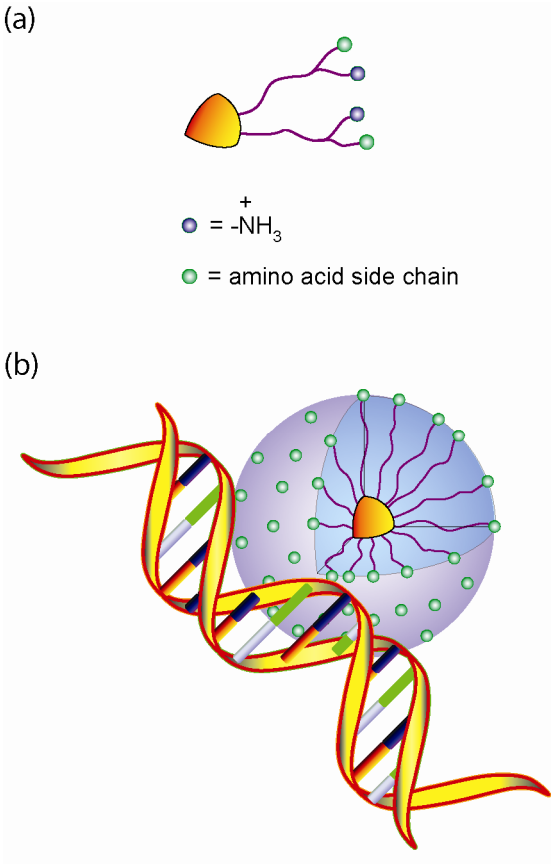

Figure 3.1: Schematic representation of (a) amino acid-functionalized nanoparticle and (b) interaction between DNA and amino acid-coated nanoparticle (drawn to scale).

3.2 Results and Discussion

Fabrication of amino acid functionalized nanoparticles. In this study, a series of amino acid conjugated nanoparticles was synthesized to provide structural diversity on the particle surface.[22] The structural diversity of these systems originates from the side chains of amino acids. The fabrication of nanoparticles was straightforward. The thiol ligands were synthesized in three steps with high yields (Figure 3.2). Trityl protected alcohol was prepared as the starting material for amino acid conjugation by reacting trityl thiol with 11-bromoundecanol. In the next step, the alcohol terminus was coupled to the free carboxylic acid of the boc-protected amino acid using DCC/DMAP. Deprotection was carried out using TFA/TIPS to simultaneously deprotect the thiol and amine groups at the termini of ligands. The thiols were incorporated onto the particle surface via the well known Murray place-exchange reaction with 1-pentanethiol coated gold nanoparticles (Figure 3.3).[23]

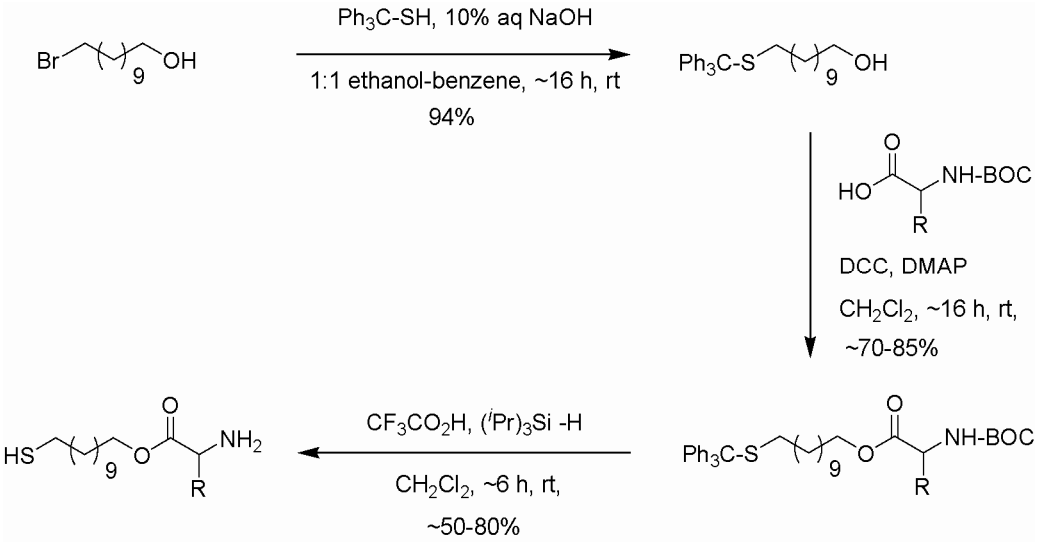

Figure 3.2: Synthesis of amino acid conjugated thiol ligands.

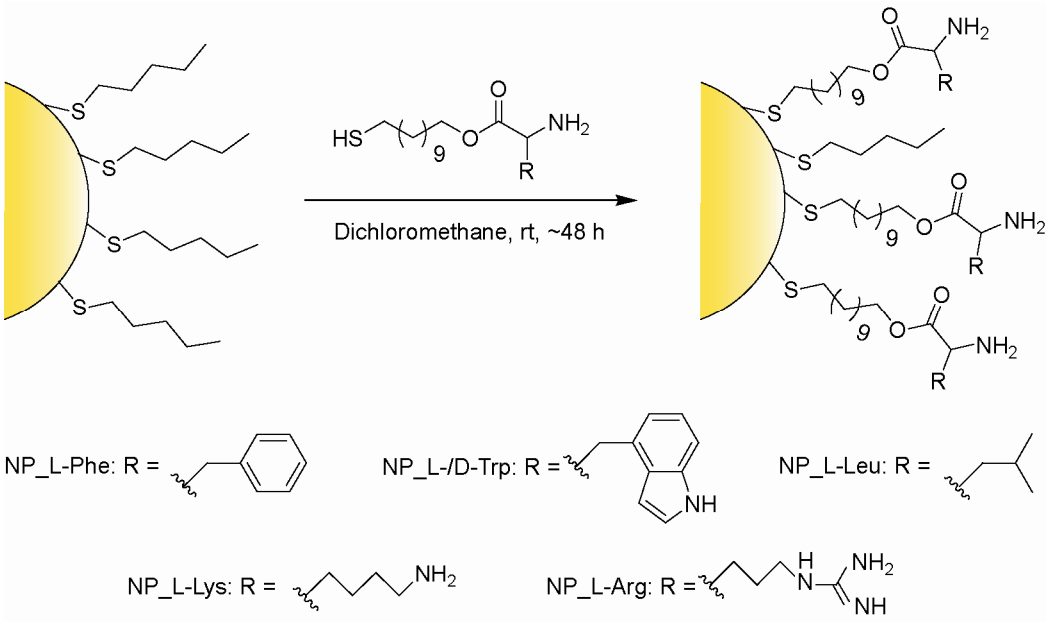

Figure 3.3: Fabrication of amino acid coated cationic nanoparticles through a place-exchange reaction.

Fluorescence titration. Fluorescence titrations were carried out to investigate the binding between DNA and nanoparticles. A FITC-labeled 37-mer DNA was used for these studies: the sequence consists of a promoter region (17 bases) recognized by T7 RNA polymerase and a template (20 bases) for RNA synthesis. Upon binding of the DNA to the particle surface, FITC-fluorescence was quenched due to energy transfer from the fluorophore to the gold core.[17] The effect of nanoparticle absorbance on the emission intensity was corrected using a non-interacting neutral TEG-OH nanoparticle.[22] The corrected intensities were plotted against nanoparticle concentrations. The binding constants and the stoichiometries of nanoparticle-DNA complexation (binding ratios) were determined by non-linear curve fitting (Figure 3.4).[22]

The calculated binding constants and binding ratios from the curve fitting are summarized in Table 3.1. Nanoparticles with cationic side chains have higher binding affinity for DNA compared to the nanoparticles bearing neutral hydrophobic side chains.

NP_L-Lys shows the strongest attraction towards DNA, ~ 3-fold higher than NP_L-Phe, the weakest one, indicating that the binding affinity can be varied moderately via functionalization of the nanoparticle surface. The trend in binding ratios indicates that the hydrophilic nanoparticles can accommodate more DNA on their surfaces than the hydrophobic particles. The results suggest that the electrostatic interaction dominates over hydrophobic interaction in nanoparticle-DNA interaction. Furthermore, we found that the chiral configuration of amino acid on nanoparticle surface does not influence the binding affinity towards DNA significantly (compare NP_L-Trp and NP_D-Trp in Table 3.1).

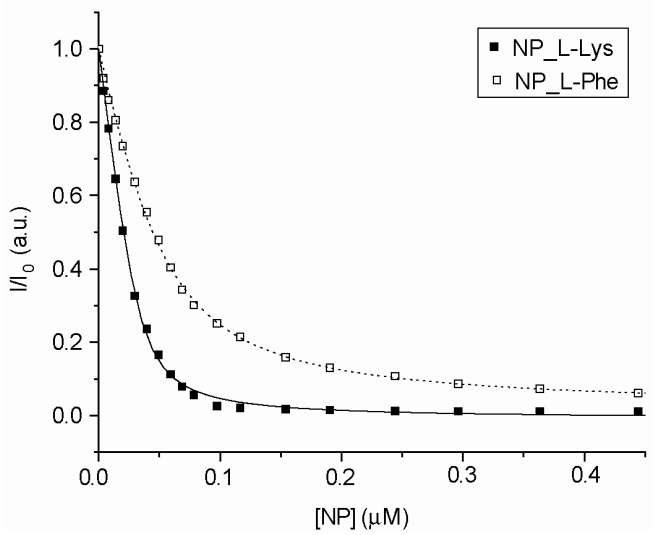

Figure 3.4: The binding curve of DNA (50 nM) with nanoparticles from fluorescence titration in 5 mM AcOH/NaOH buffer (pH = 5.0).

Table 3.1: The calculated binding constants (K_S) and binding ratios (n) of DNA-nanoparticle interaction from non-linear curve fitting.

Nature of side chain	Nanoparticles	K /10^6 M^{-1}	n
hydrophobic	NP_L-Phe	49	1.0
	NP_L-Trp	57	0.9
	NP_L-Leu	77	0.9
	NP_D-Trp	47	1.0
hydrophilic	NP_L-Lys	165	1.5
	NP_L-Arg	129	1.9

Circular dichroism. The conformational change of DNA upon interacting with the functionalized nanoparticles was investigated by circular dichroism. Recently, we have reported that quaternary ammonium-funtionalized nanoparticles change the CD signal of DNA to a substantial extent.[24] Similarly, the amine-terminated cationic nanoparticles in this study (e.g. NP_L-Phe) distort the DNA secondary structure (Figure 3.5a), as demonstrated by the decrease in ellipticity at 280 nm upon addition of nanoparticles. We continued our investigation on the structural changes of DNA with different amino acid-functionalized nanoparticles. CD spectra were collected after incubating DNA (0.25 μM) with amino acid functionalized nanoparticles. In the case of nanoparticles with hydrophobic side chains, the aromatic side chains (i.e. NP_L-Trp and NP_L-Phe) were found to unwind the DNA strand more effectively compared to the aliphatic sidechains (i.e. NP_L-Leu) (Figure 3.5b). This enhanced unwinding arises probably from π-π stacking of the aromatic rings on the sidechains with DNA bases.[25] For nanoparticles with hydrophilic side chains, NP_L-Arg perturbs the DNA structure more than NP_L-Lys (Figure 3.5c). This effect might be attributed to the possibility of

stable hydrogen bonding between the guanine moiety of arginine and interior DNA bases.[26]

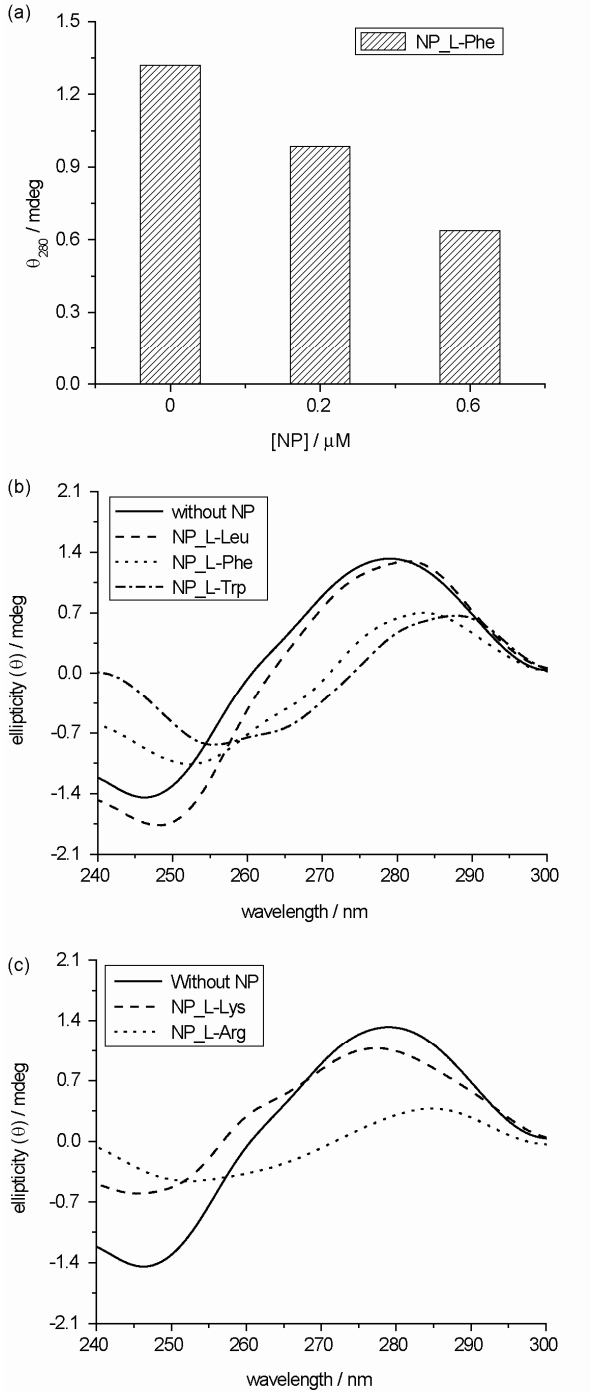

Figure 3.5: Circular dichroism spectra of 37-mer double stranded DNA (0.25 μM) in 5mM AcOH/NaOH buffer (pH = 5.0). (a) Decrease in elipticity at 280 nm (θ_{280}) upon

addition of cationic nanoparticles into DNA solution. Change in CD spectra of DNA by (b) hydrophobic nanoparticles and (c) hydrophilic nanoparticles ([NP] = 0.6 μM).

3.3 Conclusion

In conclusion, amino acid-functionalized gold nanoparticles provide a versatile scaffold for recognition of DNA. The binding affinity varies depending on the amino acid structure. Moreover, these nanoparticles perturb the DNA structure and the extent of unwinding depends on the amino acid sidechain. This study indicates that the efficiency of gene regulation or gene delivery can be modulated using this new class of nanoparticles featuring structural diversity.

3.4 Experimental Section

Materials. All chemicals were purchased from Aldrich and used as received. Solvents were bought from Pharmco-Aaper and used as received except dichloromethane and toluene which were distilled in presence of calcium hydride. The products were purified by column chromatography over silica gel (SiO_2, particle size 40-63 μm). Fluorescein Isothiocyanate (FITC) labeled DNA was purchased from Integrated DNA Technologies (IDT).

Ligand synthesis. *Preparation of tritylmercaptoundecanol.* A 60 ml solution of trityl thiol (13.2 g, 48 mmol) in 1:1 ethanol-benzene mixture was slowly added to a stirred solution (60 ml) of 11-bromoundecanol (10g, 40 mmol) in 1:1 ethanol-benzene mixture at room temperature. After cooling the reaction mixture to 0 °C, 10% aqueous NaOH solution (1.92 g, 48 mmol) was added into the flask and the reaction was continued overnight at room temperature. The solvents were removed *in vacuo* and

saturated sodium bicarbonate solution was added. The compound was extracted with dichloromethane. The organic layer was washed with brine, dried over anhydrous Na_2SO_4, and concentrated. The product was purified by flash column chromatography using a mixture of ethyl acetate and hexane (1:3, v/v) to afford the alcohol in 94% yield.

General procedure for the conjugation of amino acids. The free carboxylic acid of boc-amino acid (1.38 mmol, e.g. 366 mg Boc-L-Phenylalanine) was activated using *N*,*N*′-dicyclohexylcarbodiimide (DCC, 285 mg, 1.38 mmol) and 4-(dimethylamino) pyridine (DMAP, 168 mg, 1.38 mmol) in 20 ml of dry dichloromethane at 0 °C. After 10 min of stirring, the trityl protected alcohol (500mg, 1.12 mmol) was added. The reaction was continued overnight at room temperature. The white solid (dicyclohexylurea) was filtered out and the filtrate was washed with water. After evaporating the solvent, the residue was purified by flash chromatography on silica to yield the conjugated product (~70-85%).

General procedure for deprotection. The amino acid conjugated product (1 mmol, e.g. 690 mg of Trityl-S-C_{11}-Phe-Boc) was dissolved in 15 ml of dry distilled dichloromethane under argon. Addition of trifluoroacetic acid (TFA, 1.55 ml, 20 mmol) turned the solution yellow in color. The yellow color started to disappear after addition of triisopropylsilane (TIPS, 0.22 ml, 1.1 mmol). After 6 h, the reaction was quenched with water and extracted with dichloromethane. The organic layer was evaporated and the product was purified by column chromatography using 1:19 mixture (v/v) of methanol-dichloromethane (L-Leu, L-Phe and D-/L-Trp) or washing with hexane and diethylether (L-Lys and L-Arg).

Nanoparticle synthesis. *Amino acid functionalized nanoparticles.* As a general protocol, 50 mg of 1-pentanethiol protected gold nanoparticles (Au_C_5) and 100 mg of the thiol ligand were dissolved in dichloromethane in two separate vials. After purging both solutions with argon for 30 min, the ligand solution was poured into the particle solution. The place exchange reaction was continued for 48 h at room temperature. The amino acid-coated nanoparticles were precipitated out from the solution and the precipitate was purified by centrifugation using dichloromethane to remove the free thiols. NMR characterization of these particles in D_2O showed a high exchange of the new thiol and absence of any free ligands.

Au_TEG-OH. Tetraethylenglycol (TEG) coated neutral nanoparticle was prepared according to the literature procedure.[27]

Fluorescence titration. Fluorescence titration was carried out in a 1 cm quartz cuvette on a Shimadzu RF-5301 PC spectrofluorophotometer at room temperature (ca. 25 °C). FITC fluorescence of 50 nM DNA was monitored with addition of nanoparticle solution (4 μM NP + 50 nM DNA) in 5 mM AcOH/NaOH buffer (pH = 5.0) to ensure the complete protonation of amine groups on the particle surface. The fluorescence spectra were acquired from 490 nm to 600 nm after exciting the sample at 480 nm. The excitation and emission slit widths were 3 nm and 5 nm, respectively.

Circular dichroism. Circular dichroism (CD) experiments were performed on a Jasco 720 spectrophotometer in a 1 cm quartz cuvette. CD spectra of 0.25 μM DNA were collected with addition of nanoparticle solution (40 μM NP + 0.25 μM DNA) in 5 mM AcOH/NaOH buffer (pH = 5.0). After 5 min of equilibration at 25 °C, the spectra were

recorded as an average of three scans from 300 nm to 240 nm with 16 sec response and 10 nm/min scan rate. The final spectra were obtained after subtraction of the blank.

37-mer DNA sequence.

NMR data. In general, the proton (^{1}H) NMR spectra of all compounds were taken in $CDCl_3$ as a solvent in a 400 MHz NMR instrument.

Tritylmercaptoundecanol: δ (ppm) 7.39 (m, 6H), 7.25 (m, 6H), 7.17 (m, 3H), 3.62 (t, J = 7.4 Hz, 2H), 2.12 (t, J = 7.3 Hz, 2H), 1.53 (m, 2H), 1.37 (m, 16H).

Trit-S-C_{11}-L-Phe(Boc): δ (ppm) 7.40 (m, 6H), 7.25 (m, 9H), 7.18 (m, 3H), 7.12 (m, 2H), 4.98 (br, 1H), 4.55 (m, 1H), 4.05 (t, J = 6.8 Hz, 2H), 3.06 (m, 2H), 2.11 (t, J = 7.6 Hz, 2H), 1.56 (m, 2H), 1.40 (m, 11H), 1.24 (m, 14H).

Trit-S-C_{11}-L-Leu(Boc): δ (ppm) 7.40 (m, 6H), 7.25 (m, 6H), 7.19 (m, 3H), 4.85 (br, 1H), 4.29 (m, 1H), 4.08 (t, J = 7.6 Hz, 2H), 2.12 (t, J = 7.2 Hz, 2H), 1.61 (m, 5H), 1.42 (s, 9H), 1.25 (m, 16H), 0.93 (t, J = 3.2 Hz, 6H).

Trit-S-C_{11}-L-Trp(Boc): δ (ppm) 7.56 (m, 1H), 7.41 (m, 6H), 7.26 (m, 8H), 7.20 (m, 4H), 7.10 (m, 1H), 5.08 (br, 1H), 4.64 (m, 1H), 4.04 (m, 2H), 3.28(m, 2H), 2.13 (t, J = 7.6 Hz), 1.52 (m, 4H), 1.42 (s, 9H), 1.21 (m, 14H).

Trit-S-C_{11}-D-Trp(Boc): δ (ppm) 7.56 (m, 1H), 7.41 (m, 6H), 7.27 (m, 8H), 7.20 (m, 4H), 7.10 (m, 1H), 5.06 (br, 1H), 4.64 (m, 1H), 4.04 (m, 2H), 3.29(m, 2H), 2.13 (t, J = 7.6 Hz), 1.52 (m, 4H), 1.42 (s, 9H), 1.21 (m, 14H).

Trit-S-C_{11}-L-Lys$(Boc)_2$: δ (ppm) 7.40 (m, 6H), 7.28 (m, 6H), 7.20 (m, 3H), 5.10 (br, 1H), 4.62 (m, 1H), 4.28 (br, 1H), 4.12 (t, J=6.4 Hz, 2H), 3.11 (m, 2H) , 2.13 (t, J = 7.2 Hz, 2H), 1.82 (m, 2H), 1.56 (m, 2H), 1.55-1.16 (m, 38H).

Trit-S-C_{11}-L-Arg$(Boc)_2$: δ (ppm) 7.40 (m, 6H), 7.28 (m, 6H), 7.20 (m, 3H), 5.40 (br, 1H), 4.28 (m, 1H), 4.12 (t, J=6.4 Hz, 2H),3.90(m, 2H), 2.13 (t, J = 7.2 Hz, 2H), 1.82-1.16 (m, 40H).

HS-C_{11}-L-Phe: δ (ppm) 7.25 (m, 3H), 7.19 (m, 2H), 4.10 (t, J = 7.4 Hz, 2H), 3.73 (m, 1H), 2.97 (m, 2H), 2.50 (q, 2H), 1.59 (m, 4H), 1.26 (m, 14H).

HS-C_{11}-L-Leu: δ (ppm) 4.13 (t, J = 7.6 Hz, 2H), 3.61 (t, J = 8.1 Hz, 1H), 2.52 (q, 2H), 1.77 (m, 1H), 1.61 (m, 4H), 1.31 (m, 16H), 0.94 (t, J = 6.3Hz, 6H).

HS-C_{11}-L-Trp: δ (ppm) 7.62 (m, 1H), 7.35 (m, 1H), 7.12 (m, 3H), 4.08 (t, J = 7.6 Hz, 2H), 3.83 (m, 1H), 3.13 (m, 2H), 2.51 (q, 2H), 1.60 (m, 4H), 1.26 (m, 14H).

HS-C_{11}-D-Trp: δ (ppm) 7.42 (m, 1H), 7.28 (m, 1H), 7.09 (m, 3H), 4.10 (m, 1H), 3.96 (m, 2H), 3.35 (m, 2H), 2.51 (q, 2H), 1.56 (m, 4H), 1.32 (m, 14H).

HS-C_{11}-L-Lys: δ (ppm) 4.12 (m, 2H), 4.02 (m, 1H) , 3.03 (m,2H), 2.50 (m, 2H), 1.90-1.16 (m, 24H).

HS-C_{11}-L-Arg: δ (ppm) 4.12 (m, 2H), 3.68 (m, 2H), 3.20 (m, 1H) ,2.50 (m, 2H), 1.90-1.16 (m, 22H).

3.5 References

Notes

1. Verma, I. M.; Somia, N. *Nature* **1997**, *389*, 239.

2. Zadmard, R.; Schrader, T. *Angew. Chem. Int. Ed.* **2006**, *45*, 2703.

3. Blanco, J. B.; Vazquez, O.; Martinez-Costas, J.; Castedo, L.; Mascarenas, J. L. *Chem.-A Eur. J.* **2005**, *11*, 4171.

4. Kielkopf, C. L.; Baird, E. E.; Dervan, P. D.; Rees, D. C. *Nat. Struct. Biol.* **1998**, *5*, 104.

5. Boussif, O.; Lezoualch, F.; Zanta, M. A.; Mergny, M. D.; Scherman, D.; Demeneix, B.; Behr, J. P. *Proc. Natl. Acad. Sci.* U.S.A. **1995**, *92*, 7297.

6. Kakizawa, Y.; Furukawa, S.; Kataoka, K. *J. Control Release* **2004**, *97*, 345.

7. Greenland, J. R.; Liu, H. N.; Berry, D.; Anderson, D. G.; Kim, W. K.; Irvine, D. J.; Langer, R.; Letvin, N. L. *Mol. Ther.* **2005**, *12*, 164.

8. Jantz, D.; Amann, B. T.; Gatto, G. J.; Berg, J. M. *Chem. Rev.* **2004**, *104*, 789.

9. Vazquez, M. E.; Caamano, A. M.; Mascarenas, J. L. *Chem. Soc. Rev.* **2003**, *32*, 338.

10. Wang, C.; Ge, Q.; Ting, D.; Nguyen, D.; Shen, H. R.; Chen, J. Z.; Eisen, H. N.; Heller, J.; Langer, R.; Putnam, D. *Nature Mater*. **2004**, *3*, 190.

11. Thomas, M.; Lu, J. J.; Ge, Q.; Zhang, C. C.; Chen, J. Z.; Klibanov, A. M. *Proc. Natl. Acad. Sci. U.S.A.* **2005**, *102*, 5679.

12. Luo, D.; Haverstick, K.; Belcheva, N.; Han, E.; Saltzman, W. M. *Macromolecules* **2002**, *35*, 3456.

13. Chowdhury, E. H.; Akaike, T. *Curr. Gene Ther.* **2005**, *5*, 669.

14. Nguyen-Hackley, D. H.; Ramm, E.; Taylor, C. M.; Joung, J. K.; Dervan, P. B.; Pabo, C. O. *Biochemistry* **2004**, *43*, 3880.

15. Oyoshi, T.; Kawakami, W.; Narita, A.; Bando, T.; Sugiyama, H. *J. Am. Chem. Soc.* **2003**, *125*, 4752.

16. Thomas, M.; Klibanov, A. M. *Proc. Natl. Acad. Sci. U.S.A.* **2003**, *100*, 9138.

17. Han, G.; You, C. C.; Kim, B. J.; Turingan, R. S.; Forbes, N. S.; Martin, C. T.; Rotello, V. M. *Angew. Chem. Int. Ed.* **2006**, *45*, 3165.

18. McIntosh, C. M.; Esposito, E. A.; Boal, A. K.; Simard J. M., Martin, C. T., Rotello, V. M. *J. Am. Chem. Soc.* **2001**, *123*, 7626.

19. Han, G.; Chari, N. S.; Verma, A.; Hong, R.; Martin, C. T.; Rotello, V. M. *Bioconjugate Chem.* **2005**, *16*, 1356.

20. Sandhu, K. K.; McIntosh, C. M.; Simard, J. M.; Smith, S. W.; Rotello, V. M. *Bioconjugate Chem.* **2002**, *13*, 3.

21. Dervan, P. B. *Bioorg. & Med. Chem.* **2001**, *9*, 2215.

22. You, C. C.; De, M.; Han, G.; Rotello, V. M. *J. Am. Chem. Soc.* **2005**, *127*, 12873.

23. Hostetler, M. J.; Templeton, A. C.; Murray, R. W. *Langmuir* **1999**, *15*, 3782.

24. Goodman, C. M.; Chari, N. S.; Han, G.; Hong, R.; Ghosh, P.; Rotello, V. M. *Chem. Biol. & Drug Design* **2006**, *67*, 297.

25. Kikuta, E.; Murata, M.; Katsube, N.; Koike, T.; Kimura, E. *J. Am. Chem. Soc.* **1999**, *121*, 5426.

26. Hermann, T.; Patel, D. J. *Science* **2000**, *287*, 820.

27. Kanaras, A. G.; Kamounah, F. S.; Schaumburg, K.; Kiely, C. J.; Brust, M. *Chem. Commun.* **2002**, 2294.

CHAPTER 4

LASER DESORPTION/IONIZATION MASS SPECTROMETRY (LDI-MS): A NEW TOOL FOR SCREENING CELLULAR UPTAKE OF NANOPARTICLES

4.1 Introduction

Therapeutic nanocarriers carry drugs, genes, and/or imaging agents into cells and tissues of interests.[1-4] Various materials, such as polymeric micelles,[5] mesoporous silica nanorods,[6] carbon nanotubes,[7] and nanoparticles[8-10] have been used as therapeutic nanocarriers, as well as probes for tracking intracellular processes. Effective use of nanoparticles as carriers and intracellular probes requires the ability to monitor these particles in cells, and several techniques are available for this purpose. These techniques can be classified into two groups: (1) label-free imaging techniques such as luminescent quantum dots imaging,[10,11] atomic force microscopy (AFM),[12] and transmission electron microscopy (TEM)[13] and (2) barcoding techniques such as those that encode nanoparticles with fluorescence dyes that can be "read out" by a fluorescence spectrometer.[2] Simultaneous screening of the cellular uptake of multiple particles with different surface functional groups, however, is a challenge for existing approaches. Here, we have described a new "mass barcoding" technique for monitoring the cellular uptake of multiple functionalized gold nanoparticles (AuNPs) by using laser desorption/ionization mass spectrometry (LDI-MS).

Nanoparticles have been used in mass spectrometric analyses primarily to facilitate the laser desorption/ionization of compounds of interest. Tanaka et al[14] showed that cobalt particles (~30 nm) suspended in glycerol facilitated the ionization of proteins. Subsequently, Ag,[15] Au,[16-22] C,[23] and Si[24,25] nanomaterials have been demonstrated as

LDI-MS matrices with different degrees of success. Meanwhile, some mass spectrometric work has also been devoted to the analysis of nanoparticles themselves. For pure samples of gold nanoparticles, electrospray ionization mass spectrometry (ESI-MS)[26,27] and LDI-MS[28,29] have been used to measure the compositions of surface functionalities and atom numbers in the NP core.

In this study, we tagged AuNPs with readily ionizable surface functionalities, i.e. "mass barcodes" (shown in Figure 4.1). These alkanethiolate cationic or neutral monolayers are barriers between the nanoparticle core and the environment, effectively protecting and stabilizing the gold cluster core in biological environments.[30-32] Moreover, the chemical nature of these monolayers dictates interfacial interactions between cells and AuNPs, thus governing cellular uptake of AuNPs.[33-35] Upon laser irradiation of these AuNPs, "mass barcodes" of alkanethiolate monolayers rather than the AuNPs themselves, can be simply "read out" by LDI-MS, thus providing characteristic peaks for identifying AuNPs. Ionization of alkanethiolate monolayers on flat gold surfaces has also been observed using LDI[36,37] and matrix-assisted LDI (MALDI).[38,39] The surface ligands on the AuNPs are primarily detected because the NP core efficiently absorbs the laser light (337 nm), and this energy is readily transferred to desorb and ionize the surface ligands, probably via a mechanism similar to that proposed by Tanaka.[14] In this work, we investigated a potential advantage of such a "mass barcoding" approach – the ability to simultaneously analyze many different functionalized AuNPs. We predicted that each functionalized AuNP could be identified by its unique "mass barcode". Furthermore, we explored this LDI strategy for direct analyses of AuNPs taken up by cells. Such a multiplexed screening of AuNPs could be very valuable for rapidly assessing the

chemical and physical parameters that influence AuNP uptake by cells. We have published these results recently in *Journal of the American Chemical Society* (**2008**, *130*, 14139-14143).

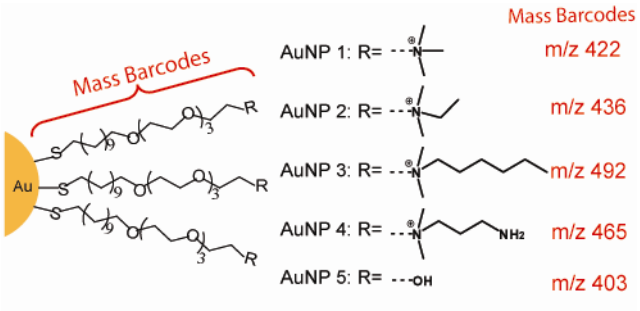

Figure 4.1: Structural representation of the gold nanoparticles (AuNPs). The mass-charge-ratios (m/z) attached to each AuNP act as "mass barcodes" used for identification of the AuNPs.

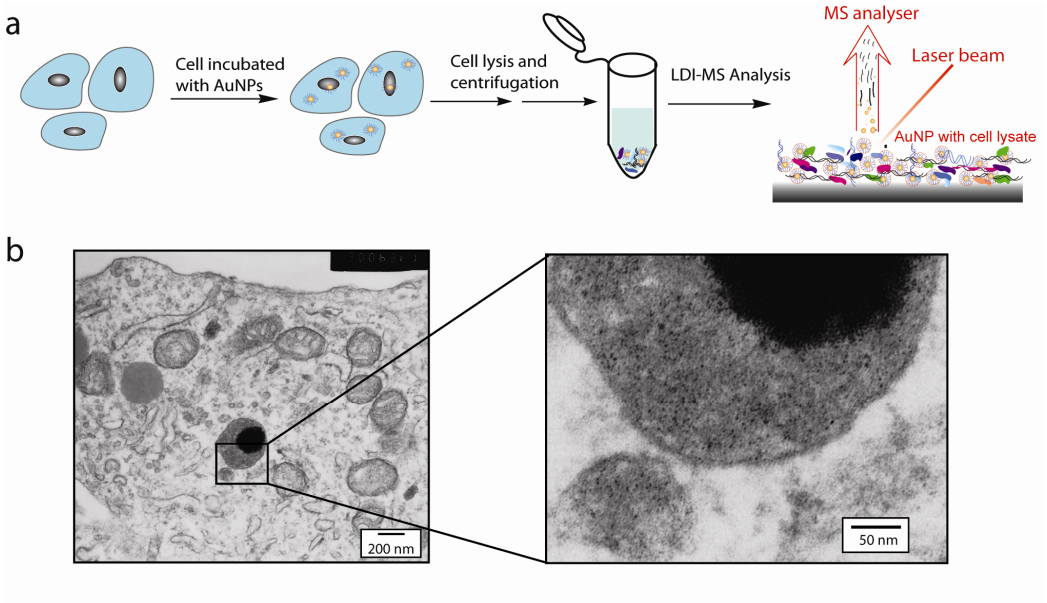

Figure 4.2: (a) Schematic illustration of the analysis of the AuNPs in cell lysates by laser desorption/ionization mass spectrometry (LDI-MS). (b) Transmission electron microscopy (TEM) images of cellular uptake of AuNP **1.**

4.2 Results and Discussion

To explore the viability of "mass barcodes" for determining uptake efficiency of AuNPs, we cultured monkey kidney cells (COS-1) with AuNPs (500 nM) for 6 h (Figure 4.2a). This concentration of AuNPs was non-toxic to the cells,[40] and indeed after 6 h of incubation, no cell morphology change was observed. The cells were washed three times with cold phosphate-buffered saline (PBS) to remove extra AuNPs that were not taken up by the cells. Before lysing the cells, transmission electron microscopy (TEM) was used to verify the cellular uptake of AuNPs. As shown for a single cell (Figure 4.2b), a large amount of gold nanoparticles was trapped in vesicles (most likely via endosomal entrapment) in the cytoplasm, which was in agreement with results from other groups.[13,41,42] It is possible that some AuNPs have escaped from the vesicles, and that depends on the NP surface functionalities.[42,43] However, no such evidence was found in the TEM images. After the cells were lysed, the AuNPs taken up by the cells were collected as part of the precipitate after centrifugation of the lysate. The precipitate was subjected to LDI-MS, and spectra similar to that shown in Figure 4.3a were obtained. Figure 4.3a illustrates the characteristic peaks that were observed for AuNP **1**. The spectrum of AuNP **1** showed an ion at m/z 422, which corresponds to the molecular ion (M^+) of the ligand attached to AuNP **1**. The spectrum also had a peak at m/z 388, which corresponds to $[M\text{-}H_2S]^+$, m/z 197 and 394, which correspond to Au^+ and Au^{2+}, respectively, and m/z 184, which corresponds to the head-group fragment of one of the most abundant lipids in animal cell membranes – phosphatidylcholine (PC). Moreover, a series of peaks spaced by 14 Da from m/z 262 to m/z 360 indicated successive losses of CH_2 units from the alkyl chains of the surface ligands. Each of the other AuNPs in this

study had similar mass spectral patterns, with each AuNP featuring different m/z ratios allowing identification.

The different "mass barcodes" of each AuNP facilitated multiplexed screening by LDI-MS. After simultaneously exposing cells to two different types of AuNPs, LDI-MS analysis of the resulting cell lysate indicated that both AuNPs can be readily identified. For example, in Figure 4.3b, diagnostic molecular ions at m/z 422 and m/z 436 indicated the cellular uptake of AuNP **1** and AuNP **2**, respectively. Other characteristic peaks, such as $[M\text{-}H_2S]^+$ (m/z 388 for AuNP **1** and m/z 402 for AuNP **2**), also assisted the identification of two AuNPs.

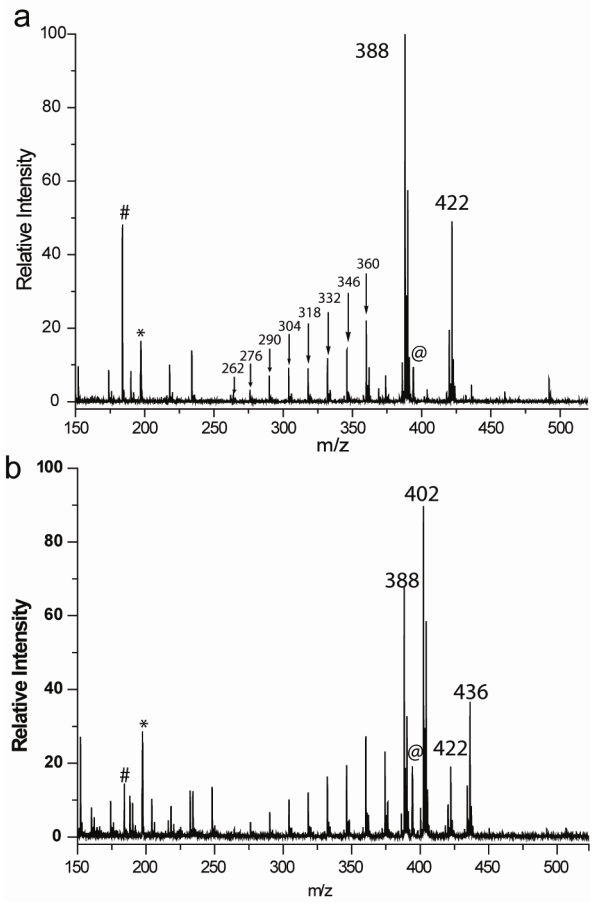

Figure 4.3: LDI mass spectrum of COS-1 cell lysate after uptake of (a) AuNP **1** and (b) AuNP **1** and AuNP **2**. m/z 422 and m/z 436 correspond to the molecular ion (M^+) of the ligands attached to AuNP **1** and AuNP **2**, respectively; "*" is Au^+ (m/z 197); "@" is Au_2^+

(m/z 394); "#" is the molecular ion corresponding to the head-group fragment of phosphatidylcholine (m/z 184).

Quantifying the relative cellular uptake of these two different AuNPs should be possible by comparing the ion abundances of their respective molecular ion peaks. To do so, however, the relative ionization efficiencies of the ligands in cell lysates must be considered. The ionization efficiencies of the surface ligands were investigated under two sets of control conditions. First, equimolar amounts of AuNP **1** and AuNP **2** (300 pmol each) were directly analyzed by LDI-MS, indicating that the ligands on AuNP **2** were ionized more readily as indicated by a molecular ion abundance ratio (AuNP **2**/AuNP **1**) of 1.79 ± 0.04. Then equimolar amounts of AuNP **1** and AuNP **2** (300 pmol each) were mixed with cell lysates and analyzed by LDI-MS, and again, the surface ligands on AuNP **2** were more readily ionized, giving rise to a molecular ion abundance ratio (AuNP **2**/AuNP **1**) of 1.41 ± 0.09 (Table 4.1). Since the data from the second set of experiments was more comparable to the cell uptake experiments, the ion abundance ratio of 1.41 can be used to determine the relative quantity of the AuNPs taken up by the cells. After correcting the experimentally observed ratio of 1.70 ± 0.14 (Figure 4.3b and Table 4.1) by the ratio observed from the analysis of the cell lysates, the cellular uptake of AuNP **2** was determined to be 1.21 (± 0.13) times greater than AuNP **1**. A similar analysis can be done for each of other AuNPs in comparison to AuNP **1** (Figure 4.4 and Table 4.1).

Table 4.1: LDI-MS relative quantification of cellular uptake of AuNPs (**1-5**).

	Mass barcodes (m/z)	Control Ratio[a]	Experimental Ratio[b]	Relative Ratio[c]
AuNP **2** / AuNP **1**	436 / 422	1.41 ± 0.09	1.70 ± 0.14	1.21 ± 0.13
AuNP **3** / AuNP **1**	492 / 422	0.72 ± 0.08	0.40 ± 0.10	0.50 ± 0.20
AuNP **4** / AuNP **1**	465 / 422	0.19 ± 0.05	0.21 ± 0.03	1.10 ± 0.30
AuNP **5** / AuNP **1**	369 / 388	0.26 ± 0.05	0.09 ± 0.02	0.34 ± 0.09

[a] 300 pmol of each AuNP was mixed with 300 pmol AuNP **1** in lysed COS-1 cells and subjected to LDI-MS analysis. [b]300 pmol of each AuNP was mixed 300 pmol AuNP **1** and then cultured with living COS-1 cells. These cells were then washed, lysed, and analyzed by LDI-MS. [c]Relative ratios are generated by comparing experimental ratios with control ratio.

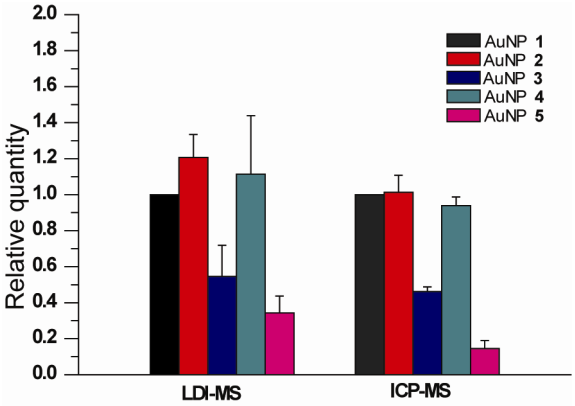

Figure 4.4: Relative quantities of the AuNPs in COS-1 cell lysates determined by LDI-MS and ICP-MS. In both cases, the AuNP amounts are normalized to AuNP **1**.

The relative uptake amounts of each AuNP provided by the LDI-MS data were validated using inductively coupled plasma mass spectrometry (ICP-MS). ICP-MS provides high sensitivity and robustness for elemental analysis,[13] but it lacks the capacity to identify AuNPs with different surface functionalities. So, the cellular uptake amounts of each AuNP had to be determined separately (see experimental section for details). The relative uptake amounts for each AuNP (compared to AuNP **1**) as determined by ICP-MS (Figure 4.4) were very similar to the LDI-MS data, indicating that LDI-MS can reliably

provide the relative quantities of each AuNP taken up by COS-1 cells. Interestingly, the similarity of the ICP-MS data, which was acquired after uptake of individual AuNPs, and the LDI-MS data, which was acquired after uptake of two different AuNPs, indicated that interactions between the AuNPs in their cellular uptake were minimal.

Taken as a whole, the quantitative data in Figure 4.4 indicated that AuNP **2** and AuNP **4** were more readily taken up by COS-1 cells than AuNP **3** and AuNP **5**. The exact mechanism by which the AuNP were taken up by the cells is probably complex and is still an active area of investigation. Nonetheless, several factors have been recognized to govern the cellular uptake efficiency of nanoparticles, such as size,[13,41] shape,[13] and surface properties.[12,33-35] Since the cell membrane is negatively charged, positively charged nanoparticles are generally found to have higher uptake efficiencies.[33,35] So, it was perhaps not surprising that AuNP **5** with its neutral surface was less readily taken up by the cells than the cationic AuNP (**1**-**4**).[33,35] While taken up more efficiently than AuNP **5**, the four cationic NPs (AuNP **1** through AuNP **4**) all exhibited slightly different uptake efficiencies. From this limited set of AuNPs, it is difficult to conclude what other factors control uptake, but surface ligand hydrophobicity might be an important parameter. AuNP **3** was the most hydrophobic of the cationic AuNPs, and it was least efficiently taken up by the COS-1 cells. Obviously, more work is needed to better understand the effect of hydrophobicity on AuNP cell uptake, and this mass barcode approach along with LDI-MS detection will be helpful in this regard.

To ensure that the results in Table 4.1 and Figure 4.4 do not simply reflect different AuNP stabilities in a cellular environment, the AuNPs were kept in cell lysate for different periods of time before analysis by LDI-MS. As an example, equal amounts

of AuNP **1** and AuNP **2** (300 pmol each) were incubated with cell lysate for different amounts of time, and the relative ratios between the two nanoparticles were found to remain steady for up to 24 hrs (Figure 4.5), which indicated that these two nanoparticles have essentially the same stability in the cellular environment.

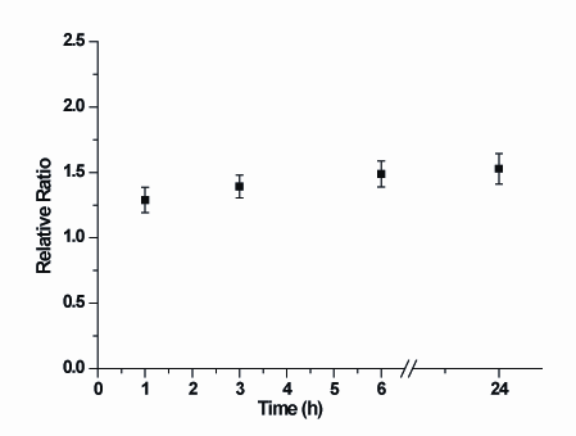

Figure 4.5: Stability of AuNPs in the cellular environment. Equal amounts of AuNP **1** and AuNP **2** (300 pmol each) were incubated with cell lysate for different times. Relative ratios of AuNP **2**/AuNP **1** were calculated by comparing intensities of m/z 436 and m/z 422 in spectra.

We also investigated the sensitivity of our LDI-MS approach by culturing COS-1 cells with differing amounts of AuNPs. We found that AuNPs present at levels as low as 30 pmol (50 nM) in cell cultures could be readily detected. Figure 4.6 illustrates this for experiments with AuNP **1**. The characteristic peak for AuNP **1** was readily apparent m/z 422 with a signal-to-noise ratio of 75. With such good signal, we feel that the AuNPs could be detected even when present at even lower amounts.

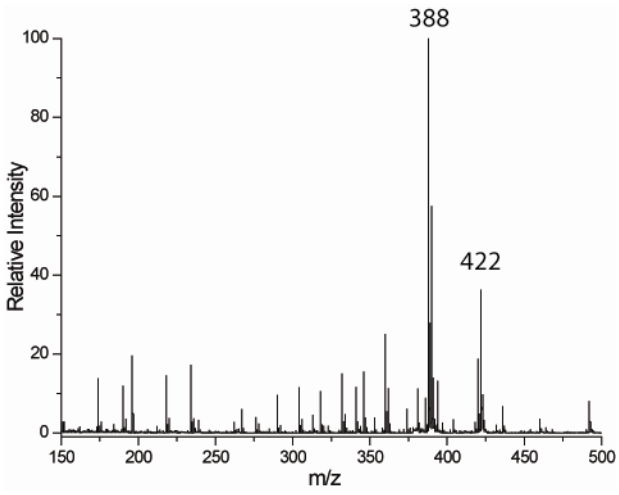

Figure 4.6: LDI mass spectrum of COS-1 cell lysate after uptake of 30pmol AuNP **1** (50nM AuNP **1** in 600uL culture solution). Peak m/z 422 has a signal-to-noise ratio 75.

A key advantage of the LDI-MS measurements over the ICP-MS measurements or other measurements is the ability to simultaneously identify and quantitate the uptake of multiple AuNPs. To demonstrate the advantages of such a multiplexed analysis, COS-1 cells were cultured with four cationic AuNPs (AuNP **1-4**) (300 pmol each), and the resulting cellular contents were analyzed by LDI-MS (Figure 4.7a). Diagnostic molecular ions peak at m/z 422, m/z 436, m/z 492, and m/z 465 indicated the presence of AuNP **1**, AuNP **2**, AuNP **3**, and AuNP **4** respectively. The relative quantities of each AuNP (Figure 4.7b) indicated that AuNP **2** was the most readily taken up by the cells, while AuNP **3** was the least readily taken up, quite similar to the results in Figure 4.4. The slight differences might be explained by an increase in the total amount of AuNPs present in the experiments. This increase may have caused uptake competition between the AuNPs, causing AuNP **4**, for example, to be taken up less readily.

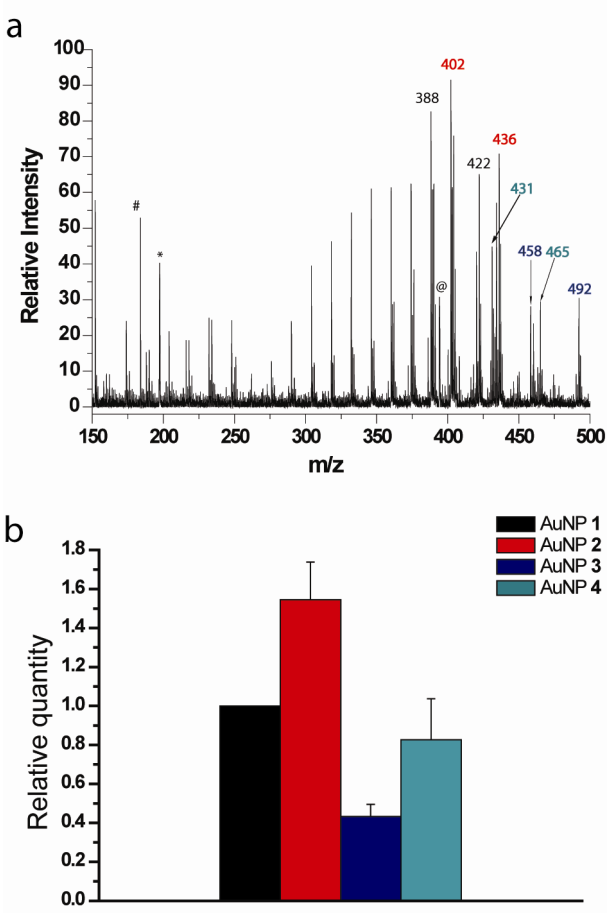

Figure 4.7: (a) Multiplexed LDI mass spectrum of COS-1 cell lysate with the four cationic AuNPs (AuNP **1-4**). m/z 422, m/z 436, m/z 492 and m/z 465 correspond to AuNP **1**, AuNP **2**, AuNP **3**, and AuNP **4**, respectively; notations: "*","@", "#" are same as in Figure 4.3. (b) Relative amounts of AuNPs (**1-4**) obtained from the LDI-MS. The AuNP amounts are normalized to AuNP **1**.

4.3 Conclusion

In conclusion, we have described the use of AuNPs with mass barcodes for the multiplexed screening of AuNP cellular uptake. We demonstrated that the relative quantities of 4 different AuNPs taken up by cells can be simultaneously determined using LDI-MS with this approach. We also found that the cellular uptake of the functionalized AuNPs was dependent on NP surface functionality, suggesting that differential cellular uptake and cell-specific targeting might be possible if the appropriate surface

functionalities are chosen. In the future, we plan to use this technique to evaluate differential AuNP uptake by different cell states (e.g. normal and diseased). A future improvement will be to combine the LDI-MS approach with sub-cellular fractionation. This combination should be able to identify the intracellular targets for the AuNPs. On the whole, this LDI-MS technique has great potential for both the development of AuNP-based delivery vectors and for probing transport of nanomaterials *in vitro* and *in vivo*.

4.4 Experimental Section

AuNP 1-5 synthesis. The Brust-Schiffrin two phase synthesis method[31] was used for synthesis of AuNPs with core diameters around 2 nm. After that, the Murray place-exchange method was used to obtain functionalized AuNPs **1-4** (Figure 4.8).[30,32] AuNP **5** was synthesized using one phase reduction method as reported.[31]

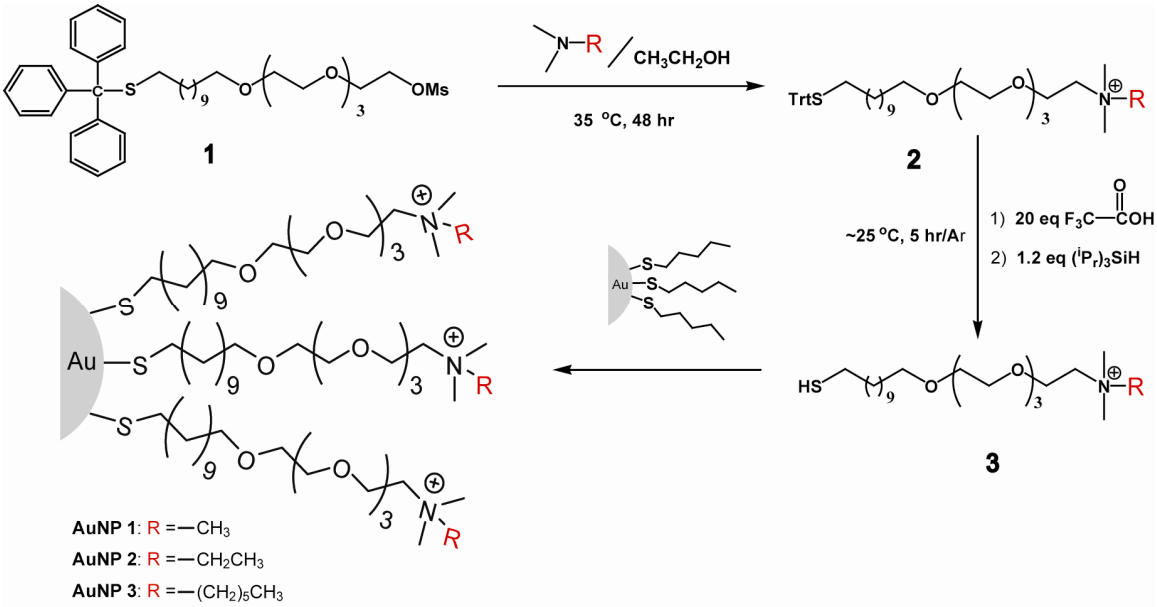

Figure 4.8: General scheme for synthesis of cationic gold nanoparticles (AuNP **1-3**).

Cell culture and cellular uptake of AuNPs. Monkey kidney COS-1 cells (75,000 cells/well) were grown on a 24-well plate in high-glucose Dulbecco's Modified Eagle Medium (DMEM; glucose (4.5 gL^{-1})) containing 4-(2-hydroxyethyl)-1-piperazineethanesulfonic acid (HEPES) buffer (pH 7.4, 25 mM) supplemented with fetal bovine serum (FBS, 10%, Aldrich). Cultures were maintained at 37 °C under a humidified condition with 5% CO_2. After 24 h of plating, the cells were washed once with cold phosphate-buffered saline (PBS), and the solutions of nanoparticles (Table 4.2) were added. Following 6 h of incubation, the cells were washed three times with PBS to remove extra nanoparticles and lysed for 15 minutes with a lysis buffer according to the kit from GENLANTIS. A quick freeze/thaw cycle (freeze 2 h at -20 °C then thaw at room temperature) was performed to improve lysis. The lysed cells were then prepared for LDI-MS or ICP-MS analyses. For screening of four cationic nanoparticles (AuNP **1- 4**) simultaneously, the COS-1 cells were plated on a 6-well plate with (75000 × 4.8) cells/well. The cells were treated in manner similar to that mentioned above. A mixture of four AuNPs (Table 4.2) was added into each well and incubated for 6 h.

Control experiments for quantification: COS-1 cells were first lysed, and then the solutions of nanoparticles in PBS only (Table 4.3) were added into each well and kept in the incubator for 6 h. The amount of nanoparticles and sample preparations were the same as described above except that no media was added.

Table 4.2: Gold nanoparticles solution preparation for cellular uptake of AuNPs.

Nanoparticles	Nanoparticles Solutions	(Vol. and Conc.)/well
(a) Individual AuNP	100 μl of 3 μM AuNP in PBS + 500 μl of DMEM	600 μl 500 nM AuNP
(b) Mixture of two AuNPs (AuNP **1** with AuNP **2-5**)	50 μl of 6 μM NP **1** in PBS + 250 μl of DMEM AND 50 μl of 6 μM NP **2**or NP **3** or NP **4** or NP **5** in PBS + 250 μl of DMEM	600 μl 500 nM AuNP **1** AND 500 nM AuNP **2** or AuNP **3** or AuNP **4** or AuNP **5**
(c) Mixture of four AuNP (AuNP**1-4)**	100 μl of 3 μM AuNP (**1-4**) in PBS + 500 μl of DMEM; then mix these four solution	2.40ml 125 nM AuNP **1** and AuNP **2** and AuNP **3** and AuNP **4**

Table 4.3: Gold nanoparticles solution preparation for control experiments for quantification

Nanoparticles	Nanoparticles Solutions
(a) Mixture of two AuNPs (AuNP **1** with AuNP **2-5**)	50 μl of 6 μM AuNP **1** in PBS AND 50 μl of 6 μM AuNP **2** or AuNP **3** or AuNP **4** or AuNP **5** in PBS
(b) Mixture of four AuNP (AuNP **1-4)**	100 μl of 3 μM AuNP (**1-4**) in PBS

Cell TEM: Cells were treated with AuNP **1** (1μM NP of 600μl solution per well in a 24-well plate) and washed with PBS buffer after 6 hrs. Then cells were removed from the plate by trypsinization and centrifuged to collect a pellet. The pellet was fixed with 2% gluteraldehyde for 30 min and postfixed with 1% OsO_4 for 1 hr. OsO_4 is highly

poisonous and must be used with extreme caution! Following agarose (1.5%) enrobing, Spurr's resin embedding, and ultrathin (50 nm) sectioning, the samples were stained with 2% aqueous uranyl acetate and 25 mg/ml lead citrate. The image was taken under a JEOL 100S microscope.

LDI-MS instrumentation: The sensitivity experiments were performed on a Waters Micromass M@LDI L/R mass spectrometer. All other LDI-MS analyses were done on a Bruker Reflex III time-of-flight mass spectrometer. The Bruker Reflex III is equipped with a 337-nm nitrogen laser, a 1.0-m flight tube, and a stainless steel sample target. All mass spectra were acquired in reflectron mode using a voltage of 16 kV. All reported spectra represent an average of 50 shots acquired at 90% laser power. The accelerating voltage was set to 20 kV. The Waters instrument was operated with positive reflection mode. Pulse voltage was set to 2400 V, source 15 000 V, MCP 1850 V. Matrix suppression delay was set to m/z 100. The spectrum represents an average of 50 shots acquired at 70% high laser power.

LDI-MS sample preparation and measurements: The lysed cells were centrifuged at 14000 rpm for 10 min. AuNPs precipitated together with the cell lysates were washed with 60% acetonitrile/ 40% water, applied directly to a stainless steel target, and allowed to dry. The dry samples were washed again on the target with 60% acetonitrile/40% water and then allowed to dry before LDI analysis. Each AuNP experiment was performed in triplicate, and at least 5 spots of each replicate were measured by LDI-MS.

ICP-MS Instrumentation: All ICP-MS measurements were performed on a Perkin Elmer Elan 6100. Operating conditions of the ICP-MS are listed below: RF

power: 1200 W; plasma Ar flow rate: 15 L/min; nebulizer Ar flow rate: 0.96 L/min; isotopes monitored: ^{197}Au and ^{103}Rh (as an internal standard); dwell time: 50 ms; nebulizer: cross flow; spray chamber: Scott.

ICP-MS sample preparation and measurements: Each AuNP was incubated with COS-1 cells separately as described above (Table 4.2). After incubation and lysing the cells, the resulting cell lysate was digested overnight using 3 mL of HNO_3 and 1 mL of H_2O_2. On the next day, 3 mL of aqua regia, which is highly corrosive and must be used with extreme caution, was added, and then the sample was allowed to react for another 1-2 h. A hot plate (~100 °C) was used to reduce the above digested solution down to 1-2 mL. The concentrated sample solution was then diluted to 100 mL with de-ionized water, and aqua regia and a ^{103}Rh internal standard solution were also added. The final AuNP sample solution contained 5% aqua regia and 10 ppb ^{103}Rh. The AuNPs sample solution was measured by ICP-MS under the operating conditions described above. Cell uptake experiments with each AuNP were repeated 3 times, and each replicate was measured 10 times by ICP-MS. A series of gold standard solutions (20, 10, 5, 2, 1, 0.5, 0.2, 0 ppb) were prepared before each experiment. Each gold standard solution contained 5% aqua regia and 10 ppb ^{103}Rh. Each standard solution was measured 10 times by ICP-MS using the operating conditions described above. The resulting calibration line was used to determine the gold amount in taken up by the cells in each sample. A ~100 ppm solution of dithiothreitol was used to wash the instrument between analyses to facilitate gold removal.

4.5 References

1. Peer, D.; Karp, J. M.; Hong, S.; Farokhzad, O. C.; Margalit, R.; Langer, R. *Nat. Nanotech.* **2007**, *2*, 751.

2. Rosi, N. L.; Giljohann, D. A.; Thaxton, C. S.; Lytton-Jean, A. K. R.; Han, M. S.; Mirkin, C. A. *Science* **2006**, *312*, 1027.

3. Michalet, X.; Pinaud, F. F.; Bentolila, L. A.; Tsay, J. M.; Doose, S.; Li, J. J.; Sundaresan, G.; Wu, A. M.; Gambhir, S. S.; Weiss, S. *Science* **2005**, *307*, 538.

4. Han, G.; You, C.-C.; Kim, B.-J.; Turingan, R. S.; Forbes, N. S.; Martin, C. T.; Rotello, V. M. *Angew. Chem. Int. Ed.* **2006**, *45*, 3165.

5. Savic, R.; Luo, L.; Eisenberg, A.; Maysinger, D. *Science* **2003**, *300*, 615.

6. Giri, S.; Trewyn, B. G.; Stellmaker, M. P.; Lin, V. S. Y. *Angew. Chem. Int. Ed.* **2005**, *44*, 5038.

7. Kam, N. W. S.; O'Connell, M.; Wisdom, J. A.; Dai, H. *Proc. Natl. Acad. Sci. U.S.A.* **2005**, *102*, 11600.

8. Hong, R.; Han, G.; Fernandez, J. M.; Kim, B. j.; Forbes, N. S.; Rotello, V. M. *J. Am. Chem. Soc.* **2006**, *128*, 1078.

9. Lewin, M.; Carlesso, N.; Tung, C.-H.; Tang, X.-W.; Cory, D.; Scadden, D. T.; Weissleder, R. *Nat. Biotechnol.* **2000**, *18*, 410.

10. Gao, X.; Cui, Y.; Levenson, R. M.; Chung, L. W. K.; Nie, S. *Nat. Biotechnol.* **2004**, *22*, 969.

11. Jaiswal, J. K.; Mattoussi, H.; Mauro, J. M.; Simon, S. M. *Nat. Biotechnol.* **2003**, *21*, 47.

12. Yang, P. H.; Sun, X.; Chiu, J. F.; Sun, H.; He, Q. Y. *Bioconjugate Chem.* **2005**, *16*, 494.

13. Chithrani, B. D.; Ghazani, A. A.; Chan, W. C. W. *Nano Lett.* **2006**, *6*, 662.

14. Tanaka, K.; Waki, H.; Ido, Y.; Akita, S.; Yoshida, Y.; Yoshida, T.; Matsuo, T. *Rapid Commun. Mass Spectrum.* **1988**, *2*, 151.

15. Owega, S.; Lai, E. P. C.; Bawagan, A. D. O. *Anal. Chem.* **1998**, *70*, 2360.

16. Novikov, A.; Caroff, M.; Della-Negra, S.; Lebeyec, Y.; Pautrat, M.; Schultz, J. A.; Tempez, A.; Wang, H. Y. J.; Jackson, S. N.; Woods, A. S. *Anal. Chem.* **2004**, *76*, 7288.

17. McLean, J. A.; Stumpo, K. A.; Russell, D. H. *J. Am. Chem. Soc.* **2005**, *127*, 5304.

18. Castellana, E. T.; Russell, D. H. *Nano Lett.* **2007**, *7*, 3023.

19. Huang, Y. F.; Chang, H. T. *Anal. Chem.* **2006**, *78*, 1485.

20. Su, C. L.; Tseng, W. L. *Anal. Chem.* **2007**, *79*, 1626.

21. Nagahori, N.; Nishimura, S.-I. *Chem. - Eur. J.* **2006**, *12*, 6478.

22. Spencer, M. T.; Furutani, H.; Oldenburg, S. J.; Darlington, T. K.; Prather, K. A. *J. Phys. Chem. C* **2008**, *112*, 4083.

23. Sunner, J.; Dratz, E.; Chen, Y.-C. *Anal. Chem.* **1995**, *67*, 4335.

24. Wei, J.; Buriak, J. M.; Siuzdak, G. *Nature* **1999**, *399*, 243.

25. Northen, T. R.; Yanes, O.; Northen, M. T.; Marrinucci, D.; Uritboonthai, W.; Apon, J.; Golledge, S. L.; Nordstrom, A.; Siuzdak, G. *Nature* **2007**, *449*, 1033.

26. Tracy, J. B.; Kalyuzhny, G.; Crowe, M. C.; Balasubramanian, R.; Choi, J. P.; Murray, R. W. *J. Am. Chem. Soc.* **2007**, *129*, 6706.

27. Tracy, J. B.; Crowe, M. C.; Parker, J. F.; Hampe, O.; Fields-Zinna, C. A.; Dass, A.; Murray, R. W. *J. Am. Chem. Soc.* **2007**, *129*, 16209.

28. Schaaff, T. G. *Anal. Chem.* **2004**, *76*, 6187.

29. Tsunoyama, H.; Negishi, Y.; Tsukuda, T. *J. Am. Chem. Soc.* **2006**, *128*, 6036.

30. Templeton, A. C.; Wuelfing, W. P.; Murray, R. W. *Acc. Chem. Res.* **2000**, *33*, 27.

31. Kanaras, A. G.; Kamounah, F. S.; Schaumburg, K.; Kiely, C. J.; Brust, M. *Chem. Commun.* **2002**, 2294.

32. You, C.-C.; Miranda, O. R.; Gider, B.; Ghosh, P. S.; Kim, I.-B.; Erdogan, B.; Krovi, S. A.; Bunz, U. H. F.; Rotello, V. M. *Nat. Nanotech.* **2007**, *2*, 318.

33. Leroueil, P.; Hong, S.; Mecke, A.; Baker, J.; Orr, B.; Banaszak Holl, M. *Acc. Chem. Res.* **2007**, *40*, 335.

34. Sandhu, K. K.; McIntosh, C. M.; Simard, J. M.; Smith, S. W.; Rotello, V. M. *Bioconjugate Chem.* **2002**, *13*, 3.

35. Xu, Z. P.; Zeng, Q. H.; Lu, G. Q.; Yu, A. B. *Chem.Eng. Sci.* **2006**, *61*, 1027.

36. Trevor, J. L.; Lykke, K. R.; Pellin, M. J.; Hanley, L. *Langmuir* **1998**, *14*, 1664.

37. Gong, W.; Elitzin, V. I.; Janardhanam, S.; Wilkins, C. L.; Fritsch, I. *J. Am. Chem. Soc.* **2001**, *123*, 769.

38. Su, J.; Mrksich, M. *Langmuir* **2003**, *19*, 4867.

39. Mrksich, M. *ACS Nano* **2008**, *2*, 7.

40. Goodman, C. M.; McCusker, C. D.; Yilmaz, T.; Rotello, V. M. *Bioconjugate Chem.* **2004**, *15*, 897.

41. Jiang, W.; Kim, B. Y. S.; Rutka, J. T.; Chan, W. C. W. *Nat. Nanotech.* **2008**, *3*, 145.

42. Nativo, P.; Prior, I. A.; Brust, M. *ACS Nano* **2008**, *2*, 1639.

43. Yezhelyev, M. V.; Qi, L.; O'Regan, R. M.; Nie, S.; Gao, X. *J. Am. Chem. Soc.* **2008**, *130*, 9006.

44. Brust, M.; Walker, M.; Bethell, D.; Schiffrin, D. J.; Whyman, R. *J. Chem. Soc., Chem. Commun.* **1994**, 801.

CHAPTER 5

EFFICIENT TRANSFECTION BY TUNING THE SURFACE CHARGE DENSITY OF AMINO ACID-FUNCTIONALIZED NANOPARTICLE VECTORS

5.1 Introduction

Gene therapy offers great promise for curing cancer and genetic disorders of both innate and acquired origin.[1,2] Successful therapy requires the transport of nucleic acids into cells by delivery vehicles, as DNA is not efficiently translocated through the cell membrane.[3] Recombinant viruses provide effective transfection vectors,[4] however issues of immunogenicity, carcinogenicity and inflammation raise serious concerns for clinical applications.[5,6,7] The challenges faced with viral vectors have inspired the parallel development of non-viral vectors based on polymers,[8,9] dendrimers[10,11] and liposomes.[12,13] These synthetic systems, however, are less efficient than viral systems.[14,15] Therefore, efforts continue to focus on designing safe and efficient vectors.[16]

Inorganic nanoparticles including silica,[17] iron oxide[18] and CdSe,[19] have been exploited recently as alternate non-viral vectors. Gold nanoparticles provide particularly attractive scaffolds for the creation of transfection agents.[20,21,22] Gold colloids are bio-inert, non-toxic and readily synthesized and functionalized.[23,24] They also provide a multifunctional platform for both therapeutic and diagnostic purposes.[25,26,27,28] Finally, through proper functionalization, these particles can be engineered to accumulate preferentially at tumor sites using targeting ligands, providing a powerful tool for cancer gene therapy.[29,30]

The use of these nanoparticles for DNA transfection has been described here. There are several challenges to the design of polycations for gene transfection, including

the need for effective complexation and condensation of the DNA, cellular uptake through endocytosis coupled with endosomal escape, protection from nuclease digestion in the cytoplasm, and finally delivery of the DNA to the nucleus.[31] Nature provides insight into DNA packaging, where DNA wraps around histone octamers, the nucleosome core proteins ~6 nm in diameter featuring a large proportion of basic residues (lysine and arginine) that form salt bridges with the phosphate backbone of DNA.[32] Using this structure as a starting point we designed DNA packaging agents using tiny spherical gold nanoparticles (core diameter ~2 nm, overall diameter 6 nm) featuring amino acids (Figure 5.1), which resemble histones in shape, size and surface functionality. In these studies we found that compaction of DNA can be improved by increasing the density of ammonium groups on the nanoparticle surface, which facilitated delivery. Conjugation of lysines on particles in a dendritic fashion yielded efficient vectors, ~28-fold higher than polylysine for *in vitro* transfections. Amino acid coated-particles showed no cytotoxicity. Finally, the gold-thiolate binding of ligands to particles allowed the transfection ability of these materials to be regulated by manipulation of intracellular glutathione levels. These results have been published recently in *ACS Nano* (**2008**, *2*, 2213-2218).

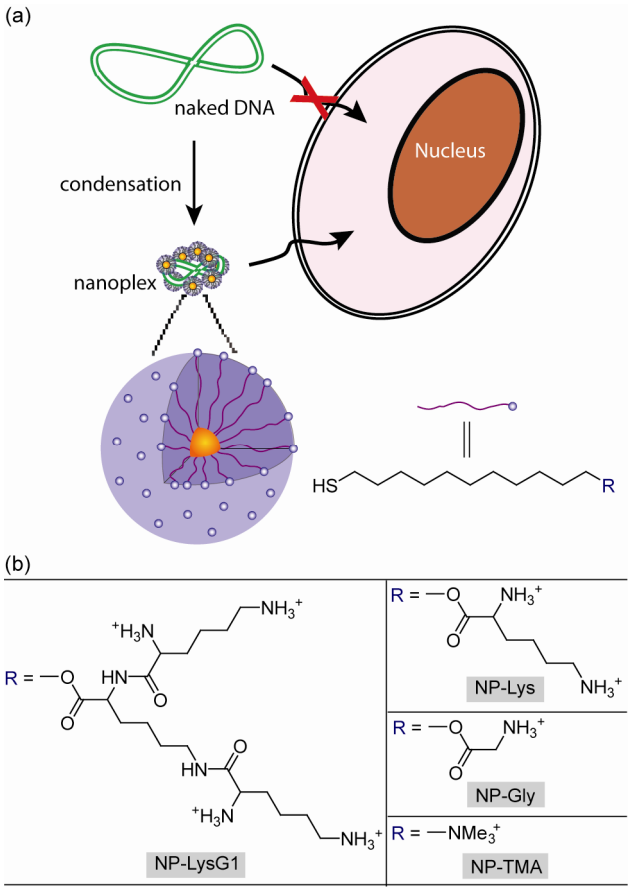

Figure 5.1: (a) Schematic illustration of the monolayer protected gold nanoparticles used as transfection vectors in this study. (b) Chemical structures of headgroups presented on the surface of the nanoparticles.

5.2 Results and Discussion

Fabrication of vectors: Amino acid-conjugated thiols were synthesized in a straightforward procedure with terminal ammonium group(s). 1-Pentanethiol-protected gold clusters (Au-C_5, core diameter ≈ 2 nm) were functionalized with these ligands via the Murray place-exchange reaction providing water-soluble particles.[33] To explore the structural effect of headgroup structure on tranfection efficiency, we fabricated three vectors (NP-LysG1, NP-Lys, and NP-Gly) featuring varying density of cationic sites (Figure 5.2).

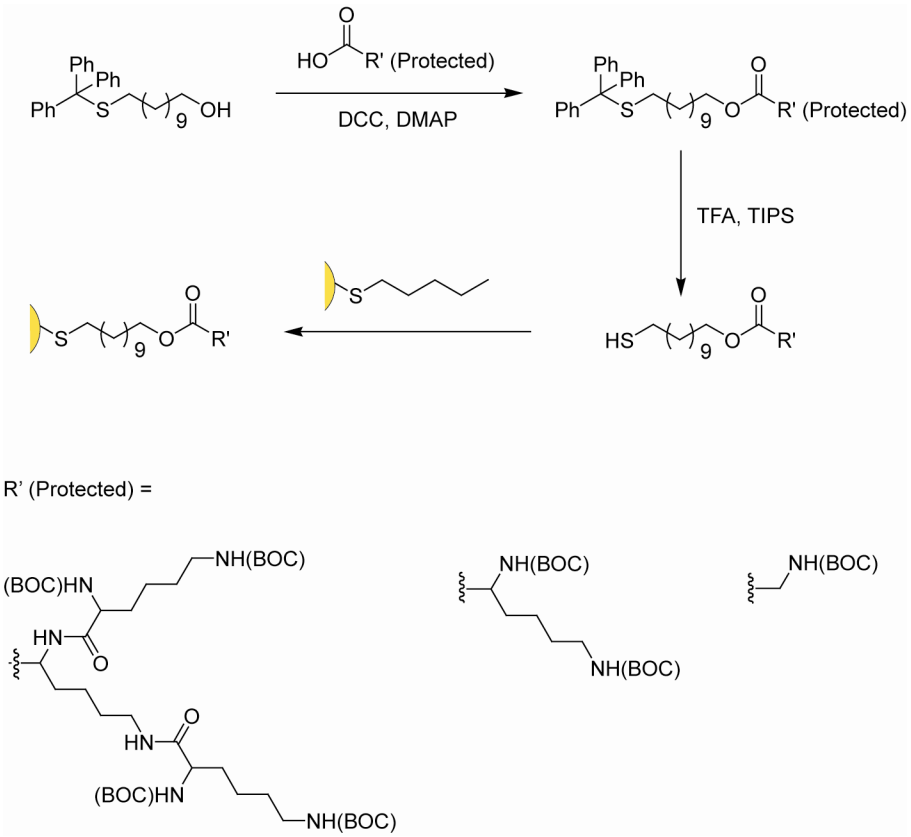

Figure 5.2: General scheme for synthesis of amino acid-coated nanoparticles.

Nanoparticle-DNA complexation: The comparable sizes of DNA and small functionalized nanoparticles facilitate their interaction.[34] In our previous studies, we have demonstrated that quaternary ammonium-functionalized gold colloids effectively recognize DNA strands.[35] Nanoparticles bearing primary ammonium groups ($pK_a \approx 10$) on the surface are also expected to bind with anionic DNA via ion-pairing at physiological pH (pH = 7.4).[36] Gel electrophoresis was carried out initially to test the association of nanoparticles with DNA (gWiz β-gal plasmid). Nanoparticle-DNA mixtures at molar ratios (MR = mol_{NP}:mol_{DNA}, at a fixed amount of DNA) of 200 (MR_{200}) and 2000 (MR_{2000}) were electrophoresed on agarose gel and stained with ethidium bromide (EtBr). While a band corresponding to free DNA was observed at

MR_{200} suggesting incomplete complexation, electrophoretic mobility of DNA toward the positive electrode was completely retarded at MR_{2000} (Figure 5.3). Binding was further verified by an EtBr exclusion assay, which indicated complexation between DNA and nanoparticles by quenching of EtBr-fluorescence (Figure 5.4).

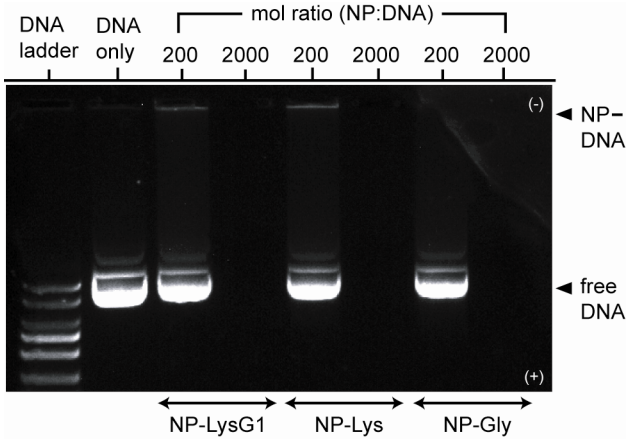

Figure 5.3: Gel retardation assay demonstrating DNA-nanoparticle complexation. A constant amount of DNA (333 ng/well) was complexed with nanoparticles at two different ratios in HEPES (10 mM, pH 7.4). No NP-DNA band is observed because of fluorescence quenching by NP complexation.

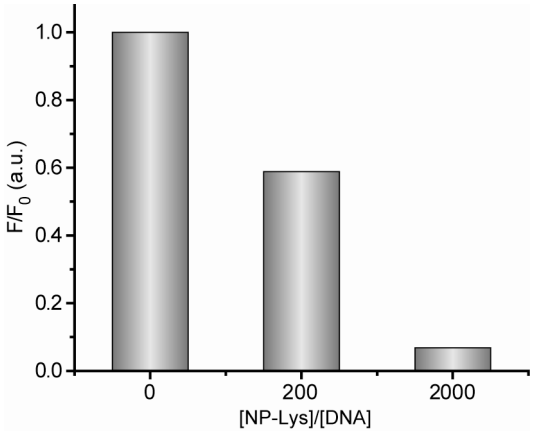

Figure 5.4: Addition of cationic nanoparticles (NP-Lys) displaced intercalated ethidium bromide within DNA and resulted in a decrease in fluorescence.

Characterization of nanoplexes: Surface charge and size of DNA complexes are two important parameters in determining the efficiency of cellular uptake. Zeta potential measurements revealed that complexes of each headgroup (MR_{2000}) bear positive surface potentials ranging from +25 mV to +34 mV (Table 5.1) that should promote initial adhesion on negatively charged cell surface.[37] In general, polycation-DNA complexes enter into mammalian cells via endocytosis, a process that is limited to particles smaller than ~150 nm in diameter.[38] Dynamic light scattering (DLS) showed that NP-Gly formed large complexes (> 150 nm). However, efficient condensation was achieved by increasing the density of ammonium groups on the particle surface. NP-LysG1 condensed DNA (<100 nm) most effectively (Table 5.1). In addition to enhanced cellular uptake, the tight packing with NP-LysG1 should prove useful for cancer gene therapy, where particles ~100 nm can more easily extravasate through open endothelial gaps in tumor tissues.[39,40]

Table 5.1: Surface charge and size of nanoparticle-DNA complexes (mol ratio 2000) in HEPES buffer (10 mM, pH 7.4) at 25 °C.

nanoparticles	zeta potential (mV)	size (nm)
NP-LysG1	30 ± 2	91 ±2
NP-Lys	34 ± 1	112 ±1
NP-Gly	25 ± 1	233 ±40
NP-TMA	34 ± 2	118 ±10

Transfection of mammalian cells: We have shown earlier that trimethyl ammonium-functionalized nanoparticles (NP-TMA) can protect DNA substantially from DNAse digestion,[41] and transfect 293T cells in the presence of serum and chloroquine.[20]

An X-gal staining assay was conducted to qualitatively assess the amino acid-coated nanoparticles mediated transfection of monkey kidney cells (Cos-1) with a β-galactosidase (β-gal) reporter plasmid at MR_{2000}. After 3h of staining, blue spots were detected under an optical microscope from cells transfected with NP-LysG1 and NP-Lys, indicating that these particles serve as effective gene delivery agents (Figure 5.5).

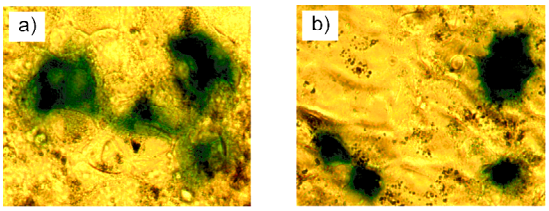

Figure 5.5: Optical micrographs showing transfected cells turned blue after 3h of X-gal staining. Cos-1 cells were transfected with β-gal reporter gene using (a) NP-LysG1 and (b) NP-Lys.

The expression of the β-gal reporter gene was monitored by enzyme activity assay to quantify the efficiency of DNA delivery. First, Cos-1 cells were treated with nanoparticle-DNA complexes at various ratios (MR_{1000}, MR_{2000}, MR_{4000} and MR_{6000}) to determine the optimal ratio for transfection. Expression of β-gal was maximal at MR_{2000} (Figure 5.6), consistent with our previous studies.[20] We next compared transfection efficiency of the synthesized nanoparticles at MR_{2000}. As illustrated in Figure 5.7, lysine-coated particles NP-Lys and LP-LysG1 efficiently expressed the reporter gene, whereas NP-Gly showed negligible enzyme activity. Cells were also transfected with two other effective vectors as positive controls, previously reported NP-TMA[20] and extensively studied polylysine.[42,43] Lysine and lysine dendrimer-coated particles were significantly better than both positive controls (Figure 5.7). In particular, NP-LysG1 and NP-Lys were

superior to polylysine by ~28 fold and ~5 fold, respectively. As expected, no measurable β-gal activity was detected when cells were treated with naked DNA.

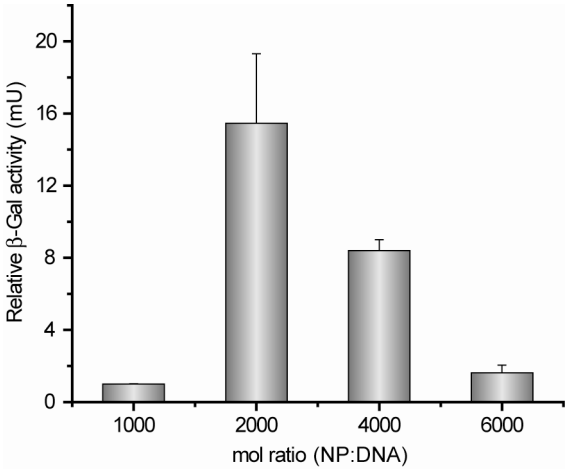

Figure 5.6: Transfection efficiency of NP-LysG1 at different mixing ratio. MR_{2000} was the optimal ratio.

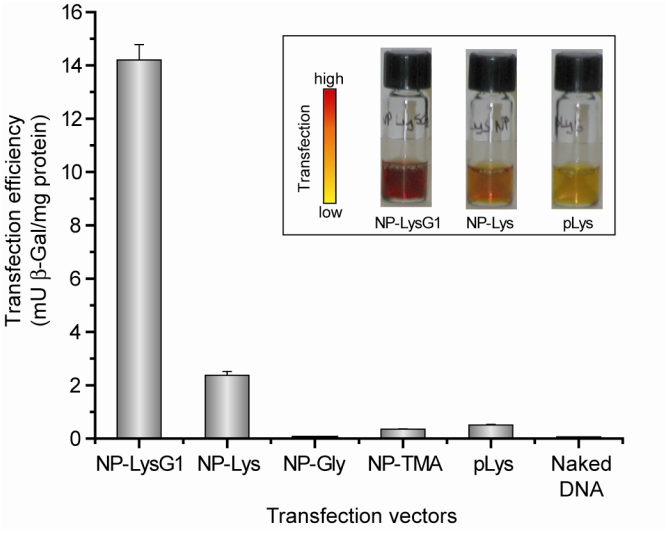

Figure 5.7: Enhanced transfection using NP-LysG1 and NP-Lys relative to positive controls, NP-TMA and polylysine (pLys). No appreciable enzyme activity was observed in the absence of vectors. Inset shows solution colors during a β-Gal activity assay performed after transfection. The color changes from yellow (substrate) to red (product) in the presence of active enzyme.

Cytotoxicity: Cellular metabolic activity was measured by an alamar blue assay to evaluate possible toxicity that might arise from nanoparticles during transfection. As

depicted in Figure 5.8, amino-acid coated particles displayed no decrease in viability. However, trimethyl ammonium functionalized particles were moderately toxic, which probably originates from their strong interaction with the cell surface.[44]

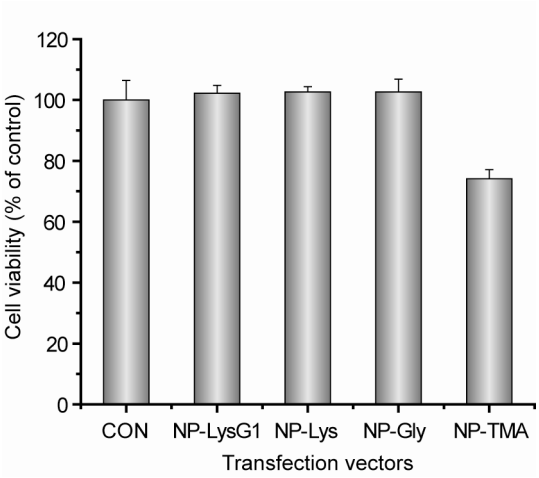

Figure 5.8: Cell viability determined by an alamar blue assay at the end of transfection (total period 48 h) using the optimum molar ratio (MR_{2000}).

Glutathione regulation of transfection efficiency: The cationic ligands of Au nanoparticles can be displaced by glutathione (GSH), which would alter the surface charge and loosen the DNA-NP association (Figure 5.9a).[45,46] This mode of release utilizes the dramatic differential between extra- and intracellular GSH levels. Moreover, manipulation of intracellular GSH levels provides a potential mechanism for external control of transfection. We investigated the regulation of transfection efficiency of nanoparticles, NP-Lys (MR_{2000}), by both increasing and decreasing intracellular GSH concentration. The glutathione level was transiently increased by treating cells with glutathione monoester (GSH-OEt).[26] Glutathione monoester is rapidly internalized by cells and processed into glutathione (GSH) by esterases.[47] Transfection efficiency increased upon treatment of cells with GSH-OEt in a concentration-dependent fashion (Figure 5.9b). In a complementary study, baseline GSH production was suppressed by

prolonged (24 h) treatment of cells with L-buthionine-[S,R]-sulfoximine (BSO), an inhibitor of γ–glutamylcysteine synthetase.[48] As expected, BSO-treated cells showed lower transfection efficiency compared to untreated cells (Figure 5.9c).

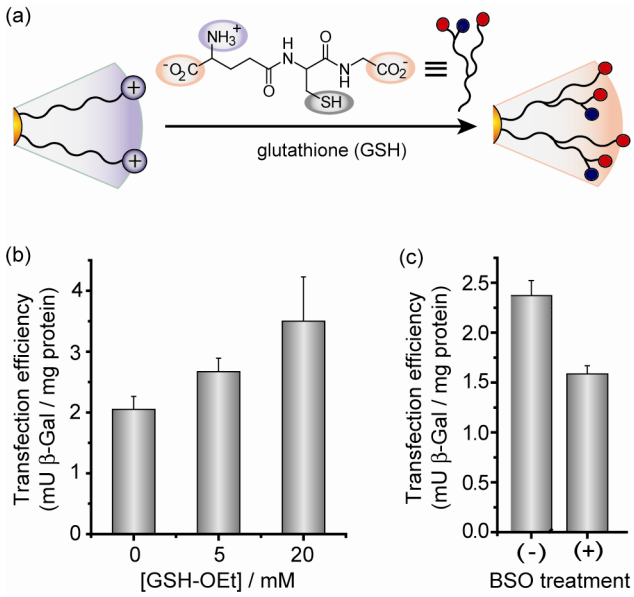

Figure 5.9: (a) Schematic depiction of place-exchange between native cationic ligands and cellular glutathione (GSH) on nanoparticle surface. (b) Elevation in transfection level depending on dose of glutathione monoester (GSH-OEt). Cells were pre-incubated with GSH-OEt for 1 h then washed prior to transfection. (c) Decrease in transfection efficiency upon L-buthionine-[S,R]-sulfoximine (BSO) treatment. Cells were plated in BSO-added (2 mM) media and incubated for 24 h.

5.3 Conclusion

In summary, we have demonstrated that coating gold nanoparticles with lysine-based headgroups produces effective transfection vectors. DNA delivery efficiency strongly depends on the structure of headgroups and their concomitant ability to condense DNA. The lysine dendron-functionalized nanoparticle NP-LysG1 was most effective at condensing DNA, and was the most potent vector, ~28 times more effective than polylysine. Importantly, these amino acid-functionalized particles showed no cytotoxicity

when used as transfection agents. These materials were also responsive to cellular glutathione level during *in vitro* transfection, providing insight into their mode of activity as well as being a potential tool for orthogonal control of transfection.

5.4 Experimental Section

Materials. All chemicals were purchased from Aldrich unless otherwise stated. The organic solvents were bought from Pharmco-Aaper and used as received except dichloromethane and toluene which were distilled in the presence of calcium hydride. Flash column chromatography was carried out for purification using silica gel (SiO_2, particle size 40-63 μm). gWiz *β*-gal plasmid (8278 bp) was purchased from Aldevron (Fargo, ND). L-Glutathione reduced ethyl ester (GSH-OEt) was obtained from Fluka. Cell culture medium powder and phosphate buffer saline (PBS) were bought from Aldrich.

Gel electrophoresis: To prepare each mixture (27 μl total volume), 400 ng DNA was incubated with required amount of nanoparticles at room temperature in 10 mM HEPES buffer (pH = 7.4). After 10 min of incubation, 3 μl gel loading dye (6x) was added into each mixture. 25 μl from the resulting 30 μl solution was loaded into 0.6% agarose gel, pre-stained with EtBr. The samples were electrophoresed at 100 V for 60 min in TBE buffer (0.045 M Tris-borate; 0.001 M EDTA) and the bands were visualized on a UV trans-illuminator.

Ethidium bromide (EtBr) exclusion assay: The dye exclusion assay was tested with NP-Lys. A mixture of pDNA (1.2 nM), EtdBr (5 μM) and NP-Lys (0 μM, 0.24 μM and 2.4 μM) were incubated for 10 min in phosphate buffered saline (PBS, Sigma). Then

fluorescence (λ_{em} = 595 nm, λ_{ex} = 545 nm) was monitored on a SpectroMax M5 micro-plate reader (Molecular Device). Nanoparticle absorbance was corrected using NP-TEG, a neutral particle. Addition of particles resulted in release of intercalated dyes and hence decreases fluorescence intensity.

Cell culture: Cos-1 cells were cultured in a humidified atmosphere (5% CO_2) at 37 °C. The cells were grown in Dulbecco's Modified Eagle's Medium (DMEM, 4.0 g/L glucose) supplemented with 10% fetal bovine serum and antibiotics (100 U/ml penicillin and 100 μg/ml streptomycin). All transfection experiments were performed with complete growth medium without antibiotics and in the presence of 100 μM chloroquine. 1×10^5 cells per well were seeded on a 24-well plate 24 h prior the experiments. For GSH-OEt treatment, old medium was removed after 24 h of plating, and cells were incubated with fresh medium containing GSH-OEt for 1 h and washed three times with PBS before adding transfection medium.[26]

Transfection protocol: All experiments were done in triplicate. Nanoplexes were first prepared at room temperature as follows (for 3 wells): (a) a 100 μl solution of 2.4 μg plasmid and a 200 μl solution of the required concentration of nanoparticles were prepared separately in PBS, (b) after 5 min, particles were mixed with DNA and incubated together for 10 min. The nanoplexes were diluted with 1600 μl pre-warmed DMEM with 100 μM chloroquine. The resulting transfection medium was added into wells (600 μl/well, 3 wells) after washing cells once with PBS. 6 h later, the medium was removed, cells were washed 3X with PBS, and complete medium (600 μl/well) was added for another 42 h of incubation. Cells were transfected similarly with

polylysine/DNA at a mass ratio of 2.5 as previously reported (M_w of pLys ≈ 50K).[42] Gene expression and cytotoxicity were tested after 48 h of total transfection period.

X-Gal assay: Cells were stained following the assay kit (Genlantis, USA). After 3h of staining, cells were washed twice with PBS and visualized on an optical microscope (Zeiss, 20x).

Reporter gene expression: β-Gal activity was assayed using chlorophenol red-β-D-galactopyranoside as a substrate (CPRG kit, Genlantis, USA). Absorbance (A_{570}) was measured on a SpectroMax M5 micro-plate reader (Molecular Device), and the amount of expressed protein was calculated from a calibration curve constructed with pure β-gal. Total cellular protein was determined by bicinchoninic acid assay (Pierce, USA) according to the manufacturer's protocol.

Cytotoxicity assay: The alamar blue assay was performed according to the manufacturer's protocol (Invitrogen Biosource, USA). After 48 h of transfection, cells were treated with 10% alamar blue solution and kept at 37°C for another 2 h. Red fluorescence, resulting from the reduction of alamar blue, was monitored (excitation/emission: 535/590) on a SpectroMax M5 micro-plate reader (Molecular Device).

DLS and zeta potential: DLS experiments and zeta potential measurements were carried out using a Malvern Zetasizer (Nano series, Malvern Instruments Inc, USA). Nanoplexes were prepared as mentioned above in transfection protocol using HEPES (10 mM, pH = 7.4) only instead of PBS/media. After 10 min of incubation, data were collected and reported as an average of three measurements.

Synthesis of NP-Gly and NP-Lys: NP-Gly and NP-Lys were prepared according to literature procedures.[49,50]

Synthesis of Trit-C_{11}-LysG1-$(Boc)_4$: A dichloromethane solution of LysG1-$(Boc)_4$-OH[51] (2.50 g, 3.11 mmol), Trit-C_{11}-OH (1.00 g, 2.24 mmol), *N*, *N*′-dicyclohexylcarbodiimide (DCC, 0.69 g, 3.34 mmol), and 4-dimethylaminopyridine (DMAP, 0.08 g, 0.65 mmol) was stirred at room temperature for 12 h. The solution was poured into a mixture of dichloromethane and distilled water. The organic layer was collected and purified by column chromatography on silica gel using n-hexane/ethyl acetate (1:2, v/v) as an eluent, to give **Trit-C_{11}-LysG1-$(Boc)_4$** as a white solid (Yield 2.40 g, 87 %). ^{1}H NMR (400 MHz, $CDCl_3$) δ 7.41 (m, 6H, *Ph*-), 7.27 (m, 6H, *Ph*-), 7.20 (m, 3H, *Ph*-), 7.00 (brs, 1H) 5.93 (brs, 1H), 5.60 (brs, 1H), 4.92 (brs, 1H), 4.76 (brs, 1H), 4.35 (brs, 2H), 4.11 (brm, 3H, -C*H*$_2$-O- and COC*H*(R)NH-), 3.10 (brs, 6H, -C*H*$_2$NHBoc), 2.12 (t, J = 7.3 Hz, 2H, -S-C*H*$_2$-), 1.40 (m, 72H, -C*H*$_2$- and C*H*$_3$-); MS (ESI-MS) calcd for $C_{68}H_{106}N_6O_{12}S$ 1231.7, found 1254.0 $[M+Na]^+$.

Synthesis of HS-C_{11}-LysG1: A dichloromethane solution of **Trit-C_{11}-LysG1-$(Boc)_4$** (0.2 g, 0.16 mmol), trifluoroacetic acid (TFA, 0.6 ml), and triisopropylsilane (TIPS, 0.03 ml) was stirred at room temperature for 6 h under argon. After removal of the solvent at reduced pressure, the residue was purified by washing with diethyl ether (20 ml x 5). After drying residue under high vacuum, white solid of product was obtained (Yield 0.09 g, 94 %). ^{1}H NMR (400 MHz, CD_3OD) major peaks assigned δ 4.41 (brs, 1H), 4.13 (brs, 2H, -C*H*$_2$-O-), 4.00 (brs, 1H), 3.86 (brs, 1H), 3.50 (brs, 1H), 3.23 (brs, 2H), 2.95 (brs, 6H, -C*H*$_2$NHBoc), 2.51 (q, J=7.2 Hz, 2H, HS-C*H*$_2$-), 1.40 (m, 36H, -C*H*$_2$- and C*H*$_3$-); MS (ESI-MS) calcd for $C_{21}H_{47}N_7O_3S$ 588.89, found 589.6 $[M+H]^+$

Synthesis of NP-LysG1: 1-Pentanethiol-protected gold colloids were dissolved in dichloromethane (DCM) and ligands were dissolved in DCM-methanol (10:1, v/v) mixture. These solutions were separately purged with argon. After 30 min of purging, they were mixed together and stirred at room temperature for ~ 48 h. Then solvents were evaporated and excess ligands were removed by 5X washing with DCM-methanol (50:1, v/v) followed by dialysis (cut off 10 kDa, Pierce) for 2 days.

5.5 References

Notes

1. McCormick, F. *Nat. Rev. Cancer* **2001**, *1*, 130.
2. Opalinska, J. B.; Gewirtz, A. M. *Nat. Rev. Drug Discovery* **2002**, *1*, 503.
3. Sokolova, V.; Epple, M. *Angew. Chem. Int. Ed.* **2008**, *47*, 1382.
4. Kay, M. A.; Glorioso, J. C.; Naldini, L. *Nat. Med.* **2001**, *7*, 33.
5. Check, E. *Nature* **2005**, *433*, 561.
6. Raper, S. E.; Chirmule, N.; Lee, F. S.; Wivel, N. A.; Bagg, A.; Gao, G. P.; Wilson, J. M.; Batshaw, M. L. *Mol. Genet. Metab.* **2003**, *80*, 148.
7. Hacein-Bey-Abina, S.; von Kalle, C.; Schmidt, M.; Le Deist, F.; Wulffraat, N.; McIntyre, E.; Radford, I.; Villeval, J. L.; Fraser, C. C.; Cavazzana-Calvo, M.; Fischer, A. *N. Engl. J. Med.* **2003**, *348*, 255.
8. Pack, D. W.; Hoffman, A. S.; Pun, S.; Stayton, P. S. *Nat. Rev. Drug Discovery* **2005**, *4*, 581.
9. Liu, Y. M.; Reineke, T. M. *J. Am. Chem. Soc.* **2005**, *127*, 3004.
10. Nishiyama, N.; Iriyama, A.; Jang, W. D.; Miyata, K.; Itaka, K.; Inoue, Y.; Takahashi, H.; Yanagi, Y.; Tamaki, Y.; Koyama, H.; Kataoka, K. *Nat. Mater.* **2005**, *4*, 934.
11. Dufes, C.; Uchegbu, I. F.; Schatzlein, A. G. *Adv. Drug Delivery Rev.* **2005**, *57*, 2177.
12. de Lima, M. C. P.; Neves, S.; Filipe, A.; Duzgunes, N.; Simoes, S. *Curr. Med. Chem.* **2003**, *10*, 1221.

13. Mahato, R. I. *Adv. Drug Delivery Rev.* **2005**, *57*, 699.

14. Luo, D.; Saltzman, W. M. *Nat. Biotechnol.* **2000**, *18*, 33.

15. Kodama, K.; Katayama, Y.; Shoji, Y.; Nakashima, H. *Curr. Med. Chem.* **2006**, *13*, 2155.

16. Cavazzana-Calvo, M.; Thrasher, A.; Mavilio, F. *Nature* **2004**, *427*, 779.

17. Torney, F.; Trewyn, B. G.; Lin, V. S. Y.; Wang, K. *Nature Nanotech.* **2007**, *2*, 295.

18. Medarova, Z.; Pham, W.; Farrar, C.; Petkova, V.; Moore, A. *Nat. Med.* **2007**, *13*, 372.

19. Derfus, A. M.; Chen, A. A.; Min, D. H.; Ruoslahti, E.; Bhatia, S. N. *Bioconjugate Chem.* **2007**, *18*, 1391.

20. Sandhu, K. K.; McIntosh, C. M.; Simard, J. M.; Smith, S. W.; Rotello, V. M. *Bioconjugate Chem.* **2002**, *13*, 3.

21. Thomas, M.; Klibanov, A. M. *Proc. Natl. Acad. Sci. U. S. A.* **2003**, *100*, 9138.

22. Rosi, N. L.; Giljohann, D. A.; Thaxton, C. S.; Lytton-Jean, A. K. R.; Han, M. S.; Mirkin, C. A. *Science* **2006**, *312*, 1027.

23. Daniel, M. C.; Astruc, D. *Chem. Rev.* **2004**, *104*, 293.

24. Connor, E. E.; Mwamuka, J.; Gole, A.; Murphy, C. J.; Wyatt, M. D. *Small* **2005**, *1*, 325.

25. Bhattacharya, R.; Mukherjee, P.; Xiong, Z.; Atala, A.; Soker, S.; Mukhopadhyay, D. *Nano Lett.* **2004**, *4*, 2479.

26. Hong, R.; Han, G.; Fernandez, J. M.; Kim, B. J.; Forbes, N. S.; Rotello, V. M. *J. Am. Chem. Soc.* **2006**, *128*, 1078.

27. Ghosh, P.; Han, G.; De, M.; Kim, C. K.; Rotello, V. M. *Adv. Drug Delivery Rev.* **2008**, *60*, 1307.

28. Shi, X. G.; Wang, S. H.; Meshinchi, S.; Van Antwerp, M. E.; Bi, X. D.; Lee, I. H.; Baker, J. R. *Small* **2007**, *3*, 1245.

29. Bhattacharya, R.; Patra, C. R.; Earl, A.; Wang, S. F.; Katarya, A.; Lu, L. C.; Kizhakkedathu, J. N.; Yaszemski, M. J.; Greipp, P. R.; Mukhopadhyay, D. *et al. Nanomedicine* **2007**, *3*, 224.

30. Paciotti, G. F.; Kingston, D. G. I.; Tamarkin, L. *Drug Dev. Res.* **2006**, *67*, 47.

31. Davis, M. E. *Curr. Opin. Biotechnol.* **2002**, *13*, 128.

32. Voet, D.; Voet, J. G. Biochemistry, 2nd ed.; John Wiley & Sons, Inc.: New York, 1995; pp 1124–1131.

33. Templeton, A. C.; Wuelfing, M. P.; Murray, R. W. *Acc. Chem. Res.* **2000**, *33*, 27.

34. Verma, A.; Rotello, V. M. *Chem. Commun.* **2005**, 303.

35. McIntosh, C. M.; Esposito, E. A.; Boal, A. K.; Simard, J. M.; Martin, C. T.; Rotello, V. M. *J. Am. Chem. Soc.* **2001**, *123*, 7626.

36. Andre, I.; Linse, S.; Mulder, F. A. A. *J. Am. Chem. Soc.* **2007**, *129*, 15805.

37. Mansouri, S.; Cuie, Y.; Winnik, F.; Shi, Q.; Lavigne, P.; Benderdour, M.; Beaumont, E.; Fernandes, J. C. *Biomaterials* **2006**, *27*, 2060.

38. Je, J. Y.; Cho, Y. S.; Kim, S. K. *Biomacromolecules* **2006**, *7*, 3448.

39. Hobbs, S. K.; Monsky, W. L.; Yuan, F.; Roberts, W. G.; Griffith, L.; Torchilin, V. P.; Jain, R. K. *Proc. Natl. Acad. Sci. U. S. A.* **1998**, *95*, 4607.

40. Mozafari, M. R.; Reed, C. J.; Rostron, C. *Micron* **2007**, *38*, 787.

41. Han, G.; Martin, C. T.; Rotello, V. M. *Chem. Biol. Drug Des.* **2006**, *67*, 78.

42. Ramsay, E.; Hadgraft, J.; Birchall, J.; Gumbleton, M. *Int. J. Pharm.* **2000**, *210*, 97.

43. Zauner, W.; Ogris, M.; Wagner, E. *Adv. Drug Delivery Rev.* **1998**, *30*, 97.

44. Goodman, C. M.; McCusker, C. D.; Yilmaz, T.; Rotello, V. M. *Bioconjugate Chem.* **2004**, *15*, 897.

45. Han, G.; Chari, N. S.; Verma, A.; Hong, R.; Martin, C. T.; Rotello, V. M. *Bioconjugate Chem.* **2005**, *16*, 1356.

46. Li, D.; Li, G. P.; Guo, W. W.; Li, P. C.; Wang, E. K.; Wang, J. *Biomaterials* **2008**, *29*, 2776.

47. Levy, E. J.; Anderson, M. E.; Meister, A. *Proc. Natl. Acad. Sci. U. S. A.* **1993**, *90*, 9171.

48. Balakirev, M.; Schoehn, G.; Chroboczek, J. *Chem. Biol.* **2000**, *7*, 813.

49. Ghosh, P. S.; Han, G.; Erdogan, B.; Rosado, O.; Rotello, V. M. *J. Pept. Sci.* **2008**, *14*, 134.

50. Ghosh, P. S.; Han, G.; Erdogan, B.; Rosado, O.; Krovi, S. A.; Rotello, V. M. *Chem. Biol. Drug Des.* **2007**, *70*, 13.

51. Dykes, G. M.; Brierley, L. J.; Smith, D. K.; McGrail, P. T.; Seeley, G. J. *Chem. Eur. J.* **2001**, *7*, 4730.

CHAPTER 6

NANOPARTICLE-MEDIATED DELIVERY OF A MEMBRANE-IMPERMEABLE ENZYME WITH RETENTION OF ITS ACTIVITY

6.1 Introduction

Delivery of functional proteins inside living cells provides a powerful tool for therapeutics and fundamental study of cell biology.[1,2,3] This technique allows introduction of proteins in a rapid, time-specific and dose-dependent fashion.[4] While significant progress in DNA-recombinant technology has lead to availablity of any protein of interest, protein transduction has been limited by the poor membrane permeability of most proteins, and hence requires a transporter.[5] In one strategy, cell-penetrating peptides (CPPs) have been attached to proteins genetically or chemically to promote their translocation across plasma membrane.[6] Nevertheless, covalent modification can generate challenges such as alteration of activity or the possibility of the tag being buried internally, and therefore a non-covalent approach has attracted tremendous attention.[7,8] Recently, supramolecular approaches using nanomaterials including silica nanoparticles, carbon nanotubes, and quantum dots have emerged as an alternative delivery strategy.[9,10,11] However, efficient delivery with retention of bioactivity still remains a major challenge.

Gold colloids are promising candidates in nanomedicine due to their bio-inertness, non-toxicity and cellular imaging ability.[12,13,14,15,16,17] They have been reported for DNA delivery, however, their use as protein carriers is largely unexplored[18,19,20] due to challenges in protein recognition and structure retention.[21] The large surface area and tunable functionality of gold nanoparticles makes them an excellent scaffold for protein

surface recognition.[22,23] Moreover, the conformation of proteins can be preserved by tailoring the monolayer of particles.[24] Herein, we have demonstrated the effective intracellular delivery of β-galactosidase (β-gal), a membrane-impermeable protein with high molecular weight (465 kDa) in a variety of cell lines, with endosomal escape and retention of activity inside the cells (Figure 6.1).

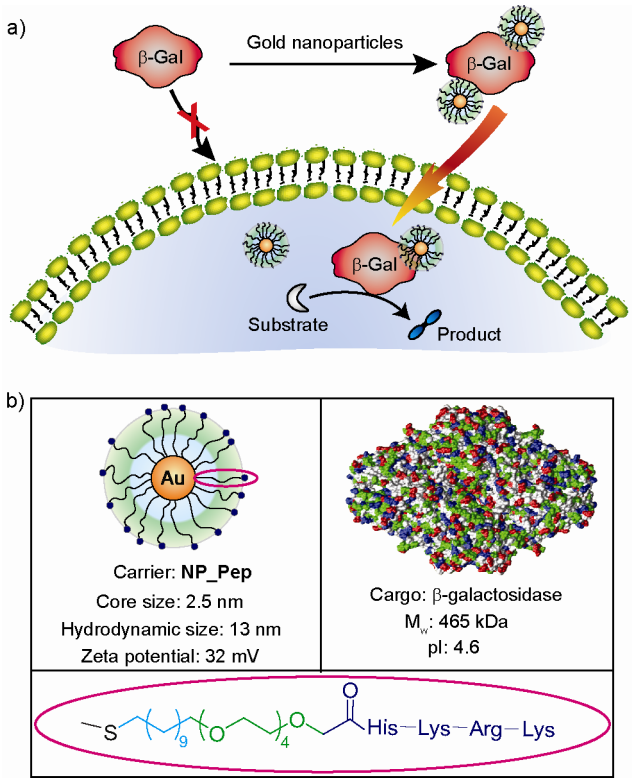

Figure 6.1: (a) Schematic representation of intracellular delivery of functional protein using gold nanoparticles. (b) Structure of the nanoparticle, the protein cargo, and the ligand onto particle.

6.2 Results and Discussion

We fabricated peptide-coated gold nanoparticles (**NP_Pep**, core diameter ~2.5 nm) to serve as a protein transporter. Three functional domains were incorporated into particle structure: the interior alkyl chains impart stability to the core, a corona of tetraethylene glycol (TEG) prevents both non-specific interaction with biomolecules and

denaturation,[24] the exterior peptide-tags serve as a recognition unit. Polyarginine is well-known for translocating molecules across the plasma membrane.[25,26,27,28,29] Therefore, our initial attempt was to functionalize the particles with a short peptide containing three arginine residues (NP-RRR), however, it rendered particles not dispersible in water. On the other hand, we have earlier experienced lysine-coated particles as water-soluble and stable for at least a year.[30] As a result, we chose a reported sequence comprising of both arginine and lysine,[31] with an additional histidine residues which is known to facilitate endosomal escape of the cargo.[32,33] Overall, the peptide headroup consisting of strong and weak basic amino acid residues (Arg, Lys and His) serves multiple roles: (a) protein surface recognition and plasma membrane association through favorable electrostatic interaction and hydrogen bonding of the guanidino moiety, and (b) "endosomal buffering" due to the presence of the proton-sponge imidazole group of histidine.[34,35,36] Importantly, these particles (**NP_Pep**) were nicely dispersed in aqueous media with similar to anticipated hydrodynamic diameter of 12.9 ± 0.3 nm.[37] They were cationic in nature with zeta potential of 32 ± 1 mV.

Nanoparticle-β-gal complexation was assessed by fluorescent titration using fluorescein isothiocyanate-labeled β-galactosidase (FITC-β-gal). As expected, FITC-fluorescence was quenched by the gold core upon addition of **NP_Pep** allowing us to quantify the interaction of the cationic particles and anionic β-gal (pI 4.6[38]), with a K_D of 1.0 nM observed (Figure 6.2). Surprisingly, we found that this complexation was stable enough for not dissociating in 150 mM salt solution within 2 h (long enough period for endocytosis[39]), presumably due to additional hydrogen-bonding interactions of the protein with the arginines of the nanoparticle.[40,41] Analysis of circular dichroism (CD) spectra

revealed that there was minimal change in secondary structure in presence of nanoparticles (Figure 6.2). Similarly, no shift in λ_{max} of tryptophan-fluorescence of the protein was observed (Figure 6.3), further confirming retention of the native structure of the protein.[42]

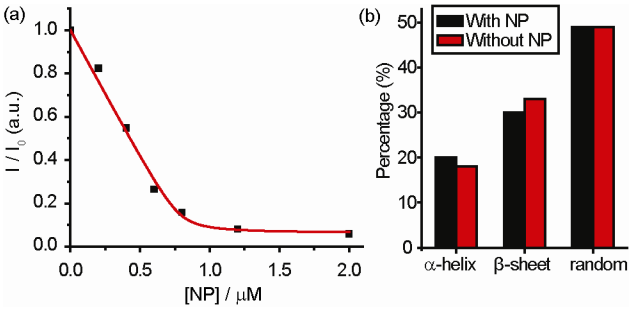

Figure 6.2: (a) Fluorescence titration of FITC-*β*-gal with NP_Pep in 5 mM phosphate buffer at 25 °C. (b) The percent of secondary structures calculated using DICHROWEB indicating minimal conformational change upon nanoparticle addition.

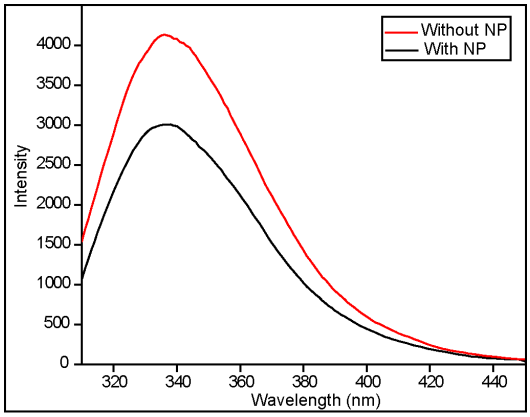

Figure 6.3: No shift in λ_{max} of tryptophan-fluorescence upon addition of nanoparticle.

Cellular delivery of *β*-gal protein was first monitored using FITC-*β*–gal as a fluorescent probe. Human cervical carcinoma cells (HeLa) were treated with 2:1 molar ratio **NP_Pep**/FITC-*β*-gal complexes, as precipitation occurred at higher particle/protein ratios in media. Following 3 h of incubation, cells were washed and cultured for another 3 h. Green fluorescence was observed when cells were treated with particle-protein complexes, while cells incubated with FITC-*β*-gal alone displayed no fluorescence

(Figure 6.4a-b). Cells treated with the complexes also showed presence of gold from inductively coupled plasma mass spectrometry (ICP-MS), consistent with the expected nanoparticle-promoted co-translocation of this membrane-impermeable protein (Figure 6.4c). The delivery process could also take place in presence of serum as evident from microscope images (Figure 6.5).

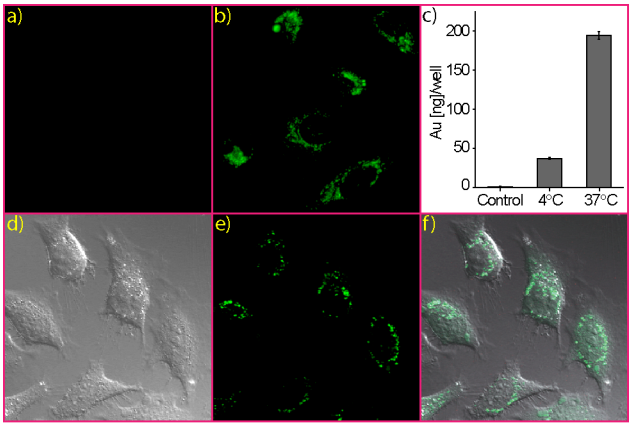

Figure 6.4: Fluorescence micrographs of Hela cells transfected with FITC-β-gal (50 nM) (a) in absence or (b) in presence of NP_Pep (100 nM). (c) ICP-MS measurements after treating cells with NP_Pep/β-gal (100 nM/50 nM) complex at different temperatures, and cells treated with β-gal alone as a control. (d-f) CLSM images of HeLa cells after protein transfection (NP_Pep/FITC-β-gal: 100 nM/50 nM): (d) bright field, (e) fluorescence and (f) their merge.

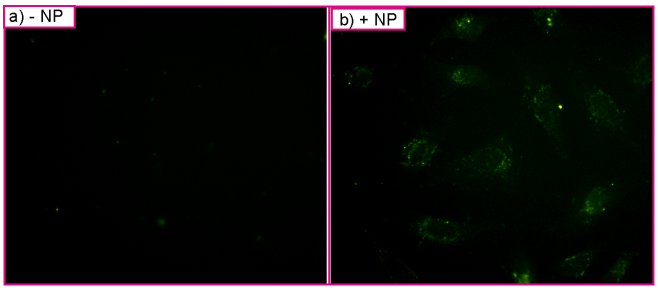

Figure 6.5: Images captured by fluorescence microscopy after protein transfection in presence of serum (a) without and (b) with nanoparticles. Cell were treated with **NP_Pep**/FITC-β-gal (100 nM/50 nM) complex in DMEM media with 10% serum for 3 h, then washed with PBS and cultured for another 3 h before taking the images.

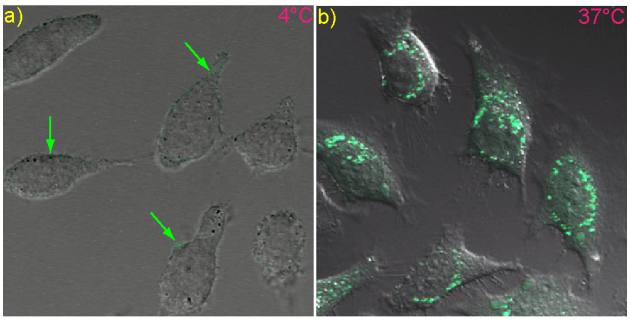

Figure 6.6: CLSM images of HeLa cells treated with **NP_Pep**/FITC-β-gal (100 nM/50 nM) at 4 °C and 37 °C. Protein signal was less at 4 °C, and located mainly near the surface as indicate by arrows.

We next performed confocal laser scanning microscope (CLSM) experiments to confirm that the observed fluorescence was coming from inside the cells as opposed to adsorbed on the cell surface. As shown in micrographs, punctate fluorescence was present in the perinuclear region of the cells, indicating protein internalization, presumably via endocytosis (Figure 6.4d-f).[43] This mechanism was supported by substantial decrease in fluorescence (Figure 6.6) coupled with a decrease in gold (via ICP, Figure 6.4c) with uptake experiments performed at 4 °C.[44]

Current research has been focused on cytoplasmic delivery of proteins. As the complex entered into cells via the endocytic pathway, we investigated whether the cargo was able to escape from the endosome or not. For this purpose, cells were treated with FM 4-64, a red color endosome-specific marker.[45] FITC-fluorescence that arises from delivered FITC-β–Gal was monitored along with red-fluorescence from FM 4-64 using CLSM (Figure 6.7a-b). After merging the green and the red channels, we observed presence of significant amount of green dots within the cells with some yellow dots, indicating most of the proteins were outside the endosomes (Figure 6.7c). The proteins

entrapped inside the vesicles appeared as yellow dots that originated from overlapping of green and red spots.

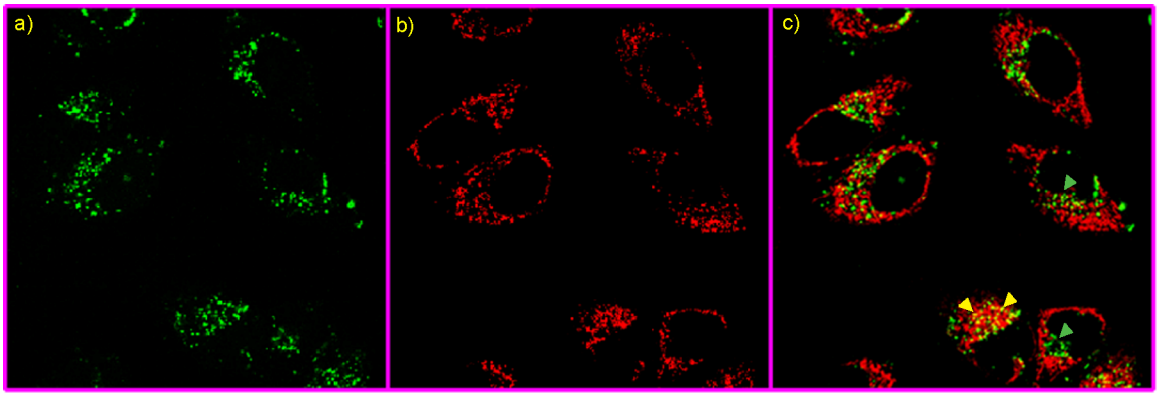

Figure 6.7: A colocalization study using CLSM after protein transfection (NP_Pep/FITC-β-gal: 100 nM/50 nM) of HeLa cells in presence of FM 4-64: (a) green fluorescence from FITC-β-gal, (b) red fluorescence from FM 4-64, an endosome-specific marker, and (c) overlap of the green and the red channels. In the merged image, green spots (shown with green arrowheads) are indicating proteins outside endosomes, while entrapped proteins inside endosomes appear as yellow dots (shown with yellow arrowheads).

Enzymatic activity provides a particularly stringent test for the retention of bioactivity after transduction, a key concern in protein delivery. The **NP_Pep**/protein complex was incubated with HeLa cells for 6 h followed by treatment with X-gal, a colorless substrate for β-gal that turns blue upon enzymatic hydrolysis. Significantly, blue precipitates appeared inside cells transfected with the particle-protein complex, demonstrating preservation of enzymatic activity after delivery (Figure 6.8b). No color was observed, as expected, when cells were treated with protein alone (Figure 6.8a). As shown earlier in the CLSM images, X-gal staining of the cells after trypsin digestion also suggested that the proteins were internalized by the cells as opposed to adsorbed onto cell surface (Figure 6.9). With longer culture period (24 h) after transfection, we observed the expected decrease in the enzymatic activity (Figure 6.10).

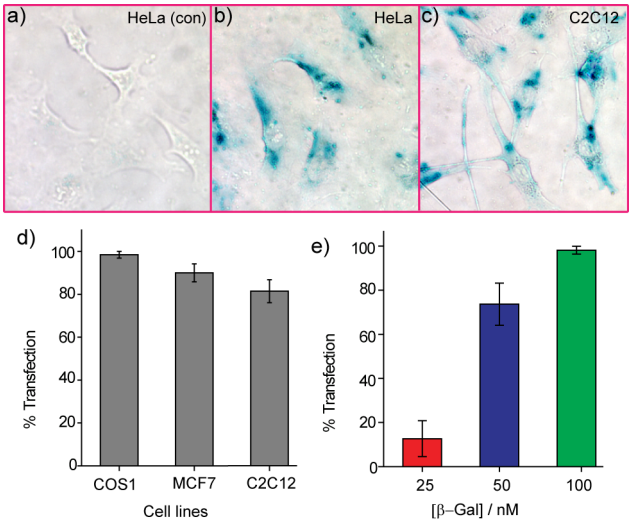

Figure 6.8: (a-c) X-gal staining after transfection. (a) HeLa with protein only. Transfected (b) HeLa and (c) C2C12 cells with NP_Pep/β-gal (100 nM/50 nM). (d) The percent of transfection with NP_Pep/β-gal (100 nM/50 nM) in defferent cell lines. (e) Dose-dependent protein delivery into HeLa cells at 2:1 NP_Pep/β-gal.

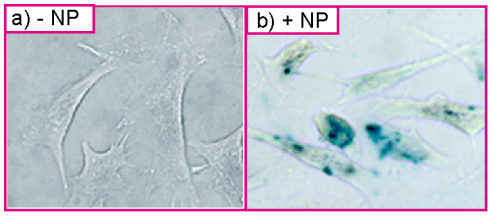

Figure 6.9: X-gal staining after trypsin digestion. After 3 h of β-gal (50 nM) transfection (a) without and (b) with **NP_Pep** (100 nM), cells were washed, trypsinized and then allowed 4 h more to reattach before X-gal staining.

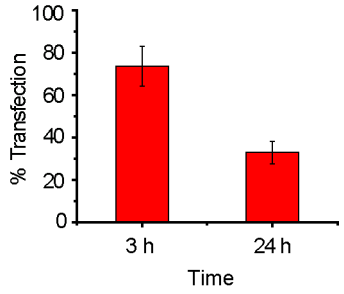

Figure 6.10: Decrease in the percent of transfection after a day as observed by X-gal staining. HeLa cells were treated with **NP_Pep**/FITC-β-gal (100 nM/50 nM) for 3 h, washed with PBS, and cultured for another 3 h and 24 h before X-gal staining.

We next studied the dose-dependent response of the delivery system, a useful tool for controlled protein delivery. Cells were treated with varied concentration of the enzyme, and protein delivery was assessed by X-gal histochemical staining. The percentage of transfected cells, judged by positively stained cells, increases with dose, with quantitative transfection (~98%) achieved at 100 nM of protein concentration (Figure 6.8e). Significantly, efficient transfection (>80%) was observed at 50 nM of protein in a diverse array of cell lines, including COS-1 (monkey kidney cells), MCF7 (human breast cancer cells), and even hard-to-transfect muscle cells (C2C12) (Figure 6.8c-d).[46]

Concurrent with our delivery studies we investigated the cytotoxicity of the **NP_Pep** particles. From a trypan blue exclusion test, we observed no cell death after 3 h of transfection as well as even after a day of transfection (Figure 6.11). This lack of toxicity was also validated from calcein AM assay (Figure 6.12). Importantly, full retention of cell vitality was observed from alamar blue assay (Figure 6.11).

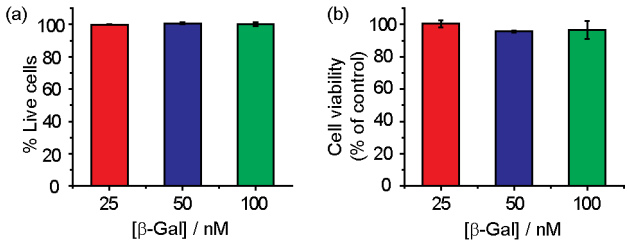

Figure 6.11: Nanoparticles showed no toxicity even after 24 h of protein transfection as measured by (a) trypan blue exclusion test and (b) alamar blue assay.

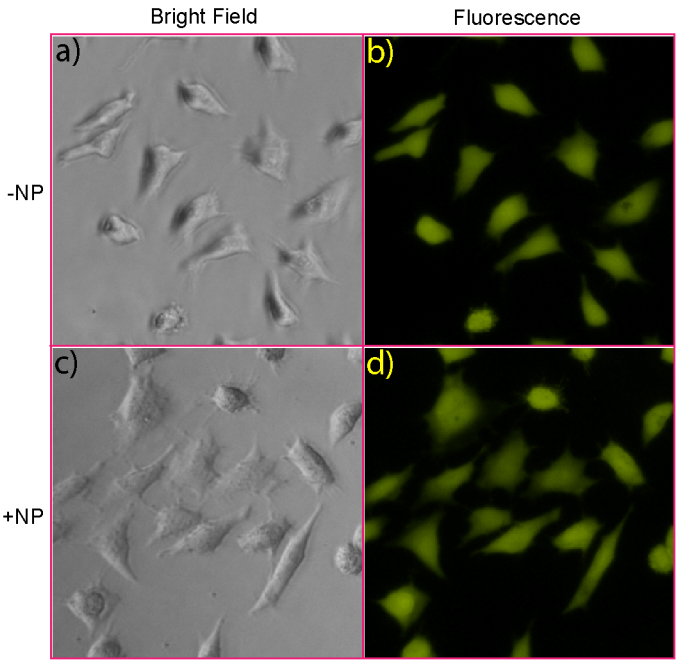

Figure 6.12: Green fluorescence from cells after calcein AM assay indicating they are alive.

6.3 Conclusion

In summary, we have reported a highly efficient strategy for intracellular protein delivery. Supramolecular complexes with engineered nanoparticles were shown to translocate exogeneous proteins into a variety of cells without exhibiting any cytotoxicity. Crucially, the transported enzyme was able to escape from endosmes and retained its biological activity, providing the potential for fundamental and therapeutic applications of this strategy. We are currently investigating delivery of therapeutic proteins.

6.4 Experimental Section

Materials. All chemicals were bought from Aldrich unless otherwise stated. The organic solvents were purchased from EMD and used as received except

dichloromethane and toluene which were distilled in presence of calcium hydride. For purification, flash column chromatography was performed using silica gel (SiO_2, particle size 40-63 μm). Amino acids and resin were purchased from Advanced ChemTech (USA). *β*-Gal, cell culture medium powder and phosphate buffer saline (PBS) were purchased from Sigma. FM 4-64 was purchased from Molecular Probes (Invitrogen, USA).

Synthesis of peptide-conjugated ligand. The peptide was synthesized manually, using standard Fmoc chemistry with Rink resin (0.7 mg/g) as a solid support. Side-chain protecting groups were as follows: trityl-chloride (Trt) for histidine; 2,2,5,7,8-pentamethylchroman-6-sulfonyl (Pmc) for arginine; *tert*-butoxycarbonyl (Boc) for lysine. Fmoc deprotection was carried out using 20% piperidine in DMF for 15 min, and amino acid (5 eq) coupling was performed using HBTU (5 eq), HOBt (5 eq) and DIPEA (10 eq) in DMF for 1 h (Figure 6.13).

The trityl-protected thiol linker (5 eq) was conjugated to the peptide using 1,3-diisopropylcarbodiimide (DIC, 6 eq) and HOBt (7.5 eq) in a overnight reaction. The thiol linked peptide was cleaved/deprotected for 1.5 h using *Reagent B*: 88% trifluoroacetic

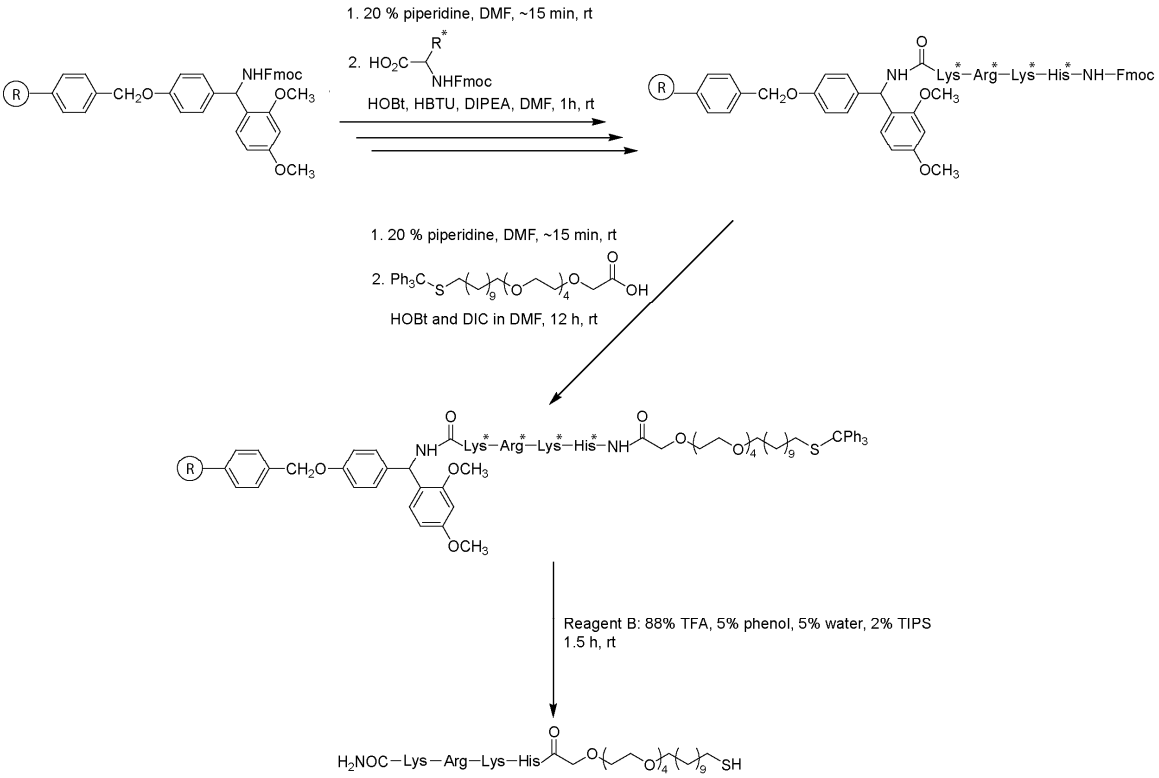

Figure 6.13: The procedures for peptide-ligand synthesis (* indicates protected side chains).

acid (TFA), 5% phenol, 5% water and 2% triisopropylsilane (TIPS). TFA was then removed under vacuum, and the ligand was precipitated with cold diethylether. The crude product was purified by reverse phase high pressure liquid chromatography (RP-HPLC) and then analyzed by mass spectrometry (calculated 986.6, obtained 987.6; $M+H^+$) (Figure 6.14).

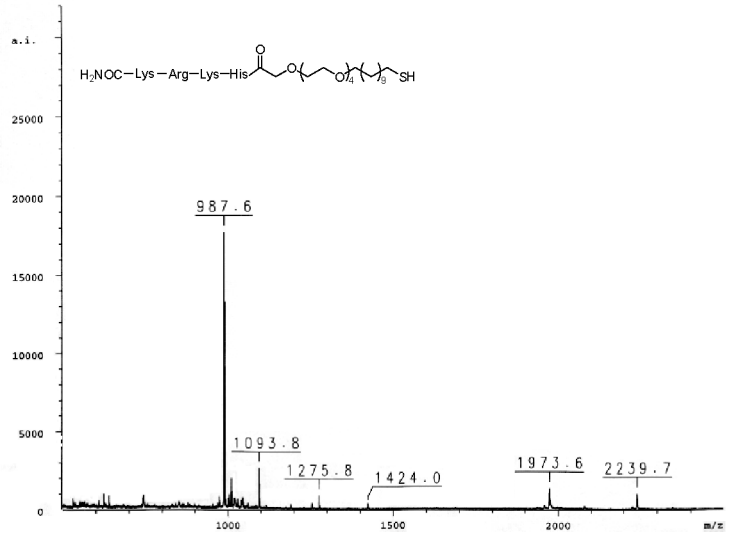

Figure 6.14: The MALDI-TOF mass spectra of the synthesized peptide ligand.

Synthesis of functionalized gold nanoparticle. 1-Pentanethiol-coated gold nanoparticles (10 mg) were dissolved in dichloromethane (DCM), and peptide ligands (20 mg) were taken in methanol. After purging argon into them separately for 30 min, they were mixed together and stirred for ~2 days at room temperature (Figure 6.15). Then solvents were rotavaped, and excess ligands were washed away with DCM-methanol (20:1, v/v; 5X)) followed by dialysis (cut off 10 kDa, Pierce) for 2 days. Absence of free ligand was verified by NMR, and particles were characterized by UV, DLS and TEM (Figure 6.16).

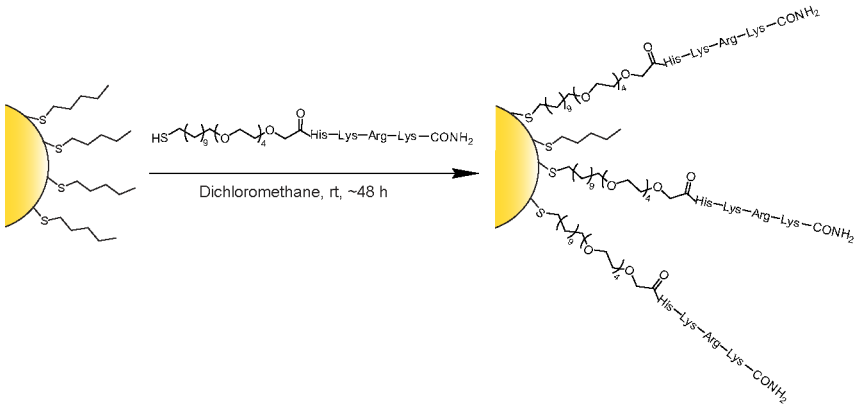

Figure 6.15: Functionalization of nanopaticles via Murray place-exchange reaction.

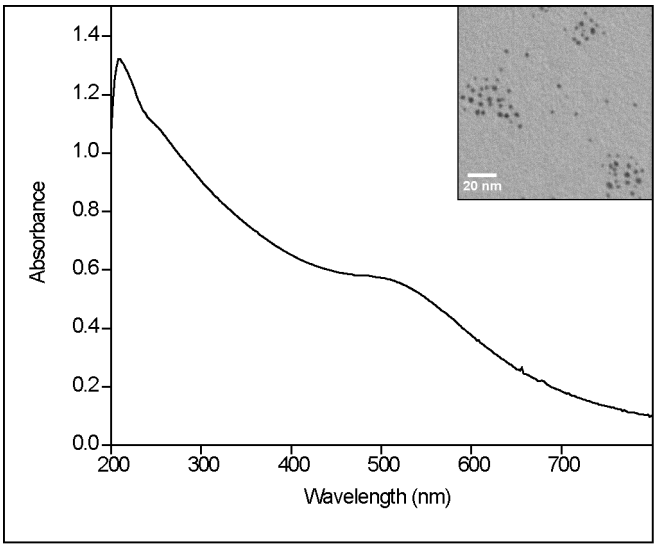

Figure 6.16: UV spectra and TEM image of the peptide functionalized gold nanoparticles.

Labeling of *β*-gal with FITC. Fluorescein isothiocyanate isomoer I (FITC) was dissolved in dimethyl sulfoxide at a concentration of 4 mg/mL. The *β*-gal (2.5mg) was dissolved in 900 μL of 0.1 M sodium bicarbonate solution (pH 9.0), and mixed with 250 μL freshly prepared FITC solution. The mixture was protected from light and stirred at room temperature for 2 h. The resulting FITC labeled *β*-gal was purified by size exclusion chromatography with Sephadex G-25 as stationary phase and phosphate buffer (5mM, pH 7.4) as mobile phase. Finally, the *β*-gal concentration and labeling efficiency (*β*-gal:FITC=1:16) were measured by ultraviolet-visible absorption spectroscopy.

***β*-Gal-nanoparticle binding experiment.** FITC-*β*-gal (100 nM) was mixed with **NP_Pep** at various molar ratios in 5 mM phosphate buffer (pH 7.4) for 10 min at room temperature. The fluorescence was recorded on a Spectro-Max M5 microplate reader (Molecular Device) (Ex 490 nm and Em 520 nm). Absorbance due to nanoparticles was corrected with control TEG-OH nanoparticle.[47] The corrected intensities were plotted and

fitted with a nonlinear equation (eqn 1) using Origin 8, providing K_D value (0.97 ± 0.58 nM) and binding ratio (**NP_Pep**:β-gal = ~ 8:1).[42] The effect of salt on the complex (**NP_Pep**:β-gal = 8:1) was monitored for 2 h.

$$\frac{I}{I_0} = \frac{\alpha}{2}\{([\beta\text{-gal}]_0 + n[NP]_0 + 1/K_s) - \sqrt{([\beta\text{-gal}]_0 + n[NP]_0 + 1/K_s)^2 - 4n[\beta\text{-gal}]_0[NP]_0}\} \quad \text{eqn 1}$$

Where K_s = association constant, n = binding ratio (considering identical binding site)

Circular Dichroism. CD spectra of β-gal (100 nM) were taken with or without nanoparticles (200 nM) in 5 mM phosphate buffer after 10 min of complexation. It was performed on a Jasco 720 spectrophotometer using a quartz cuvette of 1-mm path length. After equilibration at 25 ºC for 5 min, the spectra were acquired by scanning from 250 nm to 190 nm. Average of three scans was recorded at a rate of 20 nm/min with 8 sec response and 0.1 nm interval. The final spectra were obtained by subtracting the blank one and it was fitted into secondary structure algorithm CDSSTR (protein ref. set 7 comprising of 49 proteins, http://www.cryst.bbk.ac.uk/cdweb/html/home.html) using DICHROWEB.

Tryptophan fluorescence measurement. Fluorescence spectra were measured in a 1 cm quartz cuvette on a Photon Technology International fluorescence spectrometer at 25 °C. Tryptophan fluorescence was monitored at 310~450 nm wavelength by exciting at 295 nm. Spectra of 100 nM of β-gal solution were collected without/with **NP_Pep** (200 nM) in 5 mM phosphate buffer (pH 7.4) at 25 °C.

Cell culture. HeLa cells were cultured in a humidified atmosphere (5% CO_2) at 37 °C, and grown in Dulbecco's modified eagle's medium (DMEM, low glucose) supplemented with 10% fetal bovine serum (FBS, Aldrich). C2C12 and COS-1 cells were cultured in high glucose media (DMEM, high glucose) with 10% FBS. MCF7 cells were cultured in low glucose media (DMEM, low glucose) with 10% FBS.

***β*-Gal delivery.** Cells (HeLa: $3x10^4$ per well, C2C12: 6×10^4 per well, COS-1: $6x10^4$ per well) were seeded on 24 well plate. Next day the *β*-gal-nanoparticle mixture was added onto cells after washing with phosphate buffer saline (PBS). *β*-Gal was mixed with **NP_Pep** in 5 mM phosphate buffer (pH 7.4) for 10 min, and then diluted 6X with DMEM without serum. The cells were incubated with the transfection medium (protein-nanoparticle complex in DMEM without serum) for 3 h, and then washed with PBS (3X) followed by another 3h of culture in DMEM with 10 % FBS.

Fluorescence and confocal microscopy. Cells were washed twice with PBS before capturing images. Fluorescence pictures were taken on an Olympus IX51 inverted microscope keeping all parameters the same for different samples. Confocal pictures were obtained on a Zeiss LSM 510 Meta microscope using a 40X objective.

ICP- MS measurements. ICP-MS measurements were performed on a Perkin-Elmer Elan 6100. The operating conditions were as follows: RF power: 1250 W; plasma Ar flow rate: 15 L/min; nebulizer Ar flow rate: 0.96 L/min; dwell time: 50 ms; nebulizer: cross-flow; spray camber: Scott.

After enzyme **(NP_Pep**/*β*-gal: 100 nM/50 nM**)** delivery, cells were washed twice with PBS and then lysis buffer (250 µL/well, 30 min; Genlantis, USA) was added. Cell lysate was digested overnight with 3 mL nitric acid and 1 ml of hydrogen peroxide. The

following morning, 1 ml of freshly prepared aqua regia (caution!) was added and allowed to react with the sample for one more hour. The sample was heated to 100 °C to reduce volume of the above digestion to ~1 mL. It was then diluted to 10 mL using a volumetric flask with ultra pure water and additional aqua regia (5% final concentration). Each sample was measured in quadruplet via ICP-MS as described above. A series of gold standards containing 5% aqua regia was prepared and ran prior to the samples (20, 10, 5, 2, 1, 0.5, 0.2, 0 ppb). The gold uptake in each sample was determined from the resulting calibration line. Deionized water was used to wash the instrument between each sample analysis.

X-gal assay. Cells were stained according to the assay kit (Genlantis, USA). After 12 h of staining, cells were washed once with PBS and observed under an optical microscope (Nikon/Spot-RT). Experiments were performed in duplicate. For counting, four pictures (each having ~30 cells) were taken randomly from each replica and then averaged.

Cytotoxicity assays. A trypan blue exclusion test was performed to count live cells. After transfction with mentioned concentration of β-gal at molar ratio of 2, cells were cultured for some period (3 h or 24 h) and then they were trypsinized. Then cells were centrifuged, redispersed in PBS, mixed with 1:1 trypan blue (Fluka) and counted (duplicate, more than 100 cells for each replicate) on hemocytometer.

Live/dead cells were also assayed using **calcein AM** (Viability/Cytotoxicity Kit, Invitroge, USA) after transfection with **NP_Pep**/ β-gal (200 nM/100 nM) according to the manufacturer's protocol.

The alamar blue assay was carried out following the manufacturer's protocol (Invitrogen Biosource, 102SA). After delivery, cells were treated with 10% alamar blue solution and kept at 37 °C for another 2 h. Red fluorescence, resulting from the reduction of alamar blue, was monitored (Ex: 560 nm, Em: 590 nm) on a SpectroMax M5 microplate reader (Molecular Device).

6.5 References

Notes

1. Mitragotri, S.; Blankschtein, D.; Langer, R. *Science* **1995**, *269*, 850.

2. Kobsa, S.; Saltzman, W. M. *Pediatr. Res.* **2008**, *63*, 513.

3. Gombotz, W. R.; Pettit, D. K. *Bioconjugate Chem.* **1995**, *6*, 332.

4. Schwarze, S. R.; Ho, A.; Vocero-Akbani, A.; Dowdy, S. F. *Science* **1999**, *285*, 1569.

5. Murthy, N.; Xu, M. C.; Schuck, S.; Kunisawa, J.; Shastri, N.; Frechet, J. M. J. *Proc. Natl. Acad. Sci. U.S.A.* **2003**, *100*, 4995.

6. Phelan, A.; Elliott, G.; O'Hare, P. *Nat. Biotechnol.* **1998**, *16*, 440.

7. Morris, M. C.; Depollier, J.; Mery, J.; Heitz, F.; Divita, G. *Nat. Biotechnol.* **2001**, *19*, 1173.

8. Myrberg, H.; Lindgren, M.; Langel, U. *Bioconjugate Chem.* **2007**, *18*, 170.

9. Slowing, I. I.; Trewyn, B. G.; Lin, V. S. Y. *J. Am. Chem. Soc.* **2007**, *129*, 8845.

10. Kam, N. W. S.; Jessop, T. C.; Wender, P. A.; Dai, H. J. *J. Am. Chem. Soc.* **2004**, *126*, 6850.

11. Medintz, I. L.; Pons, T.; Delehanty, J. B.; Susumu, K.; Brunel, F. M.; Dawson, P. E.; Mattoussi, H. *Bioconjugate Chem.* **2008**, *19*, 1785.

12. Bhattacharya, R.; Mukherjee, P. *Adv. Drug Deliv.Rev.* **2008**, *60*, 1289.

13. Ghosh, P.; Han, G.; De, M.; Kim, C. K.; Rotello, V. M. *Adv. Drug Deliv. Rev.* **2008**, *60*, 1307.

14. De, M.; Ghosh, P. S.; Rotello, V. M. *Adv. Mater.* **2008**, *20*, 4225.

15. Nativo, P.; Prior, I. A.; Brust, M. *Acs Nano* **2008**, *2*, 1639.

16. Verma, A.; Uzun, O.; Hu, Y. H.; Hu, Y.; Han, H. S.; Watson, N.; Chen, S. L.; Irvine, D. J.; Stellacci, F. *Nature Mater.* **2008**, *7*, 588.

17. Pujals, S.; Bastus, N. G.; Pereiro, E.; Lopez-Iglesias, C.; Punte, V. F.; Kogan, M. J.; Giralt, E. *Chembiochem* **2009**, *10*, 1025.

18. Rosi, N. L.; Giljohann, D. A.; Thaxton, C. S.; Lytton-Jean, A. K. R.; Han, M. S.; Mirkin, C. A. *Science* **2006**, *312*, 1027.

19. Ghosh, P. S.; Kim, C. K.; Han, G.; Forbes, N. S.; Rotello, V. M. *Acs Nano* **2008**, *2*, 2213.

20. Paciotti, G. F.; Kingston, D. G. I.; Tamarkin, L. *Drug Develop. Res.* **2006**, *67*, 47.

21. Jones, S.; Thornton, J. M. *Proc. Natl. Acad. Sc. U.S.A.* **1996**, *93*, 13.

22. You, C. C.; Verma, A.; Rotello, V. M. *Soft Matter* **2006**, *2*, 190.

23. Verma, A.; Simard, J. M.; Worrall, J. W. E.; Rotello, V. M. *J. Am. Chem. Soc.* **2004**, *126*, 13987.

24. Hong, R.; Fischer, N. O.; Verma, A.; Goodman, C. M.; Emrick, T.; Rotello, V. M. *J. Am. Chem. Soc.* **2004**, *126*, 739.

25. Holowka, E. P.; Sun, V. Z.; Kamei, D. T.; Deming, T. J. *Nature Mat.* **2007**, *6*, 52.

26. Rothbard, J. B.; Jessop, T. C.; Wender, P. A. *Adv. Drug Deliv. Rev.* **2005**, *57*, 495.

27. Mitchell, D. J.; Kim, D. T.; Steinman, L.; Fathman, C. G.; Rothbard, J. B. *J. Pep. Res.* **2000**, *56*, 318.

28. Rothbard, J. B.; Garlington, S.; Lin, Q.; Kirschberg, T.; Kreider, E.; McGrane, P. L.; Wender, P. A.; Khavari, P. A. *Nat. Med.* **2000**, *6*, 1253.

29. Koch, A. M.; Reynolds, F.; Merkle, H. R.; Weissleder, R.; Josephson, L. *Chembiochem* **2005**, *6*, 337.

30. Ghosh, P. S.; Han, G.; Erdogan, B.; Rosado, O.; Krovi, S. A.; Rotello, V. M. *Chem. Biol. Drug Des.* **2007**, *70*, 13.

31. Wang, K. W.; Yan, X. H.; Cui, Y.; He, Q.; Li, J. B. *Bioconjug. Chem.* **2007**, *18*, 1735.

32. Benns, J. M.; Choi, J. S.; Mahato, R. I.; Park, J. S.; Kim, S. W. *Bioconjugate Chem.* **2000**, *11*, 637.

33. Pichon, C.; Goncalves, C.; Midoux, P. *Adv. Drug Deliv. Rev.* **2001**, *53*, 75.

34. Futaki, S. *Adv. Drug Deliv. Rev.* **2005**, *57*, 547.

35. Midoux, P.; Monsigny, M. *Bioconjugate Chem.* **1999**, *10*, 406.

36. Wang, K. W.; Yan, X. H.; Cui, Y.; He, Q.; Li, J. B., *Bioconjugate Chem.* **2007,** *18*, 1735.

37. Ghosh, P. S.; Verma, A.; Rotello, V. M. *Chem Commun.* **2007**, 2796.

38. Miranda, O. R.; You, C. C.; Phillips, R.; Kim, I. B.; Ghosh, P. S.; Bunz, U. H. F.; Rotello, V. M. *J. Am. Chem. Soc.***2007**, *129*, 9856.

39. Lu¨hmann, T.; Rimann, M.; Bittermann, A. G.; Hall, H. *Bioconjugate Chem.* **2008**, *19*, 1907.

40. Blondeau, P.; Segura, M.; Perez-Fernandez, R.; de Mendoza, J. *Chem. Soc. Rev.* **2007**, *36*, 198.

41. Salvatella, X.; Martinell, M.; Gairi, M.; Mateu, M. G.; Feliz, M.; Hamilton, A. D.; de Mendoza, J.; Giralt, E. *Angew. Chem. Int. Ed.* **2004**, *43*, 196.

42. You, C. C.; De, M.; Han, G.; Rotello, V. M. *J. Am. Chem. Soc.* **2005**, *127*, 12873.

43. Kosuge, M.; Takeuchi, T.; Nakase, I.; Jones, A. T.; Futaki, S. *Bioconjugate Chem.* **2008**, *19*, 656.

44. Khalil, I. A.; Kogure, K.; Akita, H.; Harashima, H. *Pharma. Rev.* **2006**, *58*, 32.

45. Vida, T. A.; Emr, S. D. *J. Cell Biol.* **1995**, *128*, 779.

46. Yamanouchi, D.; Wu, J.; Lazar, A. N.; Kent, K. C.; Chu, C. C.; Liu, B. *Biomaterials* **2008**, *29*, 3269.

47. Ghosh, P. S.; Han, G.; Erdogan, B.; Rosado, O.; Krovi, S. A.; Rotello, V. M. *Chem. Biol. Drug Des.* **2007**, *70*, 13-18.

CHAPTER 7

CONCLUSION AND FUTURE DIRECTIONS

The enormous power of synthetic chemistry could enable to tailor the surface coating of nanoparticles in any way we desire. As described in the previous chapters, this surface coating plays a pivotal role for communicating with biological systems. With proper design of ligand structure, we were able to use functionalized gold nanoparticles for controlling their interactions with biomolecules and delivery of therapeutics. Needless to say, more in depth investigations are required to achieve a feasible nanocarrier of therapeutics. In this chapter, some important factors to be considered have been outlined and on-going research is focusing on those aspects.

7.1 Cellular Uptake of Nanoparticles

Cellular uptake of nanoparticles is likely to be most influenced by surface functionality, as it is initiated through recognition at the plasma membrane. While small molecules (molecular weight < 500 Da) can easily diffuse through membrane, intake of nano-sized materials occurs through specific and/or non-specific interaction(s) with the cell surface.[1] Non-specific adsorption will depend on the nature of the surface charge and its density. Normally cationic nanoparticles strongly interact with cell surface through favorable electrostatic interaction, while anionic/neutral/zwitterionic particles are expected to be less readily internalized.[2]

Low uptake of zwitterionic particles can reduce the possible cytotoxicity. Considering this factor and the fact that these particles have strong resistance to serum

protein adsorption, we chose them as a carrier of small molecular drugs. Hydrophobic drugs/dyes were loaded into the "hydrophobic pocket" of NPs with high stability. We have also demonstrated release of caged molecules into cancer cells by membrane-mediated diffusion without uptake of the carrier nanoparticle (Figure 7.1). This study has been published recently in *Journal of the American Chemical Society* (**2009**, *131*, 1360). Importantly, the small size of these nanocarriers coupled with their biocompatible surface functionality should provide long circulation lifetimes and preferential accumulation in tumor tissues by the enhanced permeability and retention (EPR) effect. Additionally, the non-interacting nature of their monolayer should make these systems highly amenable to targeting strategies.

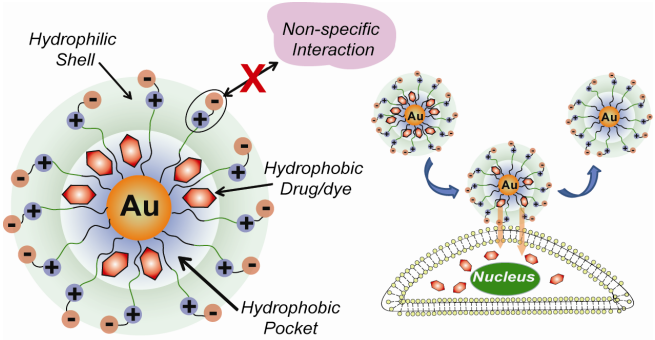

Figure 7.1: Entrapment of hydrophobic molecules into the NP monolayer and delivery of payload to cell through monolayer-membrane interactions.

7.2 Looking into the Uptake Mechanism

Surface functionalization could dictate the uptake pathway and the localization of nanoparticles into cellular compartments. A class of peptides, termed as cell penetrating peptides (CPPs), has been developed to promote efficient crossing of cell membrane barrier.[3] The CPPs are able to transport attached nanoparticles from the extracellular space through the cell membrane into the cytoplasm. In a recent study, Stellacci *et al.* have demonstrated that distribution of hydrophobic ligands on particle surface could

regulate cellular uptake of nanoparticles – 'striped' nanoparticles slipped through membrane, but 'unstructured' particles were less readily internalized.[4]

Targeting to specific organelles is of great importance in order to enhance the therapeutic efficacy. However, cytosolic delivery of payloads from nanocarriers is limited mainly by their endosomal entrapment. Nie *et al.* reported cell-penetrating quantum dots (QDs) with endosomal disrupting surface coatings.[5] The authors showed that the polyethylene glycol (PEG) grafted and hyperbranched polyethylenimine (PEI) coated QDs were able to escape from acidic intracellular organelles to cytoplasm. To this end, we are also investigating the uptake mechanism of only nanoparticles or their complexes with biomolecules. As shown in the TEM image (Figure 7.2), a large amount of gold nanoparticles (NP_Me) were trapped inside vesicles in the cytoplasm (most likely via endosomal entrapment). In some cases, we have used additives like chloroquine to assist in endosome disruption.

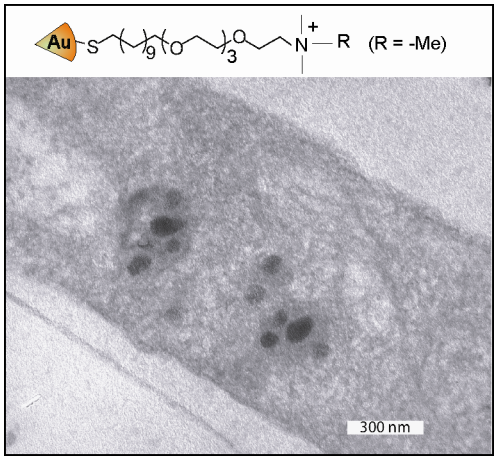

Figure 7.2: Transmission electron microscopy (TEM) image of fixed cell (HeLa) treated with NP_Me.

7.3 Toxicity of Nanoparticles

Concurrent with uptake studies, toxicity of the nanoparticles should be assessed carefully for their use as drug delivery agents. As the particles are intentionally designed to interact with cells, there is always a concern about possible adverse effects.[6] *In vitro* cytotoxicity assays, such as the alamar blue assay (metabolic activity), calcein AM and ethidium homodimer assay (live/dead), and trypan blue exclusion test (membrane integrity) are only the starting point. They should be carried out in different cell lines with various incubation times. Hemolysis is another issue in the design of drug delivery agents.[7,8] It is important to balance delivery efficiency with hemolytic activity (colorimetric assay using Drabkin's reagent) to create useful delivery agents. Genotoxicity of these particles should be considered as well. In this regard, measurements are required for DNA damage, generation of reactive oxygen species (ROS), or any change in gene expression.

To provide insight into the origins of toxicity of funtionalized gold nanoparticles, we used MTT, hemolysis, and bacterial viability assays to explore differential toxicity among cell types, using 2 nm core particles featuring cationic and anionic functionality.[9] These studies show that cationic particles are moderately toxic, with relatively little discrimination between erythrocytes, Cos-1 cells, and E. coli. In contrast, anionic particles are quite non-toxic, with no effect observed on cell viability at any of the concentrations studied. The probable mechanism for toxicity was established as lysis through dye release studies using lipid vesicles. As discussed earlier, cationic headgroups facilitate cell membrane penetration. Therefore, we are studying cytotoxicity and genotoxicity of cationic particles by varying the alkyl tail length (Figure 7.3). The results

indicated that the cell viability decreased by the particles with longer alkyl chains (NP_Me>NP_Et>NP_Bu>NP_Hex). However, NP_Me caused extensive DNA damage as observed in a comet assay.

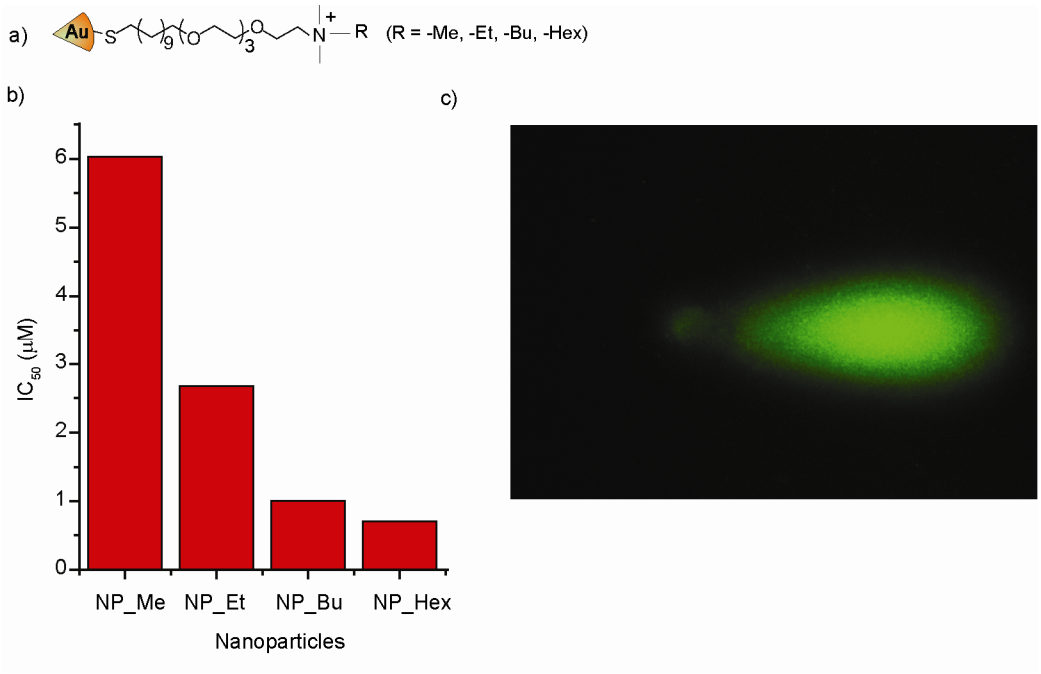

Figure 7.3: A study on toxicity of cationic particles: (b) alamar blue assay for measuring metabolic activity and (c) comet assay of cells treated with NP_Me.

7.4 *in vivo* Targeting

For *in vivo* applications, the goal of nanocarriers is to arrive at the diseased tissues after administration into circulatory system. Two approaches have been developed for targeting – namely 'passive' and 'active' targeting (Figure 7.4).[10,11] 'Passive' targeting depends on homing of the vectors in unhealthy tissues due to extravasation through leaky (gaps ~ 600 nm) blood vessels. An important aspect of carrier systems in the 5-10 nm scale is their ability to take advantage of the enhanced permeation and retention (EPR) effect (Figure 7.4).[12] On the other hand, 'active' targeting presents ligands on the carrier surface for specific recognition by cell surface receptors. The ligands could be small

molecules, peptides or proteins. Combination of both types of targeting will render an ideal carrier for *in vivo* delivery.

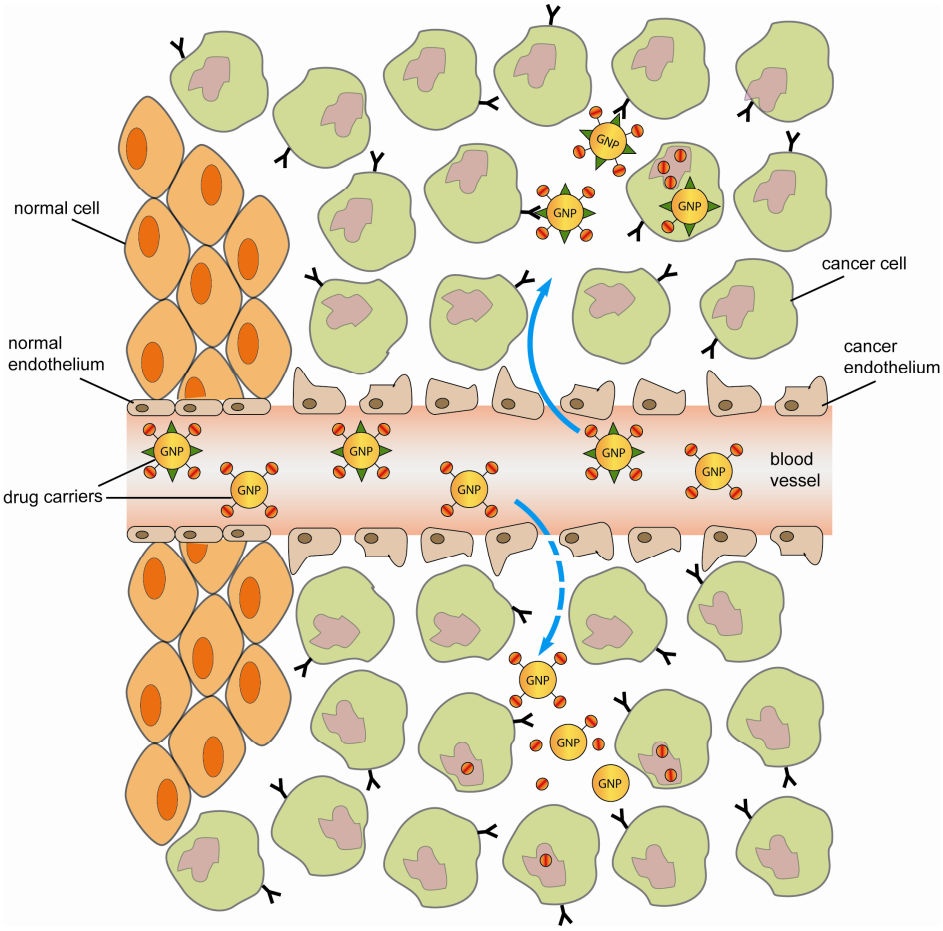

Figure 7.4: A schematic illustration of drug delivery via 'active' (solid line) and 'passive' (dotted line) targeting.

Nanocarriers suffer from non-specific uptake and potential degradation in macrophages. Therefore, targeting is crucial for maximizing drug efficacy while minimizing side effects. Pun *et al.* have studied how different physicochemical properties, such as size, PEGylation, or the ligand, regulate nonspecific versus target-specific uptake of nanoparticles.[13] They concluded that (a) PEGylation increased blood circulation life-time (comparing unmodified-NP and PEG-NP), (b) Galactose, a ligand, facilitated filtration of Gal-PEG-NPs into liver (comparing PEG-NP and Gal-PEG-NP),

and (c) the ligand rendered cell-specific targeting of hepatocytes. Folic acid (FA) and methotrexate (MTX) have been exploited by several groups as targeting molecules.[14] They are specifically recognized by folate receptors that are overexpressed on the surfaces of many tumor cells.

We have considered these known targeting molecules, like folic acid and galactose, for conjugation with our delivery systems. At the same time, using multiplexed screening ability of our newly developed tool as described in chapter 4, we are looking into finding new targeting molecules. In a preliminary study, we have already seen some degree of differentiation in uptake of the cationic particles between two cell lines (Cos-1 and SVR-Bag 4) we tried.

7.5 Outlook

Nanomaterials are now not only confined inside the four walls of a research laboratory, they have started to reach into market slowly. According to a 2008 report, more than 186 nanotech-based drugs and delivery systems have entered into preclinical or clinical trials worldwide.[15] Gold nanoparticles have emerged as a promising scaffold for delivery of therapeutics that provides a useful complement to more traditional delivery vehicles. The combination of low inherent toxicity, high surface area, and tunable stability provides them with unique attributes that should enable new delivery vectors. Full realization of their potential, however, requires addressing a number of open issues, such as acute and long-term health and environmental effects of nanomaterials, as well as scalable, reproducible manufacturing methods for these materials.

7.6 References

Notes

1. Mitragotri, S.; Blankschtein, D.; Langer, R. *Science* **1995**, *269*, 850.

2. Kim, C. K.; Ghosh, P.; Pagliuca, C.; Zhu, Z.-J.; Menichetti, S.; Rotello, V. M. *J. Am. Chem. Soc.* **2009**, *131*, 1360.

3. El-Andaloussi, S.; Holm, T.; Langel, U. *Curr. Pharm. Design.* **2005**, *11*, 3597.

4. Verma, A.; Uzun, O.; Hu, Y.; Hu, Y.; Han, H.-S.; Watson, N.; Chen, S.; Irvine, D. J.; Stellacci, F. *Nature Mater.* **2008**, *7*, 588.

5. Duan, H. W.; Nie, S. M. *J. Am. Chem. Soc.* **2007**, *129*, 3333.

6. Lewinski, N.; Colvin, V.; Drezek, R. *Small* **2008**, *1*, 26.

7. Moreau, E.; Domurado, M.; Chapon, P.; Vert, M.; Domurado, D. *J. Drug Target.* **2002**, *10*, 161.

8. Yalkowsky, S. H.; Krzyzaniak, J. F.; Ward, G. H. *J. Pharm. Sci.* **1998**, *87*, 787.

9. Goodman, C. M.; McCusker, C. D.; Yilmaz, T.; Rotello, V. M. *Bionconjugate Chem.* **2004**, *15*, 897.

10. Brannon-Peppas, L.; Blanchette, J. O. *Adv. Drug Deliver. Rev.* **2004**, *56*, 1649.

11. Brigger, I.; Dubernet, C.; Couvreur, P. *Adv. Drug Deliv. Rev.* **2002**, *54*, 631.

12. Baban, D.F.; Seymour, L.W. *Adv. Drug Deliv. Rev.* **1998**, *34*, 109.

13. Bergen, J.M.; Von Recum, H.A.; Goodman, T.T.; Massey, A.P.; Pun, S.H. *Macromol. Biosci.* **2006**, *6*, 506.

14. Dixit, V.; Van den Bossche, J.; Sherman, D.M.; Thompson, D.H.; Andres, R.P. *Bioconjugate Chem.* **2006**, *17*, 603.

15. Xia, Y. *Nature Mater.* **2008**, *7*, 758.

BIBLIOGRAPHY

Abad, M. ; Mertens, S. F. L. ; Pita, M. ; Fernandez, V. M. ; Schiffrin, D. J. *J. Am. Chem. Soc.* **2005**, *127*, 5689.

Allen, T. M. ; Cullis, P. R. *Science* **2004**, *303*, 1818.

Andre, I.; Linse, S.; Mulder, F. A. A. *J. Am. Chem. Soc.* **2007**, *129*, 15805.

Archakov, A. I.; Govorun, V. M.; Dubanov, A. V.; Ivanov, Y. D.; Veselovsky, A. V.; Lewi, P.; Janssen, P. *Proteomics* **2003,** *3*, 380.

Armitage, B. A. *DNA Binders and Related Subjects*, **2005**, *253*, 55.

Baban, D.F.; Seymour, L.W. *Adv. Drug Deliv. Rev.* **1998**, *34*, 109.

Balakirev, M.; Schoehn, G.; Chroboczek, J. *Chem. Biol.* **2000**, *7*, 813.

Bayraktar, H.; Ghosh, P. S.; Rotello, V. M.; Knapp, M. J. *Chem. Commun.* **2006**, 1390.

Benns, J. M.; Choi, J. S.; Mahato, R. I.; Park, J. S.; Kim, S. W. *Bioconjugate Chem.* **2000**, *11*, 637.

Bergen, J.M.; Von Recum, H.A.; Goodman, T.T.; Massey, A.P.; Pun, S.H. *Macromol. Biosci.* **2006**, *6*, 506.

Bhattacharya, R.; Mukherjee, P. *Adv. Drug Deliv.Rev.* **2008**, *60*, 1289.

Bhattacharya, R.; Mukherjee, P.; Xiong, Z.; Atala, A.; Soker, S.; Mukhopadhyay, D. *Nano Lett.* **2004**, *4*, 2479.

Bhattacharya, R.; Patra, C. R.; Earl, A.; Wang, S. F.; Katarya, A.; Lu, L. C.; Kizhakkedathu, J. N.; Yaszemski, M. J.; Greipp, P. R.; Mukhopadhyay, D. *et al. Nanomedicine* **2007**, *3*, 224.

Blanco, J. B.; Vazquez, O.; Martinez-Costas, J.; Castedo, L.; Mascarenas, J. L. *Chem.-A Eur. J.* **2005**, *11*, 4171.

Blondeau, P.; Segura, M.; Perez-Fernandez, R.; de Mendoza, J. *Chem. Soc. Rev.* **2007**, *36*, 198.

Blow, D. M. *Acc. Chem. Res.* **1976**, *9*, 145.

Boal, A. K.; Rotello, V. M. *J. Am. Chem. Soc.* **2000**, *122*, 734.

Boisselier, E.; Astruc, D. *Chem. Soc. Rev.* **2009**, *38*, 1759.

Boussif, O.; Lezoualch, F.; Zanta, M. A.; Mergny, M. D.; Scherman, D.; Demeneix, B.; Behr, J. P. *Proc. Natl. Acad. Sci.* U.S.A. **1995**, *92*, 7297.

Brannon-Peppas, L.; Blanchette, J. O. *Adv. Drug Deliver. Rev.* **2004**, *56*, 1649.

Brigger, I.; Dubernet, C.; Couvreur, P. *Adv. Drug Deliv. Rev.* **2002**, *54*, 631.

Brust, M.; Walker, M.; Bethell, D.; Schiffrin, D. J.; Whyman, R. *J. Chem. Soc., Chem. Commun.* **1994**, 801.

Caruso, F. *Adv. Matter.* **2001,** *13*, 11.

Castellana, E. T.; Russell, D. H. *Nano Lett.* **2007**, *7*, 3023.

Cavazzana-Calvo, M.; Thrasher, A.; Mavilio, F. *Nature* **2004**, *427*, 779.

Check, E. *Nature* **2005**, *433*, 561.

Cheng, R. P.; Gellman, S. H.; DeGrado, W. F. *Chem. Rev.* **2001**, *101*, 3219.

Chithrani, B. D.; Ghazani, A. A.; Chan, W. C. W. *Nano Lett.* **2006**, *6*, 662.

Chowdhury, E. H.; Akaike, T. *Curr. Gene Ther.* **2005**, *5*, 669.

Connor, E. E.; Mwamuka, J.; Gole, A.; Murphy, C. J.; Wyatt, M. D. *Small* **2005**, *1*, 325.

D'Andrea, L. D.; Iaccarino, G.; Fattorusso, R.; Sorriento, D.; Carannante, C.; Capasso, D.; Trimarco, B.; Pedone, C. *Proc. Natl. Acad. Sci. U. S. A.* **2005**, *102*, 14215.

Daniel, M. C.; Astruc, D. *Chem. Rev.* **2004**, *104*, 293.

Davis, M. E. *Curr. Opin. Biotechnol.* **2002**, *13*, 128.

de Lima, M. C. P.; Neves, S.; Filipe, A.; Duzgunes, N.; Simoes, S. *Curr. Med. Chem.* **2003**, *10*, 1221.

De, M.; Ghosh, P. S.; Rotello, V. M. *Adv. Mater.* **2008**, *20*, 4225.

Derfus, A. M.; Chen, A. A.; Min, D. H.; Ruoslahti, E.; Bhatia, S. N. *Bioconjugate Chem.* **2007**, *18*, 1391.

Derfus, A. M.; Maltzahn, G.; Harris, T. J.; Duza, T.; Vecchio, K. S.; Ruoslahti, E.; Bhatia, S. N. *Adv. Mater.* **2007**, *19*, 3932.

Dervan, P. B. *Bioorg. & Med. Chem.* **2001**, *9*, 2215.

Dixit, V.; Van den Bossche, J.; Sherman, D.M.; Thompson, D.H.; Andres, R.P. *Bioconjugate Chem.* **2006**, *17*, 603.

Droz, E.; Taborelli, M.; Descouts, P.; Wells, T. N. C.; Werlen, R. C. *J. Vac. Sci. Technol. B* **1996**, *14*, 1422.

Duan, H. W.; Nie, S. M. *J. Am. Chem. Soc.* **2007**, *129*, 3333.

Dufes, C.; Uchegbu, I. F.; Schatzlein, A. G. *Adv. Drug Delivery Rev.* **2005**, *57*, 2177.

Dykes, G. M.; Brierley, L. J.; Smith, D. K.; McGrail, P. T.; Seeley, G. J. *Chem. Eur. J.* **2001**, *7*, 4730.

El-Andaloussi, S.; Holm, T.; Langel, U. *Curr. Pharm. Design.* **2005**, *11*, 3597.

Fairlie, D. P.; West, M. L.; Wong, A. K. *Curr. Med. Chem.* **1998**, *5*, 29.

Fazal, M. A.; Roy, B. C.; Sun, S. G.; Mallik, S.; Rodgers, K. R. *J. Am. Chem. Soc.* **2001**, *123*, 6283.

Ferrari, M. *Nat. Rev. Cancer* **2005**, *5*, 161.

Fischer, N. O.; McIntosh, C. M.; Simard, J. M.; Rotello, V. M. *Proc. Natl. Acad. Sci. U. S. A.* **2002**, *99*, 5018.

Fischer, N. O.; Verma, A.; Goodman, C. M.; Simard, J. M.; Rotello, V. M. *J. Am. Chem. Soc.* **2003**, *125*, 13387.

Fischer, P. M. *Curr. Protein Pep. Sci.* **2003**, *4*, 339.

Futaki, S. *Adv. Drug Deliv. Rev.* **2005**, *57*, 547.

Futaki, S.; Kiwada, T.; Sugiura, Y. *J. Am. Chem. Soc.* **2004**, *126*, 15762.

Gao, X.; Cui, Y.; Levenson, R. M.; Chung, L. W. K.; Nie, S. *Nat. Biotechnol.* **2004**, *22*, 969.

Ghosh, P. S.; Han, G.; Erdogan, B.; Rosado, O.; Krovi, S. A.; Rotello, V. M. *Chem. Biol. Drug Des.* **2007**, *70*, 13-18.

Ghosh, P. S.; Han, G.; Erdogan, B.; Rosado, O.; Rotello, V. M. *J. Pept. Sci.* **2008**, *14*, 134.

Ghosh, P. S.; Kim, C. K.; Han, G.; Forbes, N. S.; Rotello, V. M. *Acs Nano* **2008**, *2*, 2213.

Ghosh, P. S.; Verma, A.; Rotello, V. M. *Chem. Commun.* **2007**, 2796.

Ghosh, P.; Han, G.; De, M.; Kim, C. K.; Rotello, V. M. *Adv. Drug Deliv. Rev.* **2008**, *60*, 1307.

Ghosh, P.; Yang, X.; Arvizo, R.; Zhu, Z.-J.; Mo, Z.; Agasti, S. S.; Rotello, V. M. *Submitted to J. Am. Chem. Soc.*

Ghosh, S. S.; Kao, P. M.; McCue, A.W.; Chappelle, H. L. *Bioconjugate Chem*. **1990**, *1*, 71.

Giljohann, D. A.; Seferos, D. S.; Patel, P. C.; Millstone, J. E.; Rosi, N. L.; Mirkin, C. A. *Nano lett.* **2007**, *7*, 3818.

Giri, S.; Trewyn, B. G.; Stellmaker, M. P.; Lin, V. S. Y. *Angew. Chem. Int. Ed.* **2005**, *44*, 5038.

Gombotz, W. R.; Pettit, D. K. *Bioconjugate Chem.* **1995**, *6*, 332.

Gong, W.; Elitzin, V. I.; Janardhanam, S.; Wilkins, C. L.; Fritsch, I. *J. Am. Chem. Soc.* **2001**, *123*, 769.

Goodman, C. M.; Chari, N. S.; Han, G.; Hong, R.; Ghosh, P.; Rotello, V. M. *Chem. Biol. & Drug Design* **2006**, *67*, 297.

Goodman, C. M.; McCusker, C. D.; Yilmaz, T.; Rotello, V. M. *Bionconjugate Chem.* **2004**, *15*, 897.

Greenland, J. R.; Liu, H. N.; Berry, D.; Anderson, D. G.; Kim, W. K.; Irvine, D. J.; Langer, R.; Letvin, N. L. *Mol. Ther.* **2005**, *12*, 164.

Gu, H. W. ; Xu, K. M.; Xu, C. J. ; Xu, B. *Chem. Commun.* **2006**, 941.

Haack, T. ; Peczuh, M. W.; Salvatella, X.; Sanchez-Quesada, J. ; de Mendoza, J.; Hamilton, A. D. ; Giralt, E. *J. Am. Chem. Soc.* **1999**, *121*, 11813.

Hacein-Bey-Abina, S.; von Kalle, C.; Schmidt, M.; Le Deist, F.; Wulffraat, N.; McIntyre, E.; Radford, I.; Villeval, J. L.; Fraser, C. C.; Cavazzana-Calvo, M.; Fischer, A. *N. Engl. J. Med.* **2003**, *348*, 255.

Han, G.; Chari, N. S.; Verma, A.; Hong, R.; Martin, C. T.; Rotello, V. M. *Bioconjugate Chem.* **2005**, *16*, 1356.

Han, G.; Martin, C. T.; Rotello, V. M. *Chem. Biol. Drug Des.* **2006**, *67*, 78.

Han, G.; You, C.-C.; Kim, B.-J.; Turingan, R. S.; Forbes, N. S.; Martin, C. T.; Rotello, V. M. *Angew. Chem. Int. Ed.* **2006**, *45*, 3165.

Hazarika, P.; Kukolka, F.; Niemeyer, C. M. *Angew. Chem. Int. Ed.* **2006**, *45*, 6827.

Hermann, T.; Patel, D. J. *Science* **2000**, *287*, 820.

Hildebrandt, N.; Charbonniere, L. J.; Beck, M.; Ziessel, R. F.; Lohmannsroben, H. G. *Angew. Chem., Int. Ed.* **2005**, *44*, 7612.

Hobbs, S. K.; Monsky, W. L.; Yuan, F.; Roberts, W. G.; Griffith, L.; Torchilin, V. P.; Jain, R. K. *Proc. Natl. Acad. Sci. U. S. A.* **1998**, *95*, 4607.

Holmberg, A.; Blomstergren, A.; Nord, O.; Lukacs, M.; Lundeberg, J.; Uhlen, M. *Electrophoresis* **2005**, *26*, 501.

Holowka, E. P.; Sun, V. Z.; Kamei, D. T.; Deming, T. J. *Nature Mat.* **2007**, *6*, 52.

Hong, R.; Han, G.; Fernandez, J. M.; Kim, B. J.; Forbes, N. S.; Rotello, V. M. *J. Am. Chem. Soc.* **2006**, *128*, 1078.

Hostetler, M. J.; Templeton, A. C.; Murray, R. W. *Langmuir* **1999**, *15*, 3782.

Huang, Y. F.; Chang, H. T. *Anal. Chem.* **2006**, *78*, 1485.

Jackson, A. M.; Myerson, J. W.; Stellacci, F. *Nat. Mat.* **2004**, *3*, 330.

Jaiswal, J. K.; Mattoussi, H.; Mauro, J. M.; Simon, S. M. *Nat. Biotechnol.* **2003**, *21*, 47.

Jantz, D.; Amann, B. T.; Gatto, G. J.; Berg, J. M. *Chem. Rev.* **2004**, *104*, 789.

Je, J. Y.; Cho, Y. S.; Kim, S. K. *Biomacromolecules* **2006**, *7*, 3448.

Jiang, W.; Kim, B. Y. S.; Rutka, J. T.; Chan, W. C. W. *Nat. Nanotech.* **2008**, *3*, 145.

Jones, S.; Thornton, J. M. *Proc. Natl. Acad. Sci.U. S. A.* **1996**, *93*, 13.

Jordan, B. J.; Hong, R.; Gider, B.; Hill, J.; Emrick, T.; Rotello, V. M. *Soft Matter* **2006**, *2*, 558.

Kakizawa, Y.; Furukawa, S.; Kataoka, K. *J. Control Release* **2004**, *97*, 345.

Kam, N. W. S.; Jessop, T. C.; Wender, P. A.; Dai, H. J. *J. Am. Chem. Soc.* **2004**, *126*, 6850.

Kam, N. W. S.; O'Connell, M.; Wisdom, J. A.; Dai, H. *Proc. Natl. Acad. Sci. U.S.A.* **2005**, *102*, 11600.

Kanaras, A. G.; Kamounah, F. S.; Schaumburg, K.; Kiely, C. J.; Brust, M. *Chem. Commun.* **2002**, 2294.

Katz, E.; Willner, I. *Angew. Chem., Int. Ed.* **2004**, *43*, 6042.

Kay, M. A.; Glorioso, J. C.; Naldini, L. *Nat. Med.* **2001**, *7*, 33.

Khalil, I. A.; Kogure, K.; Akita, H.; Harashima, H. *Pharma. Rev.* **2006**, *58*, 32.

Kielkopf, C. L.; Baird, E. E.; Dervan, P. D.; Rees, D. C. *Nat. Struct. Biol.* **1998**, *5*, 104.

Kikuta, E.; Murata, M.; Katsube, N.; Koike, T.; Kimura, E. *J. Am. Chem. Soc.* **1999**, *121*, 5426.

Kim, C. K.; Ghosh, P.; Pagliuca, C.; Zhu, Z.-J.; Menichetti, S.; Rotello, V. M. *J. Am. Chem. Soc.* **2009**, *131*, 1360.

Kobsa, S.; Saltzman, W. M. *Pediatr. Res.* **2008**, *63*, 513.

Koch, A. M.; Reynolds, F.; Merkle, H. R.; Weissleder, R.; Josephson, L. *Chembiochem* **2005**, *6*, 337.

Kodama, K.; Katayama, Y.; Shoji, Y.; Nakashima, H. *Curr. Med. Chem.* **2006**, *13*, 2155.

Kosuge, M.; Takeuchi, T.; Nakase, I.; Jones, A. T.; Futaki, S. *Bioconjugate Chem.* **2008**, *19*, 656.

Kussie, P. H.; Gorina, S.; Marechal, V.; Elenbaas, B.; Moreau, J.; Levine, A. J.; Pavletich, N. P. *Science* **1996**, *274*, 948.

Lai, C. Y.; Trewyn, B. G.; Jeftinija, D. M.; Jeftinija, K.; Xu, S.; Jeftinija, S.; Lin, V. S. Y. *J. Am. Chem. Soc.* **2003**, *125*, 4451.

Lakowicz, J. R.; Gryczynski, I.; Gryczynski, Z.; Nowaczyk, K.; Murphy, C. J. *Anal. Biochem.* **2000**, *280*, 128.

Leroueil, P.; Hong, S.; Mecke, A.; Baker, J.; Orr, B.; Banaszak Holl, M. *Acc. Chem. Res.* **2007**, *40*, 335.

Levy, E. J.; Anderson, M. E.; Meister, A. *Proc. Natl. Acad. Sci. U. S. A.* **1993**, *90*, 9171.

Lewin, M.; Carlesso, N.; Tung, C.-H.; Tang, X.-W.; Cory, D.; Scadden, D. T.; Weissleder, R. *Nat. Biotechnol.* **2000**, *18*, 410.

Lewinski, N.; Colvin, V.; Drezek, R. *Small* **2008**, *1*, 26.

Li, D.; Li, G. P.; Guo, W. W.; Li, P. C.; Wang, E. K.; Wang, J. *Biomaterials* **2008**, *29*, 2776.

Liu, Y. M.; Reineke, T. M. *J. Am. Chem. Soc.* **2005**, *127*, 3004.

Love, J. C.; Estroff, L. A.; Kriebel, J. K.; Nuzzo, R. G.; Whitesides, G. M. *Chem. Rev.* **2005**, *105*, 1103.

Lu¨hmann, T.; Rimann, M.; Bittermann, A. G.; Hall, H. *Bioconjugate Chem.* **2008**, *19*, 1907.

Luedtke, W. D.; Landman, U. *J. Phy. Chem. B* **1998**, *102*, 6566.

Luo, D.; Haverstick, K.; Belcheva, N.; Han, E.; Saltzman, W. M. *Macromolecules* **2002**, *35*, 3456.

Luo, D.; Saltzman, W. M. *Nat. Biotechnol.* **2000**, *18*, 33.

Mahato, R. I. *Adv. Drug Delivery Rev.* **2005**, *57*, 699.

Mahtab, R.; Harden, H. H.; Murphy, C. J. *J. Am. Chem. Soc.* **2000**, *122*, 14.

Mansouri, S.; Cuie, Y.; Winnik, F.; Shi, Q.; Lavigne, P.; Benderdour, M.; Beaumont, E.; Fernandes, J. C. *Biomaterials* **2006**, *27*, 2060.

McCormick, F. *Nat. Rev. Cancer* **2001**, *1*, 130.

McIntosh, C. M.; Esposito, E. A.; Boal, A. K.; Simard, J. M.; Martin, C. T.; Rotello, V. M. *J. Am. Chem. Soc.* **2001**, *123*, 7626.

McLean, J. A.; Stumpo, K. A.; Russell, D. H. *J. Am. Chem. Soc.* **2005**, *127*, 5304.

Medarova, Z.; Pham, W.; Farrar, C.; Petkova, V.; Moore, A. *Nat. Med.* **2007**, *13*, 372.

Medintz, I. L.; Pons, T.; Delehanty, J. B.; Susumu, K.; Brunel, F. M.; Dawson, P. E.; Mattoussi, H. *Bioconjugate Chem.* **2008**, *19*, 1785.

Michalet, X.; Pinaud, F. F.; Bentolila, L. A.; Tsay, J. M.; Doose, S.; Li, J. J.; Sundaresan, G.; Wu, A. M.; Gambhir, S. S.; Weiss, S. *Science* **2005**, *307*, 538.

Midoux, P.; Monsigny, M. *Bioconjugate Chem.* **1999**, *10*, 406.

Miranda, O. R.; You, C. C.; Phillips, R.; Kim, I. B.; Ghosh, P. S.; Bunz, U. H. F.; Rotello, V. M. *J. Am. Chem. Soc.***2007**, *129*, 9856.

Mirkin, C. A.; Letsinger, R. L.; Mucic, R. C.; Storhoff, J. J. *Nature* **1996**, *382*, 607.

Mitchell, D. J.; Kim, D. T.; Steinman, L.; Fathman, C. G.; Rothbard, J. B. *J. Pep. Res.* **2000**, *56*, 318.

Mito-Oka, Y.; Tsukiji, S.; Hiraoka, T.; Kasagi, N.; Shinkai, S.; Hamachi, I. *Tet. Lett.* **2001**, *42*, 7059.

Mitragotri, S.; Blankschtein, D.; Langer, R. *Science* **1995**, *269*, 850.

Moreau, E.; Domurado, M.; Chapon, P.; Vert, M.; Domurado, D. *J. Drug Target.* **2002**, *10*, 161.

Morris, M. C.; Depollier, J.; Mery, J.; Heitz, F.; Divita, G. *Nat. Biotechnol.* **2001**, *19*, 1173.

Mozafari, M. R.; Reed, C. J.; Rostron, C. *Micron* **2007**, *38*, 787.

Mrksich, M. *ACS Nano* **2008**, *2*, 7.

Murphy, C. J.; Gole, A. M.; Stone, J. W.; Sisco, P. N.; Alkilany, A. M.; Goldsmith, E. C.; Baxter, S. C. *Acc. Chem. Res.* **2008**, *41*, 1721.

Murthy, N.; Xu, M. C.; Schuck, S.; Kunisawa, J.; Shastri, N.; Frechet, J. M. J. *Proc. Natl. Acad. Sci. U.S.A.* **2003**, *100*, 4995.

Myrberg, H.; Lindgren, M.; Langel, U. *Bioconjugate Chem.* **2007**, *18*, 170.

Nagahori, N.; Nishimura, S.-I. *Chem. - Eur. J.* **2006**, *12*, 6478.

Naka, K.; Itoh, H.; Tampo, Y.; Chujo, Y. *Langmuir* **2003,** *19*, 5546.

Nativo, P.; Prior, I. A.; Brust, M. *ACS Nano* **2008**, *2*, 1639.

Neuman, D.; Ostrowski, A. D.; Absalonson, R. O.; Strouse, G. F.; Ford, P. C. *J. Am. Chem. Soc.* **2007**, *129*, 4146.

Nguyen-Hackley, D. H.; Ramm, E.; Taylor, C. M.; Joung, J. K.; Dervan, P. B.; Pabo, C. O. *Biochemistry* **2004**, *43*, 3880.

Niemeyer, C. M. *Angew. Chem., Int. Ed.* **2001**, *40*, 4128.

Nishiyama, N.; Iriyama, A.; Jang, W. D.; Miyata, K.; Itaka, K.; Inoue, Y.; Takahashi, H.; Yanagi, Y.; Tamaki, Y.; Koyama, H.; Kataoka, K. *Nat. Mater.* **2005**, *4*, 934.

Northen, T. R.; Yanes, O.; Northen, M. T.; Marrinucci, D.; Uritboonthai, W.; Apon, J.; Golledge, S. L.; Nordstrom, A.; Siuzdak, G. *Nature* **2007**, *449*, 1033.

Novikov, A.; Caroff, M.; Della-Negra, S.; Lebeyec, Y.; Pautrat, M.; Schultz, J. A.; Tempez, A.; Wang, H. Y. J.; Jackson, S. N.; Woods, A. S. *Anal. Chem.* **2004**, *76*, 7288.

Oishi, M.; Nakaogami, J.; Ishii, T.; Nagasaki, Y. *Chem. Lett.***2006**, *35*, 1046.

Opalinska, J. B.; Gewirtz, A. M. *Nat. Rev. Drug Discovery* **2002**, *1*, 503.

Orner, B. P.; Salvatella, X.; Quesada, J. S.; de Mendoza, J.; Giralt, E.; Hamilton, A. D. *Angew. Chem. Int. Ed.* **2002**, *41*, 117.

Owega, S.; Lai, E. P. C.; Bawagan, A. D. O. *Anal. Chem.* **1998**, *70*, 2360.

Oyoshi, T.; Kawakami, W.; Narita, A.; Bando, T.; Sugiyama, H. *J. Am. Chem. Soc.* **2003**, *125*, 4752.

Paciotti, G. F.; Kingston, D. G. I.; Tamarkin, L. *Drug Dev. Res.* **2006**, *67*, 47.

Paciotti, G. F.; Kingston, D. G. I.; Tamarkin, L. *Drug Develop. Res.* **2006**, *67*, 47.

Pack, D. W.; Hoffman, A. S.; Pun, S.; Stayton, P. S. *Nat. Rev. Drug Discovery* **2005**, *4*, 581.

Palegrosdemange, C.; Simon, E. S.; Prime, K. L.; Whitesides, G. M. *J. Am. Chem. Soc.* **1991**, *113*, 12.

Pasquato, L.; Pengo, P.; Scrimin, P. *J. Mat. Chem.* **2004**, *14*, 3481.

Peer, D.; Karp, J. M.; Hong, S.; Farokhzad, O. C.; Margalit, R.; Langer, R. *Nat. Nanotech.* **2007**, *2*, 751.

Peer, D.; Karp, J.; Hong, S.; Farokhzad, O.; Margalit, R.; Langer, R. *Nature Nanotech.* **2007**, *2*, 751.

Pellegrino, T.; Kudera, S.; Liedl, T.; Javier, A. M.; Manna, L.; Parak, W. J. *Small* **2005**, *1*, 48.

Phelan, A.; Elliott, G.; O'Hare, P. *Nat. Biotechnol.* **1998**, *16*, 440.

Pichon, C.; Goncalves, C.; Midoux, P. *Adv. Drug Deliv. Rev.* **2001**, *53*, 75.

Polizzi, M. A.; Stasko, N. A.; Schoenfisch, M. H. *Langmuir* **2007**, *23*, 4938.

Pujals, S.; Bastus, N. G.; Pereiro, E.; Lopez-Iglesias, C.; Punte, V. F.; Kogan, M. J.; Giralt, E. *Chembiochem* **2009**, *10*, 1025.

Ramsay, E.; Hadgraft, J.; Birchall, J.; Gumbleton, M. *Int. J. Pharm.* **2000**, *210*, 97.

Ramsden, J. J. *Q. Rev. Biophys.* **1993,** *27*, 41.

Raper, S. E.; Chirmule, N.; Lee, F. S.; Wivel, N. A.; Bagg, A.; Gao, G. P.; Wilson, J. M.; Batshaw, M. L. *Mol. Genet. Metab.* **2003**, *80*, 148.

Rosi, N. L.; Giljohann, D. A.; Thaxton, C. S.; Lytton-Jean, A. K. R.; Han, M. S.; Mirkin, C. A. *Science* **2006**, *312*, 1027.

Rosi, N. L.; Mirkin, C. A. *Chem. Rev.* **2005**, *105*, 1547.

Rothbard, J. B.; Garlington, S.; Lin, Q.; Kirschberg, T.; Kreider, E.; McGrane, P. L.; Wender, P. A.; Khavari, P. A. *Nat. Med.* **2000**, *6*, 1253.

Rothbard, J. B.; Jessop, T. C.; Wender, P. A. *Adv. Drug Deliv. Rev.* **2005**, *57*, 495.

Salvatella, X.; Martinell, M.; Gairi, M.; Mateu, M. G.; Feliz, M.; Hamilton, A. D.; de Mendoza, J.; Giralt, E. *Angew. Chem. Int. Ed.* **2004**, *43*, 196.

Sandhu, K. K.; McIntosh, C. M.; Simard, J. M.; Smith, S. W.; Rotello, V. M. *Bioconjugate Chem.* **2002**, *13*, 3.

Sastry, M.; Rao, M.; Ganesh, K. N. *Acc. Chem. Res.* **2002**, *35*, 847.

Savic, R.; Luo, L.; Eisenberg, A.; Maysinger, D. *Science* **2003**, *300*, 615.

Schaaff, T. G. *Anal. Chem.* **2004**, *76*, 6187.

Schwarze, S. R.; Ho, A.; Vocero-Akbani, A.; Dowdy, S. F. *Science* **1999**, *285*, 1569.

Shi, X. G.; Wang, S. H.; Meshinchi, S.; Van Antwerp, M. E.; Bi, X. D.; Lee, I. H.; Baker, J. R. *Small* **2007**, *3*, 1245.

Slowing, I. I.; Trewyn, B. G.; Lin, V. S. Y. *J. Am. Chem. Soc.* **2007**, *129*, 8845.

Sokolova, V.; Epple, M. *Angew. Chem. Int. Ed.* **2008**, *47*, 1382.

Spencer, M. T.; Furutani, H.; Oldenburg, S. J.; Darlington, T. K.; Prather, K. A. *J. Phys. Chem. C* **2008**, *112*, 4083.

Stites, W. E. *Chem. Rev.* **1997,** *97*, 1233.

Su, C. L.; Tseng, W. L. *Anal. Chem.* **2007**, *79*, 1626.

Su, J.; Mrksich, M. *Langmuir* **2003**, *19*, 4867.

Sunner, J.; Dratz, E.; Chen, Y.-C. *Anal. Chem.* **1995**, *67*, 4335.

Tanaka, K.; Waki, H.; Ido, Y.; Akita, S.; Yoshida, Y.; Yoshida, T.; Matsuo, T. *Rapid Commun. Mass Spectrum.* **1988**, *2*, 151.

Templeton, A. C.; Wuelfing, W. P.; Murray, R. W. *Acc. Chem. Res.* **2000**, *33*, 27.

Thomas, M.; Klibanov, A. M. *Proc. Natl. Acad. Sci. U.S.A.* **2003**, *100*, 9138.

Thomas, M.; Lu, J. J.; Ge, Q.; Zhang, C. C.; Chen, J. Z.; Klibanov, A. M. *Proc. Natl. Acad. Sci. U.S.A.* **2005**, *102*, 5679.

Torney, F.; Trewyn, B. G.; Lin, V. S. Y.; Wang, K. *Nature Nanotech.* **2007**, *2*, 295.

Tracy, J. B.; Crowe, M. C.; Parker, J. F.; Hampe, O.; Fields-Zinna, C. A.; Dass, A.; Murray, R. W. *J. Am. Chem. Soc.* **2007**, *129*, 16209.

Tracy, J. B.; Kalyuzhny, G.; Crowe, M. C.; Balasubramanian, R.; Choi, J. P.; Murray, R. W. *J. Am. Chem. Soc.* **2007**, *129*, 6706.

Trevor, J. L.; Lykke, K. R.; Pellin, M. J.; Hanley, L. *Langmuir* **1998**, *14*, 1664.

Tsou, L. K.; Tatko, C. D.; Waters, M. L. *J. Am. Chem. Soc.* **2002**, *124*, 14917.

Tsunoyama, H.; Negishi, Y.; Tsukuda, T. *J. Am. Chem. Soc.* **2006**, *128*, 6036.

Vazquez, M. E.; Caamano, A. M.; Mascarenas, J. L. *Chem. Soc. Rev.* **2003**, *32*, 338.

Verma, A.; Nakade, H.; Simard, J. M.; Rotello, V. M. *J. Am. Chem. Soc.* **2004**, *126*, 10806.

Verma, A.; Rotello, V. M. *Chem. Commun.*, **2005**, 303.

Verma, A.; Simard, J. M.; Worrall, J. W. E.; Rotello, V. M. *J. Am. Chem. Soc.* **2004**, *126*, 13987.

Verma, A.; Uzun, O.; Hu, Y.; Hu, Y.; Han, H.-S.; Watson, N.; Chen, S.; Irvine, D. J.; Stellacci, F. *Nature Mater.* **2008**, *7*, 588.

Verma, I. M.; Somia, N. *Nature* **1997**, *389*, 239.

Veselovsky, A. V.; Ivanov, Y. D.; Ivanov, A. S.; Archakov, A. I.; Lewi, P.; Janssen, P. *J. Mol. Recog.* **2002,** *15*, 405.

Vida, T. A.; Emr, S. D. *J. Cell Biol.* **1995**, *128*, 779.

Voet, D.; Voet, J. G. *Biochemistry, 2nd ed.;* John Wiley & Sons, Inc.: New York, **1995**; pp 1124–1131.

Wang, C.; Ge, Q.; Ting, D.; Nguyen, D.; Shen, H. R.; Chen, J. Z.; Eisen, H. N.; Heller, J.; Langer, R.; Putnam, D. *Nature Mater*. **2004**, *3*, 190.

Wang, G. L.; Zhang, J.; Murray, R. W. *Anal. Chem.* **2002**, *74*, 4320.

Wang, J. *Anal. Chim. Acta* **2003**, *500*, 247.

Wang, K. W.; Yan, X. H.; Cui, Y.; He, Q.; Li, J. B. *Bioconjug. Chem.* **2007**, *18*, 1735.

Wei, J.; Buriak, J. M.; Siuzdak, G. *Nature* **1999**, *399*, 243.

Wilson, D.; Perlson, L.; Breslow, R. *Bioorg. & Med. Chem.* **2003**, *11*, 2649.

Xia, Y. *Nature Mater.* **2008**, *7*, 758.

Xu, C. J.; Xu, K. M.; Gu, H. W.; Zhong, X. F.; Guo, Z. H.; Zheng, R. K.; Zhang, X. X.; Xu, B. *J. Am. Chem. Soc.* **2004**, *126*, 3392.

Xu, Z. P.; Zeng, Q. H.; Lu, G. Q.; Yu, A. B. *Chem.Eng. Sci.* **2006**, *61*, 1027.

Yalkowsky, S. H.; Krzyzaniak, J. F.; Ward, G. H. *J. Pharm. Sci.* **1998**, *87*, 787.

Yamanouchi, D.; Wu, J.; Lazar, A. N.; Kent, K. C.; Chu, C. C.; Liu, B. *Biomaterials* **2008**, *29*, 3269.

Yang, P. H.; Sun, X.; Chiu, J. F.; Sun, H.; He, Q. Y. *Bioconjugate Chem.* **2005**, *16*, 494.

Yang, Q.; Wang, S. H.; Fan, P. W.; Wang, L. F.; Di, Y.; Lin, K. F.; Xiao, F. S. *Chem. Mater.* **2005**, *17*, 5999.

Yezhelyev, M. V.; Qi, L.; O'Regan, R. M.; Nie, S.; Gao, X. *J. Am. Chem. Soc.* **2008**, *130*, 9006.

You, C. C.; De, M.; Han, G.; Rotello, V. M. *J. Am. Chem. Soc.* **2005**, *127*, 12873.

You, C. C.; De, M.; Rotello, V. M. *Curr. Opin. Chem. Biol.* **2005**, *9*, 639.

You, C. C.; Verma, A.; Rotello, V. M. *Soft Matter* **2006**, *2*, 190.

You, C.-C.; Miranda, O. R.; Gider, B.; Ghosh, P. S.; Kim, I.-B.; Erdogan, B.; Krovi, S. A.; Bunz, U. H. F.; Rotello, V. M. *Nat. Nanotech.* **2007**, *2*, 318.

Zadmard, R.; Schrader, T. *Angew. Chem. Int. Ed.* **2006**, *45*, 2703.

Zauner, W.; Ogris, M.; Wagner, E. *Adv. Drug Delivery Rev.* **1998**, *30*, 97.

Zhang, J.; Misra, R. D. K. *Acta Biomat.* **2007**, *3*, 838.

Zheng, M.; Davidson, F.; Huang, X. Y. *J. Am. Chem. Soc.* **2003**, *125*, 7790.

Zheng, M.; Huang, X. Y. *J. Am. Chem. Soc.* **2004**, *126*, 12047.

Zhu, Z. J.; Ghosh, P. S.; Miranda, O. R.; Vachet, R. W.; Rotello, V. M. *J. Am. Chem. Soc.* **2008**, *130*, 14139.